A COMPUTATIONAL STUDY OF INTERVERTEBRAL DISC DEGENERATION IN RELATION TO CHANGES IN REGIONAL TISSUE COMPOSITION AND DISC NUTRITION

Carlos Eduardo Ruiz Wills

Institute for Bioengineering of Catalonia
Technical University of Catalonia

Doctoral Thesis
December 2015

Materials Science and Engineering Doctoral Program

Supervised by Dr. Jérôme Noailly and Prof. Damien Lacroix

A mis padres Ana Isabel y Carlos Jesús mis dos fuentes de inspiración y amor incondicional

Twenty years from now you will be more disappointed by the things that you didn't do than by the ones you did do, so throw off the bowlines, sail away from safe harbour, catch the trade winds in your sails. Explore, Dream, Discover.

Mark Twain

PUBLICATIONS AND CONGRESSES

Journal papers and manuscripts

- Ruiz, C., Noailly, J. and Lacroix, D. (2013) Material property discontinuities in intervertebral disc porohyperelastic finite element models generate numerical instabilities due to volumetric strain variations. Journal of the Mechanical Behavior of Biomedical Materials, Volume 26, pp. 1-10.
- Ruiz Wills, C., Malandrino, A., Lacroix, D., Ito, K. and Noailly, J. (2014) Simulating the sensitivity of cell nutritive environment to composition changes within the intervertebral disc. Journal of the Mechanics and Physics of Solids. Submitted.
- Ruiz Wills, C., Malandrino, A., Lacroix, D. and Noailly, J. (2014) Simulating proteoglycan turnover and cell viability in the intervertebral disc: a numerical exploration of nutrition-induced changes along degeneration. Manuscript.
- Ruiz Wills, C., Foata, B., Lacroix, D. and Noailly, J. (2015) Alterations of cartilage endplates composition generate dehydration at the nucleus pulposus: a novel finite element approach for the composition gradient of the cartilage endplate. Manuscript.

Congresses and seminars

- Ruiz, C., Noailly, J. and Lacroix, D. Mesh Convergence Study of The Intervertebral Disc. 4to. Simposio del Instituto de Bioingeniería de Cataluña (IBEC) sobre Bioingeniería y nanomedicina. Poster presentation, October 18-19th of 2011, Barcelona, Spain.
- Ruiz, C., Noailly, J. and Lacroix, D. Estudio de Convergencia de Malla del Disco Intervertebral. I Reunión del Capítulo Español de la Sociedad Europea de Biomecánica (ESB). Oral presentation, November 10th of 2011, Zaragoza, Spain.
- Ruiz, C., Noailly, J. and Lacroix, D. Material discontinuities create fluid flow instabilities in intervertebral disc poroelastic finite element models. 10th International Symposium on Computer Methods in Biomechanics and Biomedical Engineering (CMBBE 2012). Oral presentation, April 11-14th of 2012, Berlin, Germany.
- Ruiz, C., Noailly, J. and Lacroix, D. Strategies to cope with fluid velocity instabilities in intervertebral disc poroelastic models. 5to. Simposio del Instituto de Bioingeniería de Cataluña (IBEC) sobre Bioingeniería y nanomedicina. Poster presentation, June 11th of 2012, Barcelona, Spain.
- Ruiz, C., Noailly, J. and Lacroix, D. Material discontinuities create fluid flow instabilities in intervertebral disc poroelastic finite element models. 18th Congress of the European Society of Biomechanics (ESB 2012). Oral presentation, July 1-4th of 2012, Lisbon, Portugal. J Biomech, 45, S600.
- Ruiz, C., Noailly, J. and Lacroix, D. Mesh convergence is affected by poroelasticity in multi-tissue intervertebral disc models. The Virtual Physiological Human Network of Excellence (VPH2012). Oral presentation, September 18-20th of 2012, London, United Kingdom.
- Ruiz, C., Noailly, J. and Lacroix, D. Estrategias para enfrentar inestabilidades en la velocidad de fluido en modelos porohiperelásticos con múltiples tejidos blandos: el ejemplo del disco intervertebral. II Reunión del Capítulo Español de la Sociedad

Europea de Biomecánica (ESB). Oral presentation, Octuber 25th of 2012, Seville, Spain.

- Ruiz, C., Malandrino, A., Lacroix, D. and Noailly, J. A composition-dependent intervertebral disc model for integrated studies of degenerative changes. 6to. Simposio del Instituto de Bioingeniería de Cataluña (IBEC) sobre Bioingeniería y nanomedicina. Poster presentation, May 8th of 2013, Barcelona, Spain.
- Ruiz, C., Malandrino, A., Lacroix, D., Ito, I. and Noailly, J., Can biochemical composition changes affect nutrition and cell viability in early intervertebral disc degeneration?. III Reunión del Capítulo Español de la Sociedad Europea de Biomecánica (ESB). Oral presentation, October 23-24th of 2013, Barcelona, Spain.
- Ruiz, C. Can biochemical composition changes affect nutrition and cell viability in early intervertebral disc degeneration?. PhD discussions of the Institute for Bioengineering of Catalonia (IBEC). Seminar, October 25th of 2013, Barcelona, Spain.
- Toumanidou, T. and Ruiz, C. Spine Finite Element Models: How can they change our understanding about low back pain?. Institute for Bioengineering of Catalonia. Seminar, March 20th of 2014, Barcelona, Spain.
- Ruiz, C., Malandrino, A., Lacroix, D., Ito, K. and Noailly, J. Composition-based tissue modelling to assess the sensitivity of cell nutritive environment to extracellular matrix changes within the intervertebral disc. 7th World Congress of Biomechanics (WCB 2014). Poster presentation, July 6-11th of 2014, Boston, United States.
- Ruiz, C., Malandrino, A., Lacroix, D., Ito, K. and Noailly, J. A composition-based intervertebral disc model to study the effects of extracellular matrix degenerative changes on nutrition. 11th World Congress on Computational Mechanics (WCCM XI). Keynote presentation, July 20-25th of 2014, Barcelona, Spain.
- Ruiz Wills, C., Malandrino, A., Lacroix, D. and Noailly, J. Intervertebral disc degeneration: How does proteoglycan loss affect the cell viability?. 7mo. Simposio del Instituto de Bioingeniería de Cataluña (IBEC) sobre Bioingeniería y nanomedicina. Poster presentation, September 15th of 2014, Barcelona, Spain.
- Foata, B., Ruiz, C. and Noailly, J. Effect of the cartilage endplate gradient of composition on the fluid exchange at the intervertebral disc - vertebra interface. 7mo. Simposio del Instituto de Bioingeniería de Cataluña (IBEC) sobre Bioingeniería y nanomedicina. Poster presentation, September 15th of 2014, Barcelona, Spain.
- Ruiz Wills, C., Malandrino, A., Lacroix, D. and Noailly, J. Simulating proteoglycan turnover and cell viability in the intervertebral disc: a numerical exploration of nutrition-induced changes along degeneration. IV Reunión del Capítulo Español de la Sociedad Europea de Biomecánica (ESB). Oral presentation, November 20-21th of 2014, Valencia, Spain.
- Reagh, J., Vizel, S., Ruiz Wills, C., Di Blasi, T., Malandrino, A., Loeser, F., Chan, S., Gantebein-Ritter, B. and Noailly, J. Multi-scale simulation of intervertebral disc biophysics under bioreactor conditions by coupling finite element and agent-based models. 21th Congress of the European Society of Biomechanics (ESB 2015). Poster presentation, July 5-8th of 2015, Prague, Czech Republic.
- Ruiz Wills, C., Malandrino, A., Lacroix, D. and Noailly, J. Simulating proteoglycan turnover and cell viability in the intervertebral disc: a numerical exploration of nutrition-induced changes along degeneration. 21th Congress of the European Society of Biomechanics (ESB 2015). Oral presentation, July 5-8th of 2015, Prague, Czech Republic.

ABSTRACT

Up to 85% of the world population suffers from low back pain, a clinical condition often related to the intervertebral disc (IVD) degeneration (DD). Altered disc cell nutrition affects cell viability and can generate catabolic cascades that degrade the extracellular matrix (ECM). Also, a major degenerative biochemical change in the disc is the proteoglycan (PG) loss, which affects the osmotic pressure and hydration that is critical for cell nutrition. However, the relationship between biochemical degradation and nutrition along degeneration is unclear. The effect of cartilage endplates (CEP) tissue changes through known composition data remains unknown as well. Experiments have limited capacity in the study of multiple IVD interactions, while theoretical models are promising tools to this aim. Thus, this PhD thesis used computer models to study the relationship between disc degeneration and cell nutrition, and focuses on indirect mechanotransduction phenomena that occur in the IVD.

Porohyperelastic IVD finite element models, including all tissues, were used. Such models consider the role of solid-fluid interaction within the IVD. In Chapter 3 a convergence study was performed to access the stability of local predictions under fast load rates. In Chapter 4 the models were updated by adding the viscoelastic collagen fibres of the annulus fibrosus (AF) and the osmotic pressure of the nucleus pulposus (NP). They were coupled to a transport-cell viability model, and a design of experiment (DOE) was used to study the effect of disc composition on cell nutrition. In Chapter 5 the transport model was modified to allow PG updates, depending on PG half-life and PG production related to predicted oxygen pressure. In Chapter 6, a composition-dependent permeability formulation was created for the CEP to focus on the impact of CEP degradation. Three days of diurnal load cycle were simulated for all transport-cell viability simulations. Solute concentrations were evaluated along the mid-sagittal plane path.

Chapter 3 showed that unrealistic spatial oscillations in the fluid velocity predictions were due to material discontinuities. Previous stabilization strategies did not eliminate the oscillations. However, the creation of a material transition zone combined with local refinement reduced them by 91%. The model obtained warranted the stability of local calculations for long lasting loads. Chapter 4 results revealed that none of DOE combinations affected the cell viability, and that water reductions altered the most disc nutrition. Moreover, NP degeneration might affect the AF nutrition, possibly explaining the tears found in grade III discs. In Chapter 5, IVD nutrition affected the PG content, which seemed to simulate natural ageing. Also, PG loss altered disc mechanical behaviour but neither cell viability nor nutrition. However, the inclusion of NP dehydration reduced solute levels, which might activate catabolic processes. Chapter 6 showed that CEP permeability would increase with DD. Also, CEP degeneration alone produced NP dehydration under compression, which affected disc nutrition. The results suggested that the CEP might play a key role in DD. Interestingly, cell death was predicted when CEP degeneration was combined to AF and NP degeneration, questioning the paradigm that CEP calcification might be responsible for cell death along DD.

This PhD thesis identified different paths related to DD. On one hand, NP dehydration and PG loss reduced glucose at the inner AF, weakening the latter due to inflammation and enzyme activation. Meanwhile, nutrition regulated the PG content, which can explain natural ageing but probably not accelerated degeneration processes. However, CEP degeneration caused NP dehydration, and the combined degeneration of all disc tissues activated the cell death. All these simulated events are important to understand DD and might promote the development of new experimental explorations and treatment strategies.

ACKNOWLEDGEMENTS

I would like to express my sincere gratitude to all the people who made possible this thesis. First of all, I would like to thank God for being with me all the time and giving me the strength to arrive to this moment.

I would like to thank the European Commission (My SPINE-269909) and the Agència de Gestió d'Ajuts Universitaris i de Recerca of the Generatitat de Catalunya (AGAUR-2012BE100979), for financing this thesis.

I am deeply thankful to my directors Prof. Damien Lacroix and Dr. Jérôme Noailly for their support and patience. Damien broke my scheme of engineer and showed me the path of research, your guidance and advices were crucial for me during this time. Jérôme knew how to encourage me to keep going, you always had the correct advice to give me, I really appreciate that you never gave the answer to a question directly, instead, you always made me think about the whole frame involved to find by myself the solution, that is something that I will keep with me for all my life and I definitely will transmit to others.

I would like to thank Prof. Keita Ito for open to me the door of the group of Orthopaedic Biomechanics of the Eindhoven University of Technology. I grew professionally and personally during my time in Eindhoven. Also, I met again with really good friends, Sol and Juan, and also made new friends, Andrés, Lorenza, Juan Carlos, Liliana, Jaqueline and David. I will always be grateful for that experience.

I am infinitely thankful to my parents Ana Isabel Wills Oliveros and Carlos Jesús Ruiz Bolívar for giving me the life, their support and unconditional love during my whole life. Dad, you taught me from the beginning to fight for what I want, to always challenge myself to become better and better, not because the others will recognize my effort but because of the satisfaction of achieve something you believe you couldn't do, you always encourage me to chase my goals and never look back, letting me know that if I fall you would always be there to give me a hand. Mom, I can't put in words how grateful I am to you. Since I was a kid, you encourage me to learn about art, music, sport and religion to have a complete vision of the world. You taught me to put the heart to everything I do and to see life with joy. You always know what to tell me to cheer me up, remembering me that if I fall 6 times I have to get up 7 times and go on. You taught me to never be embarrassed of defending my beliefs and to value the small things in the world, like landscapes and moments that sometimes go unnoticed. You taught me to feel the people that are around me and to appreciate them for what they are and not for what they have. At the end you showed me how to be a better person. I love you both mom and dad with all the strength of my heart. I dedicate this thesis to you.

I would like to thank to Dr. Andrea Malandrino who was my tutor. Most of the knowledge I gained during this thesis came from you. You were professionally like a big brother for me. You were always willing to help me; you made me focus on the important points and put aside minor things. You always had words of encouragement for the difficult times. Knowing that I had your support gave me strength to move forward. In the personal life I am glad to have you as a friend.

I would like to thanks my cousin Yuliana Wills. Having you by my side during these years filled the hole of being away from my family. You lived with me the good and

bad times, always supporting me, giving me advices and scolding me when I do something bad. Our blood made us cousins but life made us brother and sister. I love you little sister.

I would like to thanks to the current and former members of the group of Biomechanics and Mechanobiology of the Institute for Bioengineering of Catalonia (IBEC): Andy, Themis, Simone, Sarah, JJ, Clara, Cécile, Sara, Aura, Toni, Natalia, Eduard, Albert, Ernest, Zóe, Isabela, Nicole, Arsalan, Kwasi, Luca, Ariane, Felix, Leonid, Baptiste, Tony and Alex. Especially Themis who shared with me the office for the last 2 years. All of you made me feel like home. It was nice to work in a group where you have partners and not competitors. You were like a family for me during these years.

I would like to thanks my students Baptiste and Sarah. Baptiste, your work allowed me to complete one chapter of this thesis. It was very easy to guide you because you are smart, methodical and independent. Sarah, even though you were a bachelor student, I always treated you as a Master student because I knew you could fulfil that role. You are brilliant, you always faced the tasks that I gave you with enthusiasm, and you always wanted to know everything you can about the problem you were working with. You always put a smile on me. Guys, you both are nice people and I am sure you will have an excellent future in any project that you develop in life. It was a pleasure to work with you and an honor to be your tutor.

I would like to thanks all IBEC community. Especially to the IT department, Juli Bafaluy and Francisco Contreras, for the constant technical support, and the personal of communications Vienna, Pilar, Àngels and Carol who always treated me with kindness and affection.

I would like to thanks to my dear IBEC PhD student committee, of which I was member from its creation until I finished this thesis. Especially to Claudia, Montse, Marta, Anna, Isil, Rosella, Simón and Marc. It was a pleasure working with you in the scientific and social integration of all IBEC students. I will always keep the committee and you guys in my heart.

I would like to thanks to Olga and Cristina. Girls you have no idea how important was for me your companionship, constant support and encouragement in this last months. Thanks for made my last time in IBEC the best.

I will always be thankful to my dear family. Although there is an ocean that separates me from most of you, you are and you always will be with me because you are in my heart. My cousins Sofía, Rita and José Ernesto made my first months in Barcelona unforgettable. Now my cousins Bianca, Alessandra and Ricardo give me that family warmth I need to keep going forward. My dear family, I love all of you with all my heart, thanks to be part of my life.

At last but not less important I would like to thank my friends. Alejandro, Carmen, Beatriz, Jorge Mario and Ana Raquel, you are a piece of home in Barcelona, the ones who I consider family, I am very blessed to have you here with me. My friends Tamara, Igor, Jesús, Laura, Jessica, Lucía, Norys, Luis, Debora, Julián, Claudio, Martina, Maisa, Jacobo, Zory, Ludmila, Lorena and Diego, you were my connection with the world that is outside the PhD, you always supported me and gave a word of encouragement. My flatmates Adrien, Anne-Sophie, Lucie and Astrid, you made our flat a home, I enjoyed every minute I spent with you guys. My friends in Barquisimeto, Rafael, Daniela, Oscar, Carmen Alicia, Claudia Paola, Luiday, Armando, Ignacio, José Rafael, Tereyda, Vanessa and Claudia, although I was away,

you never forgot me and always made me feel as if I never had left. I am very lucky to have all of you guys as friends. Your friendship is the most valuable treasure I have. Without you guys, I never could have made it that far, from the bottom of my heart thank you very much for all.

CONTENTS

LIST OF TABLES

LIST OF FIGURES

LIST OF ABBREVIATIONS AND ACRONYMS

2D	Two dimensions	G	Shear modulus
3D	Three dimensions	G_m	Solid matrix shear modulus
ANOVA	Analysis of variance	IFW	Intra-fibrillar water
AF	Annulus fibrosus	IVD	Intervertebral disc
α	Initial permeability at zero strain	K	Bulk modulus
α_{gluc}	Death rate for glucose	κ_0	Initial permeability
α_{pH}	Death rate for pH	LBP	Low back pain
BEP	Bony endplate	M	Experimental constant
CEP	Cartilage endplate	MMP	Matrix metalloproteinase
c_{F0}	Initial fixed charge density	MMP-3	Matrix metalloproteinase-3
C_{gluc}	Glucose concentration	MRI	Magnetic resonance imaging
C_{lact}	Lactate concentration	n_{F0}	Initial water content
C_{O_2}	Oxygen concentration	NP	Nucleus pulposus
CPU	Central processing unit	p	Threshold of significance
DOE	Design of experiment	PCD	Programmed cell death
e_0	Initial void ratio	ρ_{cell}	Cell density
ECM	Extracellular matrix	$\rho_{c,tot}$	Total density of collagen
EFW	Extra-fibrillar water	RAM	Random access memory
FE	Finite element	SED	Strain energy density
FV	Fluid velocity	XFEM	Extended finite element method

1 INTRODUCTION

1.1 The problem and motivation

Low back pain (LBP) is a common disabling symptom of osteoarticular disease in the spine. It is the second most frequent human disease after the common cold (Negrini et al. 2006; Katz 2006). In fact, according to ergonomic factors and location, up to 85% of the world population suffers from back pain at some point of their lives (Andersson 1999). In the case of the European Union, back pain affects up to 25% of the active population (Podniece 2008). In addition, the direct cost estimated for LBP, excluding medications and diagnostic test, rises to $20 billons per year in The United States alone (Katz 2006). On the other hand, in the European Union, e.g. Germany, the overall cost is more than 7000 € per person and per year before any rehabilitation treatment (Juniper et al. 2009).

Nowadays most of the treatments available to face LBP, e.g. discectomy, fusion, intervertebral disc substitute or conservative treatments, lead to satisfactory short-term pain relief. Yet, the main problem is that long/mid-term outcomes are less positive in terms of incremental degeneration problems and pain resurgence (Harrop et al. 2008; Mariconda et al. 2010). Although the origins of low back pain remain unclear (Chou et al. 2009), it is often associated with the degeneration of the intervertebral disc, even though the latter may be asymptomatic in many cases (Pfirrmann et al. 2001). In fact, endplate condition, herniation or protrusion are often associated to disc degeneration, and

can be sources of pain. Pain can also appear from inflammatory responses that decrease the threshold of afferent pain fibres.

The list of factors that contribute to disc degeneration did not change in several years, e.g. environmental, genetic, autoimmune, mechanical and inflammatory. However, the degree of impact of each factor has significantly changed in the last 10 years (Shankar et al. 2009), e.g. the effects of disc nutritive environment of cell and gene expression have become more relevant for disc degeneration in the last years. Moreover, abnormal loading conditions in the lumbar spine, including immobilization and overloading, may induce tissue adaptive changes that was suggested to contribute to disc degeneration (Stokes & Iatridis 2004; Raj 2008). On the other hand, the gene expression of interleukin, e.g. IL-1beta, favours the production of inflammatory factors (Huang et al. 2008) that may play a significant role in the aetiology of low back pain (Specchia et al. 2002). Also, changes in the intervertebral disc properties affect the load distributions in the surrounding bone, resulting in further alterations of the mechanical properties of the bone (Grant et al. 2002).

Indirect mechanotransduction including disc nutrition have been identified as a relevant path that could be involved in disc degeneration (Iatridis et al. 2006). In fact, the lack of nutrition affects the ability of the cells to synthesize and maintain disc extracellular matrix, possibly leading to disc degeneration (Raj 2008). The interactions between mechanical loads and nutritional environment influenced the gene expression of nucleus cells affecting matrix turnover (Rinkler et al. 2010; Neidlinger-Wilke et al. 2012). In addition, the disc cells started to die when the concentration of nutrients decreased below some critical values (Horner & Urban 2001). While some authors reported that disc cell density decreases with ageing (Setton and Chen 2004), others have revealed an increment of cell density with time (Rodriguez et al. 2011). Indeed, the formation of cell clusters and cell invasion can happen with ageing. In any case, there is a consensus about the overall decrease of disc cell anabolic activity. The latter contribute to proteoglycan depletion and affects nucleus intradiscal pressure, generating a loss of water that might affect the transport of nutrients in the disc. Thus, there seems to be a link between disc degeneration and nutrition but the role of nutrition in disc degeneration remains unclear.

In vivo, ex vivo and *in silico* models have been used to inform the physico-chemical properties of the lower back. *In vivo* animal studies have the advantage of including both a complete bunch of biological processes and the influence of tissue and organ structures. Nonetheless, anatomic and functional differences between animals and humans make very hard the extrapolation of the experiments outcomes to humans (Comí et al. 1995). In the case of *ex vivo* models, there are two options: use of synthetic materials or cadaveric tissues. The first ones try to simulate the disc behaviour using materials that are similar to the disc soft tissues. Synthetic models developed for medical education replicate disc anatomy, represent the main tissues, and can be deformed allowing the study of the migration of the nucleus material under compression throughout the annulus that might explain the generation of pain under loads (Jaumard et al. 2007; Dynamic Disc Designs 2015). On the other hand, cadaveric specimens incorporate true information about disc anatomy and physical properties, but they provide limited information about specific points inside disc tissues, e.g. boundary annulus-nucleus, also the cadavers have availability problems, and as the animal models, their cost is high. The overall problem of experiments with synthetic and cadaveric materials is that only anatomical and biomechanical information is provided. Biological processes, e.g. nutrition cannot be included. Organ culture experiments allow having a high control of mechanical and chemical boundary conditions while keeping the mechanics of the tissues in situ. However, the setting of such experiments is complicated because of the inhomogeneity of the disc tissues and the swelling of the nucleus, in consequence there are few studies published in the literature.

In silico models consist in the numerical resolution of mathematical models that describe, e.g. the physico-chemical processes operating in the spine, via computer simulation. The use of complex computer models allows obtaining information on the properties of each component involved in disc degeneration system and on their interplay, e.g. between matrix degeneration and nutrition. Moreover, computational models have limitations related to the control of both the modelling approximations, and the impact of the latter on the simulation results. Accordingly, the validation of the calculations obtained by the models against experimental data is utmost important but challenging at the same time.

Moreover, the reproduction of the continuous changes that occur within the complex biological system of the human disc is a challenge for computational models, as well as the definition of boundary conditions,. Nevertheless, the recent advance in computational power allows the development of mathematical description of multi-physics processes that occur inside the disc. Such capacity will be exploited along the development of the present thesis.

1.2 The aim and outlines

The main aim of this thesis is the study of how intervertebral disc mechanics and tissue condition interact with disc cell nutrition, in order to achieve better understanding of the role of nutrition in disc degeneration. To achieve this aim, a composition-based intervertebral disc finite element model will be used so as to gain an educated approach for the simulation of degenerated tissues. Such a model will be used to simulate the nutrient transport, cell metabolism and cellular activity, including relations to tissue maintenance. Also, during the development of this study several points are addressed.

First, the control of the calculation time and solution stability is important for multiphysics problem simulation, and will be addressed. Second, disc tissue degeneration involves multiple changes in terms of composition and multiphysics interactions. For this reason, the influence of extracellular matrix degeneration on cell death will be evaluated, based on tissue composition measurements. Third, the depletion of proteoglycans is often as one the most important change during disc degeneration. Thus, the interaction between such loss and nutrition along disc degeneration will be studied. Finally, the cartilage endplate is recognized as an important component for disc nutrition. However, the role of the cartilage endplate degeneration on the mechanobiology of the rest of the disc remains underexplored, and will be studied. According to these specific objectives, this doctoral thesis has the following structure:

- Chapter 2 presents a brief description of the anatomy, biology, biomechanics and mechanobiology involved in the intervertebral disc to introduce the biological frame of this study. Also, previous numerical models and their contributions to the study of disc degeneration will be

described so as to highlight the strengths and limitations of theoretical modelling.

- In Chapter 3, the calculation time needed to achieve the stability of poromechanical disc models will be explored. This issue is relevant for the simulation of the disc processes, and might provide guidelines for the creation and the use of geometrically nonlinear poromechanical models.
- Chapter 4 presents a sensitivity study to identify the disc composition parameters that influence most the metabolic transport and cell viability. A relationship between disc extracellular matrix changes and nutrition will be developed in this section.
- In Chapter 5, the update of proteoglycan content due to ageing and nutrition environment, a crucial aspect in disc degeneration, will be simulated. The model will take in account the competition between the production rate and half-life of proteoglycans, and it will consider the variation of production rate according to the oxygen levels. The proteoglycan turnover model will be included in the transport-composition-based disc model to study the influence of time-related matrix changes on disc nutrition.
- Chapter 6 is dedicated to the evaluation of the effect of the cartilage endplate composition on disc hydration. A composition-based permeability formulation will be presented and used to study the influence of the cartilage endplate composition on disc nutrition and degeneration under different loading conditions.
- Chapter 7 presents the general discussion and conclusions of this thesis.

2 STATE OF ART

2.1 The spine

The human spine is a skeletal structure composed by five distinct sections: the cervical spine (C1-C7), the thoracic spine (T1-T12), the lumbar spine (L1-L5), the sacrum (S1-S5) and the coccyx (Figure. 2.1). The spine provides protection to the spinal cord and gives a structural support to the body. The spine section that supports the highest mechanical loads is the lumbar spine. In fact, the amount of loads including the action of the muscles that affect this section is higher than 55% of the total body mass.

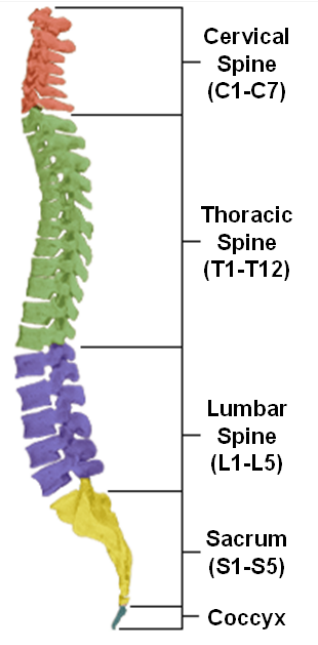

Figure 2.1: General representation of the spine sections (Adapted from http://www.nphonssketletal4.wikispaces.com)

The functional unit of the spine is the motion segment. As such, there are 24 motion segments in the spine. Each motion segment contains two vertebral bodies and an intervertebral disc (IVD) in between (Figure 2.2) (Roberts & Urban 2011). In general, the discs represent one-third of the total spine height. They are also an important structure of the spine because they provide flexibility and transmit the loads through the whole spine (Roberts & Urban 2011). Furthermore, the spine degenerative diseases are frequently related with the intervertebral disc.

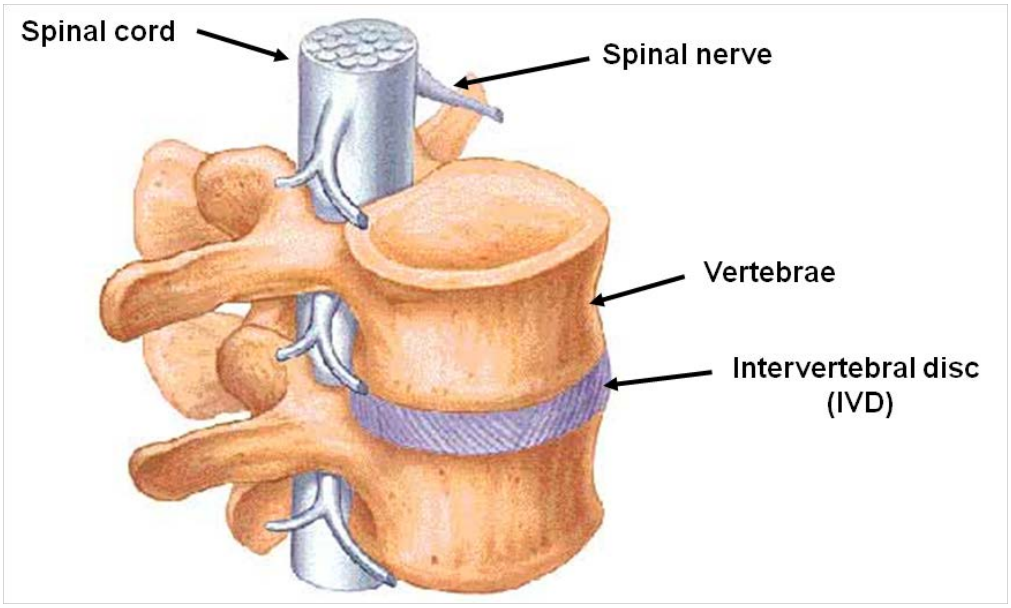

Figure 2.2: Scheme of a spine motion segment (Adapted from http://umm.edu/programs/spine/health/guides/anatomy-and-function)

2.2 Intervertebral disc anatomy

The intervertebral disc is a heterogeneous and fibrocartilaginous structure (Setton & Chen 2004; Cassinelli et al. 2001). It is composed of four distinct regions: the outer layer is the annulus fibrosus (AF), a region that surrounds a gel-like inner region known as nucleus pulposus (NP). A transition zone (TZ) connects AF and NP (Figure 2.3a), and the cartilage endplates (CEP) confines the NP and the inner AF at the top and bottom of the disc (Figure 2.3b)(Roberts & Urban 2011; Raj 2008; Cassinelli et al. 2001; Guilak et al. 1999; Chen et al. 2002). Although all disc tissues are structurally and mechanically different, together they form an integral unit that contributes to the functional mechanics of the whole disc (Setton & Chen 2004).

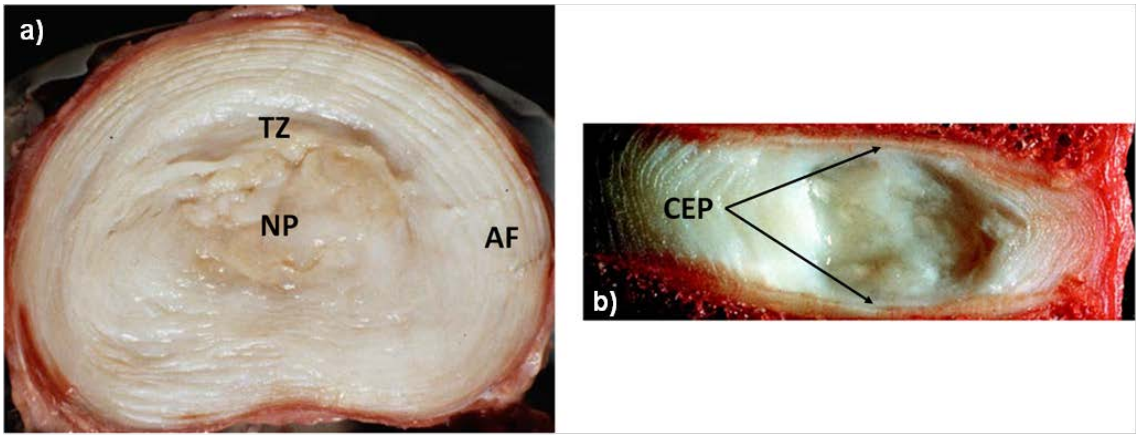

Figure 2.3: Middle-aged healthy human lumbar disc: a) sectioned in the transverse plane, showing the nucleus (NP), the annulus (AF) and the transition zone (TZ) (Top: anterior part of the disc) and b) sectioned in the sagittal plane, showing the cartilage endplates (CEP) (Left: anterior part of the disc) (Adapted from Adams et al. 2014)

2.2.1 Nucleus pulposus

The nucleus pulposus is a gelatinous and, at the millimetric scale, isotropic tissue that has a high content of water, negatively charged proteoglycans, collagens fibres randomly organized, and non-collagenous proteins (Raj 2008; Setton & Chen 2004). The high concentration of proteoglycans attracts molecules of water and gives the nucleus its swelling capacity (see Donna effect in section 2.3.1). The swelling pressure helps to pressurize the interstitial fluid that allows the confined nucleus to support compression loads (see section 2.5)(Figure 2.4)(Urban et al. 1979).

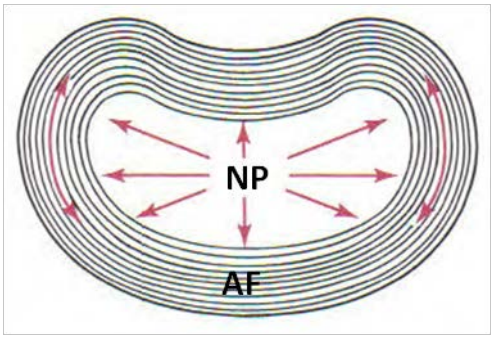

Figure 2.4: Swelling pressure distribution within the nucleus pulposus (NP) (Adapted from Neumann 2009)

2.2.2 Annulus fibrosus

The annulus fibrosus is a lamellar and fibrocartilaginous structure that consists in a series of 15 to 25 concentric layers or lamellae. Each lamella contains

collagen fibres that are parallel to each other (Raj 2008; Setton & Chen 2004). These fibres are oriented at 28º to 43º to the vertical axis, and are organized in a criss-cross manner from one lamella to another (Figure. 2.5). This organized structure gives the annulus its functional anisotropic behaviour, especially under tension, axial rotation and compression (see section 2.5) (Noailly et al. 2011).

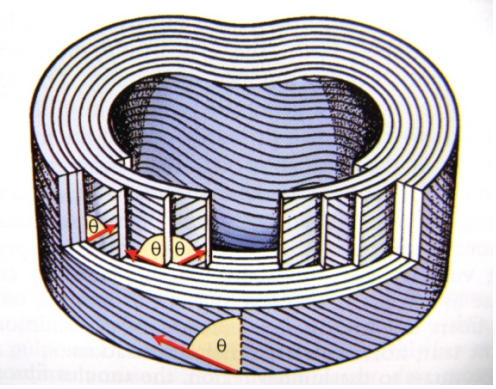

Figure 2.5: Annulus fibrosus (AF) lamellar structure (From Neumann 2009)

2.2.3 Transition zone

The transition zone is a thin region composed by fibrous tissue located between the annulus fibrosus and the nucleus pulposus (Figure 2.3). This zone presents local differences in disc biosynthesis according to observations *ex vivo*, in explants cultures, and in isolated cells. Such differences define the transition zone as the zone of greatest proteoglycan and protein biosynthesis compared to AF and NP zones (Guilak et al. 1999; Cassinelli et al. 2001; Chen et al. 2002).

2.2.4 Cartilage endplate

The CEP is a hyaline cartilage situated at the top and bottom of the disc. Generally, its thickness is not larger than 1 mm. This tissue contains collagen fibres that are arranged horizontally and parallel to the vertebrae (Figure 2.6) (Raj 2008). The cartilage endplates are believed to play a key role in the regulation of the diffusion of nutrients and waste products between the disc and the vertebrae (Setton & Chen 2004). Also, they contribute to the intradiscal fluid pressurization (see section 2.5) and it is thought that they keep the hydration of the nucleus thanks to specific balance between the distributions of porosity and permeability (see section 2.5)(Setton & Chen 2004).

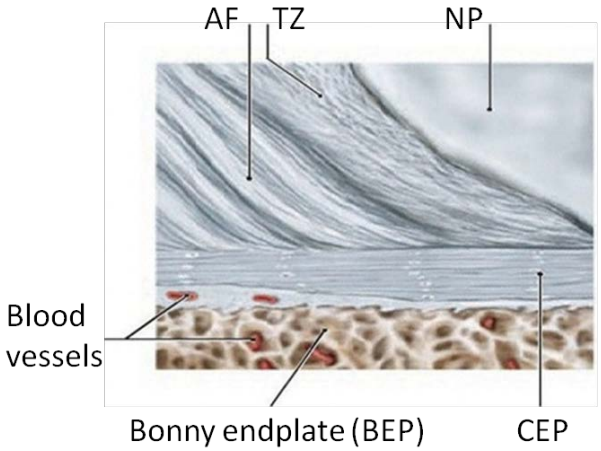

Figure 2.6: Cartilage endplate (CEP) (Adapted from http://o.quizlet.com/B8QBj4JYL3CY8KUAwNVGyQ.jpg)

2.3 Intervertebral disc biochemistry and multiphysics

The biochemistry and the ultrastructure of the extracellular matrix regulate the mechanical functions of the intervertebral disc (Raj 2008; Setton & Chen 2004). As a result, the principal disc tissues, e.g. the annulus and nucleus, provide the main mechanical function. Both tissues have the same biochemical components i.e. water, collagen and proteoglycan. However, the variations of relative contents and organization of such components make annulus and nucleus different (Figure 2.7)(Raj 2008; Schroeder et al. 2010).

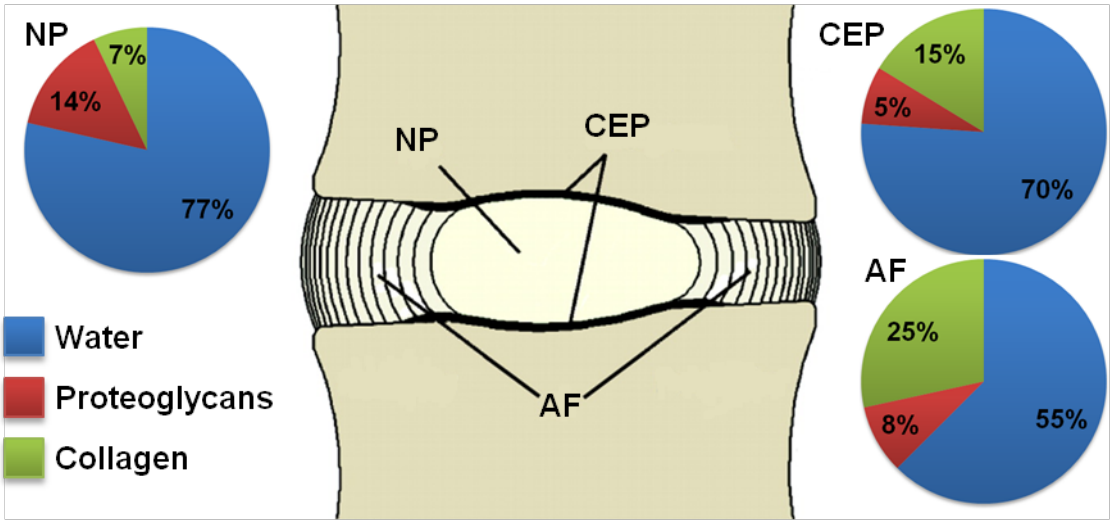

Figure 2.7: Biochemical composition of disc tissues (Adapted from Smith et al. 2011)

2.3.1 Proteoglycans

The aggrecan is the principal proteoglycan inside the intervertebral disc. It has a main protein core that has glycosaminoglycans attached (Figure 2.8) (Roberts & Urban 2011). The Donnan effect describes the equilibrium between two solutions that are separated by a semi permeable membrane that allows the pass of some ions through it. To illustrate this effect let suppose that in one side of the membrane there are a negatively charged electrolytes. Meanwhile, some of the positive ions of the solution of the other side pass through the membrane to equilibrate. In the case of the disc, the molecules of water enter inside the disc to equilibrate the negative charge of the proteoglycans, as such, a gradient of pressure is formed and the disc swells. As a result of the swelling, the proteoglycans provide hydration to the disc because they can capture large amounts of water. Moreover, proteoglycans also regulate the movement of molecules through the disc matrix (Maroudas 1968; Urban et al. 1979; Huyghe et al. 2003). The amount of proteoglycans in the nucleus is close to 15% of wet weight, and it is higher than in the other disc tissues, around 8% and 5 % for the annulus and cartilage endplates respectively (Roberts & Urban 2011; Raj 2008).

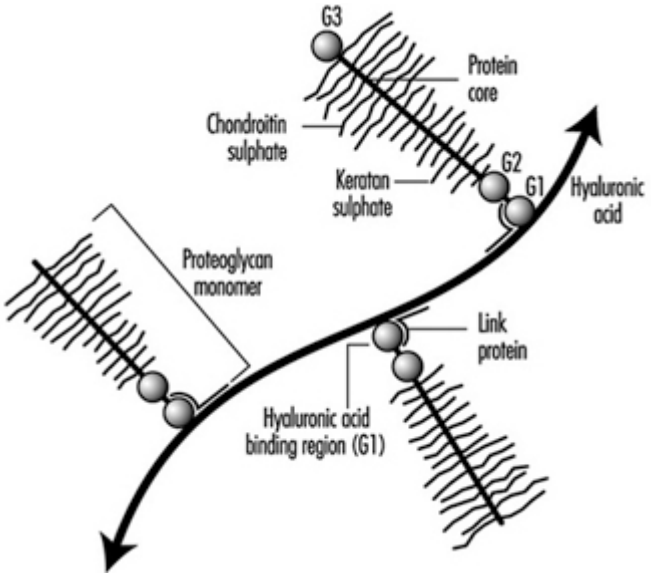

Figure 2.8: Proteoglycan aggregate (Roberts & Urban 2011)

2.3.2 Collagen fibres

Collagen is the most important structural protein of the disc and all connective tissues. Although there are many types of collagen, all of them have a

crosslink triple helix structure. This structure not only gives strength to the disc, so as to support very well tensile loads (see section 2.5), but also makes the attachment between disc and bone (Roberts & Urban 2011; Raj 2008). The outer annulus contains predominantly type I collagen forming oriented bundles (Figure 2.9). These bundles in the inner annulus are thicker than in the outer and the quantity of collagen II increases toward the disc centre (Eyre et al. 1988; Marchand & Ahmed 1990). Also, the nucleus and cartilage endplates contain predominantly type II collagen that forms crosslink networks (Roberts & Urban 2011). Moreover, the collagen fibres of the annulus are much thicker than the fibres of the nucleus (Roberts & Urban 2011).

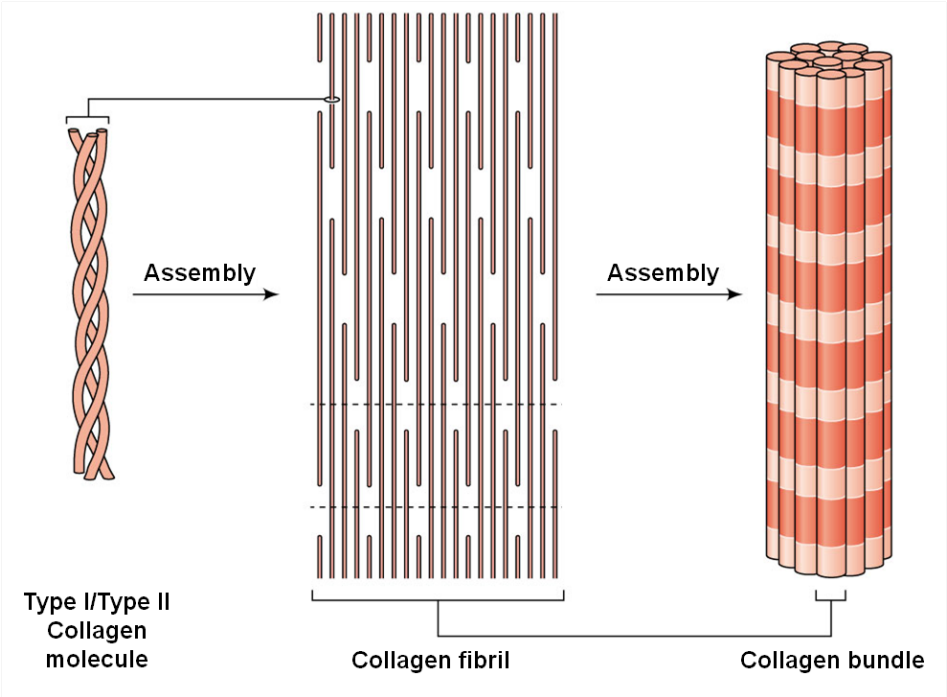

Figure 2.9: Collagen bundle (Adapted from http://pixgood.com/collagen-structure-triple-helix.html)

2.3.3 Water

Water is the principal component of the intervertebral disc. The amount of water in the disc ranges from 65 to 90% of the total volume of the tissue depending on the age of the person and the disc area (Roberts & Urban 2011). The water content of disc matrix has a direct proportional relationship with the amount of proteoglycans. Also, the application of mechanical loads to the disc makes intradiscal water be expelled out of the organ as tissues consolidate (Roberts & Urban 2011). Furthermore, the water content is very important for

both the mechanical functions of the disc and the transport of nutrient through the extracellular matrix (Roberts & Urban 2011). In relation to tissue multiphysics, the total amount of water is the sum of two parts: the intrafibrillar water (IFW) and the extrafibrillar water (EFW) (Sivan et al. 2006a). The IFW fills the space between the collagen fibres, from which proteoglycans are excluded. In contrast, the EFW is the water in contact with the proteoglycans. Whereas the IFW is important in the annulus because it may represent up to 30% of its total fluid, the EFW is crucial for the osmotic pressure present in the nucleus (Sivan et al. 2006a).

2.4 Intervertebral disc biophysics

There are several cell populations in the different regions of the disc. Whereas the outer annulus presents elongated and fibroblast-like cells, the transition zone and nucleus have spheroidal chondrocyte-like cells (Figure 2.10) (Buckwalter 1995). Finally, the cartilage endplate cells are rounded chondrocytesm (Maroudas et al. 1975). The cell type in the annulus and cartilage endplates does not significantly change along life-time. However, notochordal cells present in the nucleus in early life decreased fast until they disappear at the age of 4-10 years (Wolfe et al. 1965; Pazzaglia et al. 1989). Meanwhile, the nucleus is populated progressively by chondrocyte-like cells that might come from the inner annulus and the cartilage endplates (Kim et al. 2003).

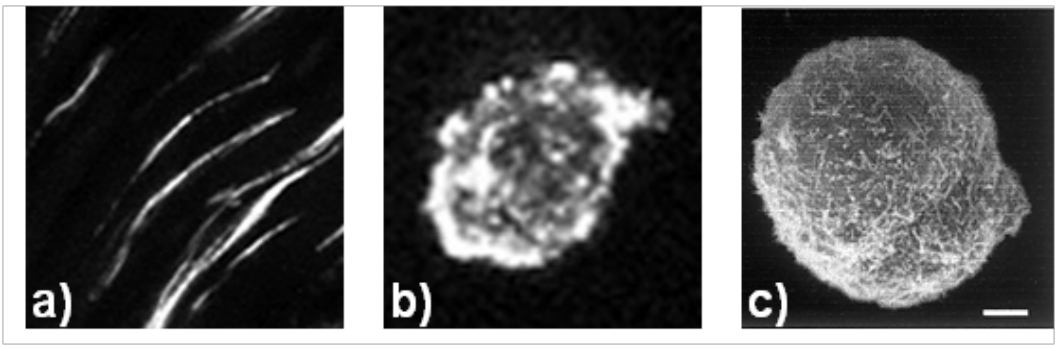

Figure 2.10: Disc cell population at: a) the outer annulus, b) the transition zone, and c) the nucleus (Adapted from Guilak et al. (1999) and Bruehlmann et al. (2002))

The amount of cells inside the disc is low and heterogeneous (Maroudas et al. 1975; Bibby et al. 2001; Roberts & Urban 2011). There are more cells in the outer annulus and cartilage endplates than in the nucleus. Furthermore, the cell density in the cartilage endplate and in the annulus is about four and two times

higher than in the nucleus, respectively. Cell concentrations in the annulus and cartilage endplates are due to their proximity to the disc nutrition supplies, i.e. the peripheral vasculature (Maroudas et al. 1975).

Although the number of cells is reduced in the disc, cell activity maintains the cell density levels constant, depending on the period of time considered. Actually, a study from Liebscher et al. (2011) suggests that disc degenerative changes are possible consequence of the loss of cell functionality rather than the loss of cells itself. Horner et al. (2002) found that the production rates of glycosaminoglycans were higher for nucleus cells than for the annulus cells. The same study reported that collagen rate of production by cells is low in all disc tissues. Additionally, disc cells also produce proteinases, e.g. aggrecanases and matrix metalloproteinases (MMP), that break down continually the components of the matrix (Sztrolovics et al. 1997; Weiler et al. 2002). Also, soluble mediators, e.g. growth factors and cytokines can regulate disc cell activity (Shinmei et al. 1988; Thompson et al. 1991). Both mechanical factors, e.g. hydrostatic pressure, and nutrient supply, e.g. glucose environment, influence the cell activity as well (Urban et al. 2000; Horner et al. 2002; Bruehlmann et al. 2002)(see section 2.6).

The cellular processes maintain the homeostasis in the disc. As a result, they control the balance between the synthesis and turnover of matrix elements, e.g. collagen and proteoglycans (Shankar et al. 2009). The study of Sivan et al. (2008) revealed that the average half-life of collagen in healthy disc is a decreasing function of the age. They found that the collagen half-life between ages 20 and 40 is about 95 years and between ages 50 and 80 is about 215 years. Moreover, the half-life of aggrecan is shorter than the one of collagen. Indeed, for healthy discs the half-life of aggrecan is about 13 and 14 years for the annulus and nucleus respectively (Sivan et al. 2006b). A possible explanation of the significant difference between the half-lives of collagen and proteoglycans is the fact that aggrecan structure is less compact making it more susceptible to proteolysis (Sivan et al. 2008). As mentioned before, the balance between cell-mediated synthesis and breakdown keeps the disc healthy. As such, if the rate of breakdown increases over the synthesis, the matrix of the disc will disintegrate and the disc would degenerate (Urban et al. 2000).

2.5 Intervertebral disc biomechanics

The intervertebral disc is part of a complex load-bearing system. In such system, the principal functions of the disc are: to provide six degrees of freedom of mobility and to transmit loads from one vertebra to the next one (Bogduk 2005).

As mentioned in the sections 2.2.1 and 2.3.1, the proteoglycan content of the nucleus generates an osmotic pressure. This pressure stretches the fibres of the annulus that are around (See Figure 2.4). On the other hand, the CEP is suggested to act as a valve characterized by a direction-dependent resistance of the fluid flow, where the resistance to the flow out of the disc is higher than the resistance to the flow in (Ayotte et al. 2001). Such direction-dependent flow resistance has been suggested as a mechanism to ensure the complete recovery of fluid during rest (Ayotte et al. 2001). The exchange of fluid in and out might be important for disc nutrition (see section 2.6.1).

Thanks to its lamellar structure, the annulus described in section 2.2.2 is capable to supporting tractions and shear loads, and to transmitting these loads from one vertebra to the next by itself (Bogduk 2005). The traction and shear loads are generated by: rotational deformations of the spine segments, and also because the NP presses the AF wall. Also, an experimental study showed that the disc maintains the same compressive stiffness when the nucleus is removed (Markolf & Morris 1974). However, when the annulus is subjected to a sustained weight-bearing, it will tend to deform. Also, the prolonged pressure makes the collagen fibres to bulge and the water flows out reducing the annulus height. To prevent annulus prolonged deformation the nucleus provides mechanism of reinforcement (Bogduk 2005). In addition, the nucleus when is subjected to a compression load reduces its height and expands radially. Such expansion produces a pressure on the annulus and stretches the collagen bundles outward, that due to their tensile properties resist this pressure (Figure 2.11). Additionally, when the nucleus expands use energy to stretch the collagen fibres of the annulus. The fibres store that energy that returns to the nucleus when the load applied is released. Also, the nucleus also exerts pressure on the CEP (Bogduk 2005). Also, the pressure applied to the CEP transmits part of the load applied from one

vertebra to the next one. In consequence, there is a high tissue consolidation in the CEP that might contribute to the valve effect.

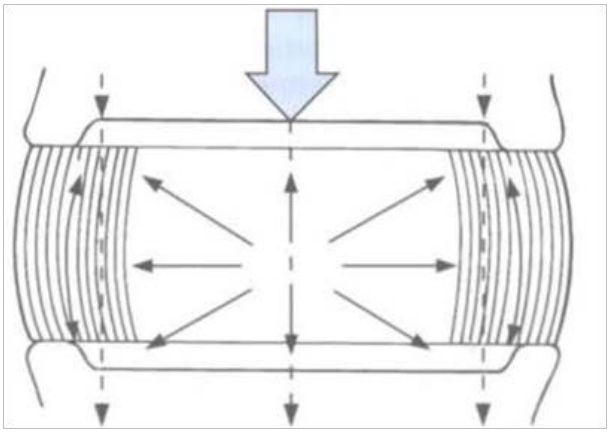

Figure 2.11: Disc load distribution under compression (Bogduk 2005)

In shear movements, all the point of one vertebra moves in parallel to those in the next vertebra (See Figure 2.12). The annulus resists to this movement but the fibres action depends on their location relative to the direction of the movement. For example in forward shear, annulus fibres oriented in direction of the movement stretch because their attachment points separate. As a result, those fibres contribute to resist the shear. On the other hand, the other annulus fibres oriented opposite to the movement are not affected because their attachment points get close (Figure 2.12a)(Bogduk 2005).

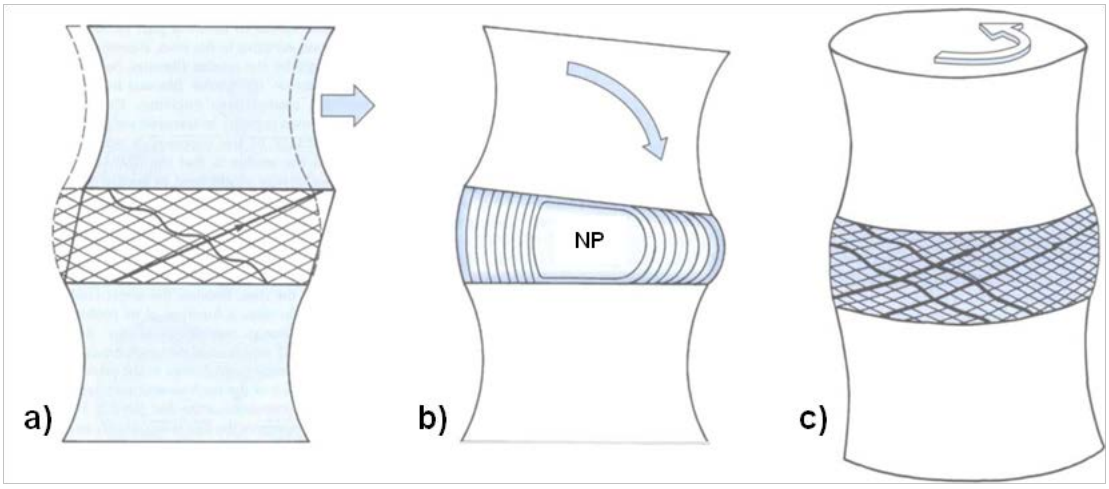

Figure 2.12: Examples of intervertebral disc movements: a) shear forward, b) bending, and c) twist (Adapted from Bogduk (2005))

Bending movements consist of lowering one rim of a vertebra and raising the opposite rim of the same vertebra (See Figure 2.12b). In the case of flexion, the

anterior part of the disc lowers while the posterior part rises. In consequence, the anterior annulus will be under compression and will tend to bulge (Brown et al. 1957; Shah et al. 1978; White & Panjabi 1978). Meanwhile, as the posterior part of the disc rises, the annulus fibres stretch. The anterior part of the nucleus also is compressed due to flexion, while the posterior nucleus is able to deform along the posterior AF (Bogduk 2005).

In axial rotation movements, all points at the lower surface of a vertebra moves in the direction of the twist (See Figure 2.12c). This movement has a particular effect on the annulus. Indeed, half of the lamellae of the annulus stretch, e.g. the ones with fibres that are inclined in direction of the movement, while the other half of lamellae are not affected by this movement.

Finally it was shown in this section that the disc can be subjected to a variety of loads, and that each tissue has a specific role to make the disc resist these loads. In section 2.4 it was mentioned that mechanical loads can affect disc cellular activity. This influence will be addressed in the next section.

2.6 Intervertebral disc mechanobiology

The disc cells respond to the stimuli that come from the mechanical loads. Indeed, cells convert those stimuli into biochemical signals and integrate them into cellular processes. There are four steps that cells follow to react to mechanical signals: mechanical coupling to matrix, mechanotransduction, intracellular signal transmission and cell response (Lotz & Hsieh 2014).

Cellular load transducers including integrins, ion channels, G protein-coupled receptor and tyrosine kinase receptors make easy the mechanical coupling to matrix (Lotz & Hsieh 2014). Integrins are important for the interactions between the cell and the extracellular matrix. They also regulate the cell survival, adhesion, cytokine responses, and mechanobiology (Setton 2005). Within the disc, there are some integrins that interact with the collagen, laminin and fibronectin of the cells. Moreover, they participate in the mediation of the cell adhesion to matrix substrates that are similar in annulus and nucleus cells (Setton 2005). On the other hand, another disc integrins present in fibroblast and chondrocytes help to obtain different mechanobiological responses in distinct disc areas (Setton 2005).

Mechanotransduction consist in the conversion of mechanical stimuli into chemical signals (Tsai et al. 2014). Such conversion occurs when the forces applied to the extracellular matrix are coupled to the cytoskeleton, inducing changes of intracellular proteins that affect substrate availability leading to phosphorylation (del Rio et al. 2009; Doyle & Yamada 2010).

The signals are transmitted within the cell by cytoskeletal filaments, e.g. F-actin, intermediate filaments, e.g. cytokeratin, and microtubules, e.g. tubulin that connect cell nucleus to the extracellular matrix (Alenghat & Ingber 2002). In addition, cells mechanical properties change according to their cytoskeleton composition. In this sense, nucleus cells are stiffer and more viscous than annulus cells (Guilak et al. 1999). Also, the intracellular signal transduction can happen through the cytoskeleton, small molecules, and transcription factors (Lotz & Hsieh 2014).

The cellular response can occur at different timescales that can define the frequency-dependent behaviour of the cells. Whereas some forces generate an immediate response through activation of ion channels, other can take hours or days as they produce changes in gene expression that affect cytoskeletal or adhesion proteins, and finally the path of force transmission (Lotz & Hsieh 2014). Additionally, nucleus cells response to pressure depend on the magnitude, frequency and duration. If the pressure is physiological, i.e. less than 1 MPa, less than 3 Hz of frequency and less than 24 hours of duration, the response is anabolic, while pressures that are out of that range generate catabolic responses. On the other hand, the response of the annulus cells to cyclic shear is anabolic up to 1 or 2 days at low magnitude, i.e. less than 1% of strain, and physiological frequencies, i.e. 1 Hz (Lotz & Hsieh 2014).

There are two mechanisms of mechanotransduction: direct and indirect (Figure 2.13). Direct mechanotransduction affects cell shape, size, and/or pressure on the cell as shown in the previous paragraphs. Meanwhile, indirect mechanotransduction is an independent phenomena that may alter the fixed charge density, pH and nutrient transport (Iatridis et al. 2006). In addition, the latter mechanisms regulates the access of nutrient to the cells. Also, experimental evidence indicated that nutrient deprivation activate catabolic processes that affect disc matrix (Rinkler et al. 2010; Neidlinger-Wilke et al. 2012). Such

experiments highlight the importance of the study of the role of indirect mechanotransduction in terms of disc nutrition.

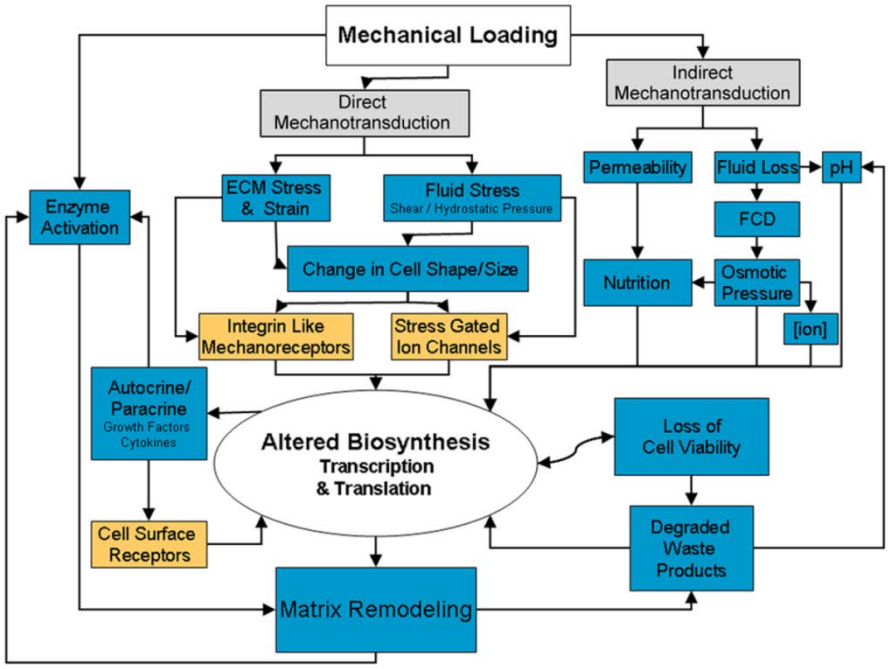

Figure 2.13: Mechanisms of mechanotransduction (Iatridis et al. 2006)

There are changes in the biology and the biochemistry of the disc in response to mechanical loads. Such changes may alter disc mechanical behaviour, and such alterations can play an important role in disc degeneration (Setton & Chen 2004). In addition, mechanical signals can alter the transport of nutrient that is necessary for the survival, and the activity of disc cells as showed in section 2.4. The transport of nutrient within the disc will be addressed in the next subsection.

2.6.1 Nutrition of the disc

The disc is the largest avascular tissue of the human body. As such, the blood vessels of disc borders are responsible for the supply of important nutrients to the disc, e.g. glucose, oxygen, and substrates for matrix production (Figure 2.14) (Urban et al. 2004). Within the disc, there are two mechanisms of transport of nutrient: convection and diffusion (Holm et al. 1981); being the last one the main mechanism (Urban et al. 1982). Also, the environment of nutrition of disc cells changes depending of the area of the disc. In fact, the cells in the centre of the disc have concentrations of oxygen and pH that are different from those cells at the borders (Holm et al. 1981).

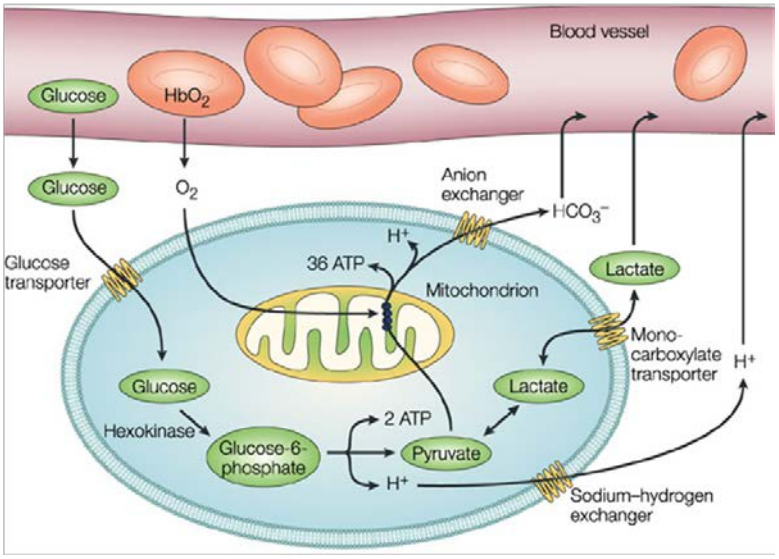

Figure 2.14: Scheme of cell nutrition (From Gatenby & Gillies 2004)

There are two possible routes for the transport of nutrients into the disc, and waste products out of the disc: the vertebral endplates and the annulus border, and the first one is the predominant path (Figure 2.15) (Holm et al. 1981; Ayotte et al. 2001; Urban et al. 2004). Also, it is suggested that any change in the vertebral endplate or in the blood supply has and important impact on disc nutrition (Urban et al. 2004). For instance, an experimental study showed that the inhibition of the vertebral endplate perfusion can obstruct the solute transport into disc nucleus (Van Der Werf et al. 2007). Moreover, both solute size and charge are important to the nutrient transport across the matrix, but most important is that disc pathology might affects the supply of solutes (Urban et al. 2004).

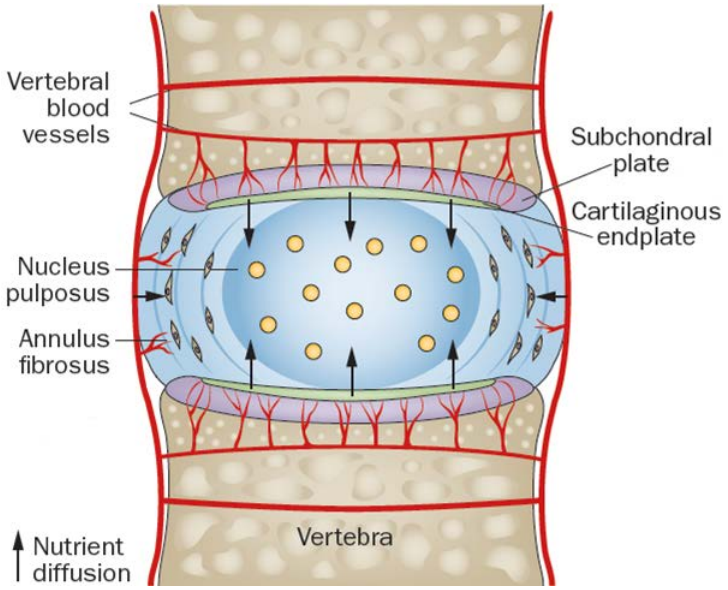

Figure 2.15: IVD blood supply (Adapted from Huang et al. 2014)

There is scarce information about the nutrition via annulus margins. Nevertheless, it is known that the blood vessels irrigate well this annulus zone. Also, different arteries supply the outer zone of the vertebral body, the mid-annulus zone, and the central core of the vertebral body, and the lumbar vertebrae have the lowest blood flow (Drescher et al. 2000). These arteries also provides nutrient to the disc via the capillaries present in the vertebral endplate (Crock & Goldwasser 1984). Additionally, there are muscarinic receptors in those capillaries that might regulate the blood flow in response to external signals (Wallace et al. 1994). Also, the amount of these capillaries decreases progressively from the centre of the endplates to the apophyseal ring, where they completely disappear (Urban et al. 2004).

The CEP can operate like a permeable selective barrier that limits the movement of nutrient from one side to the other. Also, they might be involved in the reduction of hydration and the increase in the content of proteoglycan (Urban et al. 2004). The diffusion of small, e.g. oxygen and glucose, across the cartilage endplates is easy. However, large solutes, e.g. growth factors and matrix macromolecules are excluded from the matrix, and the increment of the molecular weight and the aggrecan concentration increases the degree of exclusion (Roberts et al. 1996). Moreover, changes in the permeability of the cartilage endplates might affect the transport by convection via the fluid flow, though there is no clear consensus in the literature about this idea.

During the daily loads, the disc expels a large amount of fluid that is recovered along the night rest (McMillan et al. 1996; Malko et al. 2002). In addition, the transport of solutes into the disc is slow. In fact, the solutes can reach the centre of the nucleus in about 6 hours (Rajasekaran et al. 2004). As for the effect of mechanical loads, 4.5 hour of sustained creep loading decreased the diffusion of nutrient into the disc (Arun et al. 2009).

Solutes properties and matrix composition are factors that control the movement of the solutes along the disc. Within the matrix, a dense gel of proteoglycans contains the collagen network. The proteoglycan network might regulate the size of pores available in the tissue. For example, if the concentration of proteoglycan increases, the average pore size might decreases (Grunhagen et al.

2011). However, the influence that changes in disc composition have on the transport of nutrient remains unclear.

In a regular diurnal cycle, the disc can lose and regain more than 20% of its height possibly affecting the diffusion of nutrient. Indeed, the loss of fluid generates an increment in the proteoglycan density, leading to a reduction in the solute diffusivity. Yet, the reduction of the disc height can increase the rate of nutrient transport to the disc centre (Grunhagen et al. 2011), and increased proteoglycan densities increase the osmotic forces. Overall, proteoglycan depletion is expected to influence disc nutrition under mechanical loads, but there is poor information in the literature about such influence.

In addition, the cellular activity, especially the production of matrix macromolecules, depends on the maintenance of the levels of nutrient and metabolites. For example, the reduction of the oxygen content, pH levels or glucose might lead to the decrease in the production of sulphated glycosaminoglycans and matrix gene expression (Ishihara & Urban 1999; Razaq et al. 2003; Rinkler et al. 2010). Also, nutrient concentration can depend on the rate at which cells consume oxygen and nutrients, e.g. glucose, and produce lactic acid. For instance, all disc cells consume sulphate to produce sulphated glycosaminoglycan side chains of proteoglycans (Grunhagen et al. 2011). Nevertheless, the rates of sulphate incorporation are low compared with the concentration of sulphated available, thus, the cellular activity do not affect the sulphate concentration. In the case of the glucose, although concentrations and diffusivities of glucose and sulphate are similar, the cells consume glucose at rates that can deplete them from the centre of the disc. Finally, the rate of nutrient consumption and lactate production can be altered by other factor, e.g. the presence of cytokines and growth factors, mechanical stress and solute levels (Grunhagen et al. 2011).

2.6.2 Cell viability

The equilibrium between nutrient supply and nutrient consumption within the disc is precarious, and any disruption is thought to reduce the amount of viable cells responsible of maintaining a functional matrix (Jünger et al. 2009). Additionally, necrosis and programmed cell death (PCD) are the main types of cell death in the disc. Also, PCD can be divided in type I and type II. Apoptosis is type I

PCD, and is indentified by chromosomal concentration, cell contraction, DNA degradation, apoptotic body formation, and it depends on the participation of caspase. On the other hand, autophagic cell death is PCD type II, which has not dependence on the participation of caspase and it is identified by the emerging of autophagosome (Lockshin & Zakeri 2004; Klionsky 2005).

Cell death and disc degeneration were both associated with vertebral endplates trauma (Cinotti et al. 2005; Haschtmann et al. 2008). The obstruction of the marrow spaces might generate the loss of contact between the capillaries and the CEP, affecting the diffusion of nutrient to the disc (Huang et al. 2014). Additionally, changes in the structure of the cartilage endplate due to ageing and change of matrix due to calcification might reduce the fluid flow into the disc (Rajasekaran et al. 2004). On the other hand, damage to cartilage endplate would disrupt the permeable barrier and cause abnormal diffusion to the nucleus. This damage also can make the cartilage endplate more porous; allowing the loss of proteins in the matrix; possibly leading to disc degeneration (Buckwalter 1995). In addition, the cartilage endplate has a gradient of composition which effect on disc cell nutrition and viability is unclear

The effect of nutrient supply on cell viability was experimentally studied by Horner & Urban (2001). They cultured nucleus cell from bovine disc in agarose gels diffusion chamber. They found that cells close to the nutrient supply remained alive while the cells die at the centre of the diffusion chamber. This results indicated that the longer is the distance from the nutrient supply the lower is number of viable cells (Figure 2.16). In addition, disc cells die when there is not glucose or the environment has acid pH. Although cells remain alive for more than 13 days when the oxygen content was nil, the lack of oxygen led to a low production of proteoglycans (Horner & Urban 2001). Hence, a fall in the supply of nutrient decreased the amount of viable cells, and that nutrition constraints regulate the cell density. According to the diffusion chamber experiments, disc cell density had an inverse relationship with disc height (Rodriguez et al. 2011).

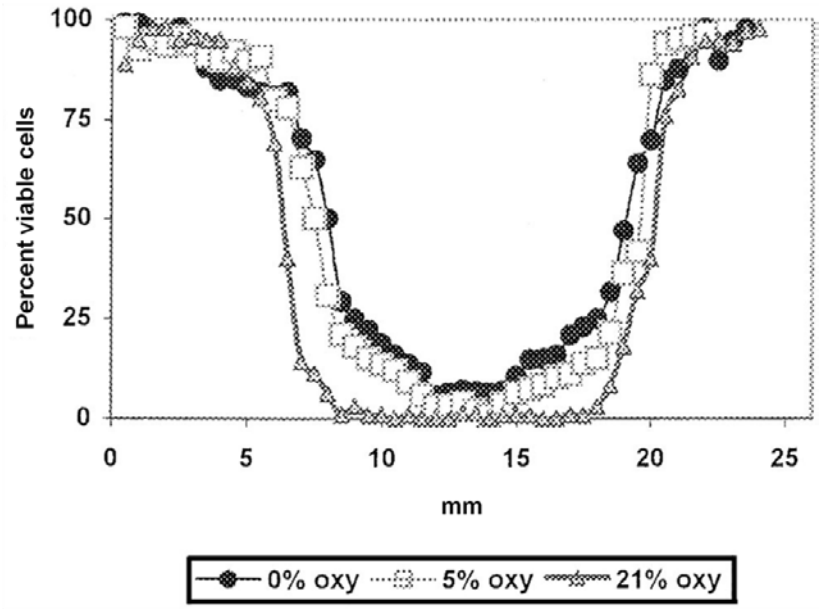

Figure 2.16: Effect of the oxygen on cell viability (From Horner & Urban 2001)

Jünger et al. (2009) explored the effect of limited nutrition on disc cells embedded in their native tissue in short- and midterm whole organ disc culture. They cultured ovine disc for 7 and 21 days under simulated physiological loads. They found that the cells remained alive up to the 21 days of culture when the glucose content was sufficient. Nevertheless, when the glucose levels were limited for 7 days, the cell viability decreased to 60% in the annulus and to 50% in the nucleus, and remained so until 3 weeks. In addition, the matrix production of the cells that remained alive did not compensate matrix breakdown in the time of the study.

The absence of glucose reduces the cell viability in the disc, independently of the oxygen content (Horner & Urban 2001; Bibby & Urban 2004). Additionally, the combination of low glucose and acid pH generates more cell death than when they are considered separately (Bibby & Urban 2004). Also, the production of lactate decreases when the pH is low after more than one day at low levels of glucose. This situation does not change as the oxygen content varies. As a result, the study of disc cell physiology should consider combined nutrient and metabolic environment instead of any single nutrient concentration (Bibby & Urban 2004).

The reduction of glucose in bovine nucleus cells downregulated significantly the gene expression of aggrecan, collagen type I and type II (Rinkler et al. 2010). It is suggested that glucose deprivation is more critical in gene

expression than mechanical loads (Rinkler et al. 2010). However, adequate mechanical loads might have a beneficial, yet limited effect on matrix turnover during disc degeneration (Rinkler et al. 2010). In addition, the simulation of degenerative glucose supply, oxygen, osmolarity and pH is suggested to influence the degradation of disc matrix through impairing matrix formation and supporting matrix degradation (Neidlinger-Wilke et al. 2012). The reduction in glucose and pH level produced the greatest effects, though the lack of glucose mainly affected cell viability, pointing out cell death as a possible important event in disc degeneration. The hydrostatic pressure had a little direct effect, however, it apparently counteracted matrix degradation by inverting or reducing the effect of some stimuli (Neidlinger-Wilke et al. 2012). Finally, as saw in the last two subsections the fall in disc nutrition and cell viability might have an important role in disc degeneration, the later will be addressed in the next section.

2.7 Intervertebral disc degeneration

As shown in Chapter 1, LBP is frequently related to disc degeneration. Disc degeneration is thought to start within the second decade of life, and it is considered as an inevitable consequence of ageing. However, whereas disc degeneration progresses slowly in some subjects, in others the destruction of the disc is fast (Antoniou et al. 1996). Moreover, disc degeneration can be defined as a cascade which begins with changes of the environment of the cells inside disc structure that progress over decades to structural breakdown and functional impairment (Urban & Roberts 2003; Freemont 2009).

During disc degeneration disc morphology changes, i.e. there is an increment in disorganization, when the degeneration and ageing increase (Figure 2.17), and also the differentiation between annulus and nucleus is less clear (Urban & Roberts 2003; Raj 2008). In this sense, the nucleus presents clefts after twenty years of life, and later these clefts lead to the generation of a fibrotic tissue as a natural attempt of repairing. Additionally, fissures in the annulus begin to appear at the third decade. Finally, in the fourth decade, the endplate reduces its thickness, and there is a development of clefts and fissures. Later, in the sixth decade, a fibrocartilagenous tissue replaces the endplate (Figure 2.18)(Shankar et al. 2009).

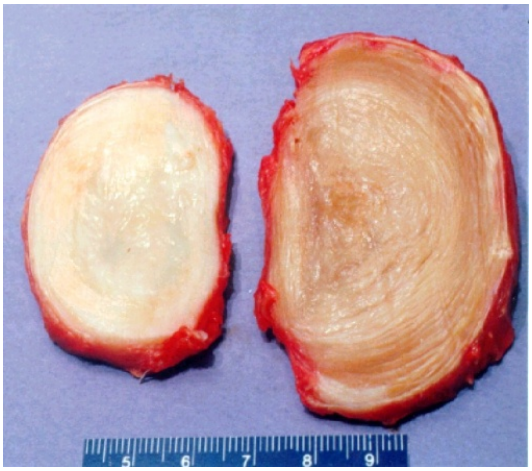

Figure 2.17: Healthy (left) and degenerate (right) human L2-L3 intervertebral disc (From http://www.emba.uvm.edu/~jiatridi/research/ratpack.jpg)

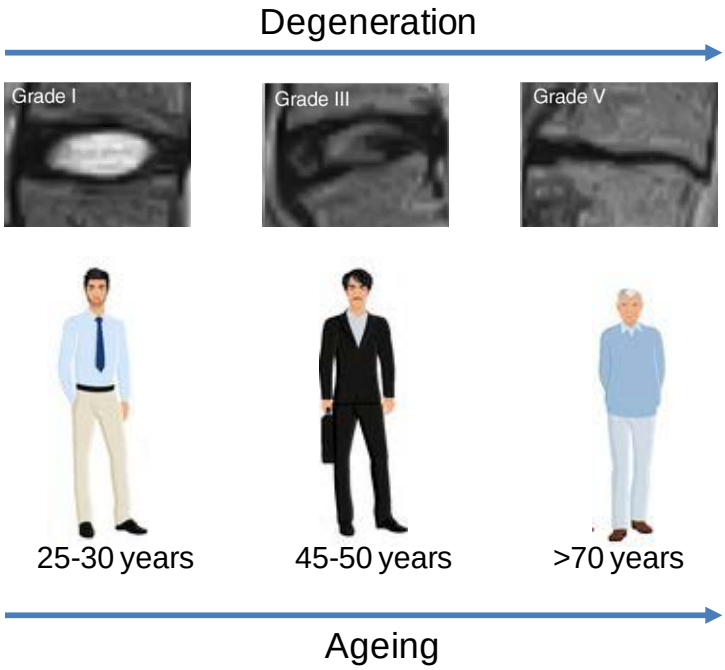

Figure 2.18: Evolution of disc degeneration with ageing (Adapted from Hangai et al. (2009))

A study of Antoniou et al. (1996) reported three phases of matrix turnover related to age and degeneration grade. The phase I, growth, is indicative of active synthesis of matrix molecules and active denaturation of collagen type II. The phase II, maturation and ageing, is characterized by a reduction in the synthetic activity and a progressive decrease in denaturation of collagen type II. The phase III, degeneration and fibrotic, there is a decrease in the synthesis of aggrecan and procollagen type II, as well as an increment in the denaturation of collagen type II and in the synthesis of procollagen type I, and the two latter depend on age and grade of degeneration.

Morphological and biochemical changes were evaluated along Thompson degeneration grades by Benneker et al. (2005). They found that in grade 1 discs, the nucleus is gelatinous with round or oval shape, the annulus has fibrous lamellae, the cartilage endplates are intact, and the vertebral body has rounded top and bottom margins. In grade 2 discs, the nucleus periphery appears fibrous, the annulus has mucinous material between lamellae, and the cartilage endplates are irregular. In grade 3 discs, the nucleus looks like a fibrous tissue and can invade the inner annulus, the annulus loses clear demarcation with the nucleus and presents concentric tears, and rim calcification and sclerosis are usually observed. In grade 4 discs, there are clefts parallel to the endplates, the nucleus can extend to the outer annulus. Finally, in discs grade 5, disc height is notably reduced, the nucleus disappears totally, and diffuse and severe sclerosis and calcification dominate.

The internal growth of nerves and blood vessels can appear during disc degeneration. Also, there is a local increment of cells in the nucleus that form clusters (Urban & Roberts 2003). Cell death also occurs in disc degeneration, and the cells that are around appear to be necrotic and apoptotic. As for concomitant tissue changes, Rodriguez et al. (2011) found that whereas with age and degeneration there is an increment in vertebral endplate permeability and porosity, the proteoglycan content decreases nonlinearly. They also found that there is an inverse correlation between disc cell density and disc height, and this correlation increases in the last stages of degeneration. Moreover, other studies suggest that changes in disc tissues can appear in a time-line sequence, i.e. the endplates change fist, then the nucleus and finally the annulus (Benneker et al. 2005; Shankar et al. 2009) .

The principal biochemical changes that might occur in disc degeneration are (Urban & Roberts 2003):

- *Loss of proteoglycan:* during disc degeneration proteoglycan loss is considered as the most important biochemical change (Lyons et al. 1981). As such, the degradation of the aggrecans leads to small fragments that can leach from the tissue more easy than the large fragments (Urban & Roberts 2003). As a result, there is a loss of glycosaminoglycans, the osmotic pressure falls and the tissue might dehydrate (Raj 2008).

- *Collagen changes:* the changes of collagen content are more difficult to observe than the changes of proteoglycans. In fact, whereas there are alterations in the collagen type and distribution, the collagen population remains almost the same (Urban & Roberts 2003). Also, there is an apparent competition between collagen loss and fibrosis, which remains poorly documented, however.
- *Increase in Fibronectin:* the amount and fragmentation of the fibronectin increases with disc degeneration (Oegema et al. 2000). In addition, these fragments limit the synthesis of proteoglycan and trigger the expression of inflammatory cytokines and matrix metalloproteinase (MMP) that can break down disc extracellular matrix (Raj 2008).
- *Enzymatic Activity:* the activity of the enzymes contributes to disc degeneration. In fact, it increases the fragmentation of the amount of collagen, proteoglycan and fibronectin (Raj 2008). Also, some enzymes, e.g. cathepsins, MMPs, and aggrecanases, may break down the components of the disc extracellular matrix (Urban & Roberts 2003).

The proteoglycan content loss affects the disc load-bearing system. Indeed, such loss generates the fall of the osmotic pressure and the disc cannot retain molecules of water when it is under compression (Urban & Roberts 2003). As such, degenerated discs have decreased water content and height, and lateral disc bulging increases under loads (Raj 2008). They lose the capacity to maintain the hydrostatic pressure under mechanical loads, and association between stress concentrations along the endplate or the annulus and discogenic pain has been proposed (Adams et al. 1996; McNally et al. 1996). However, how these changes might relate with disc cell nutrition and viability remains unclear.

The loss of height in degenerated discs has implications in LBP not only related to discogenic pain: it can produce abnormal loads at the adjacent apophyseal joints (Adams et al. 1990). Also, it can reduce the tensional forces on the ligament flavum which may produce remodelling and thickening of the ligament (Urban & Roberts 2003). As a result, the ligament can lose its elasticity and would tend to bulge into the spinal canal, leading to spinal stenosis (Postacchini et al. 1994).

2.8 Finite elements modelling in spine

Although experimental studies can provide a direct way to get information about the spine performance and biomechanics, they have the lack capacity of: a) integrate physical and biological information through experiments, b) explore spatial scale effects, e.g. cell, tissue, organ, for the study of specific mechanisms, and c) diversify the number of hypothesis to embrace the variability inherent to the problem studied. In this sense, numerical models have some advantages: first, they can generate and test infinite number and variety of specimens, second, the same specimen can be used for different load conditions and combinations, third, the specimen cannot be overload or damage, and last, the specimen can be modified to simulate any physiological condition (Fagan et al. 2002). But certainly, the most important asset of modelling it the integration of time and spatial scales, under multiple sets of hypotheses that can simulate either *ex vivo*/*in vitro* or *in vivo* conditions. Hence, simulation results can be used to interpolate and explain clinical and experimental evidences. Also, the models can provides: information about the stress distribution within the disc and the vertebral bodies, and also descriptions of the biophysical system that are impossible to obtain experimentally.

In the study of the spine, the finite element models can be used in four ways (Fagan et al. 2002):

- To evaluate the healthy spine,
- To evaluate the spine that is altered by disease, degeneration, trauma, ageing or surgery,
- To evaluate the spine with spinal instrumentation, and
- To assist in the development and design of that spinal instrumentation.

2.8.1 Elements to consider for computational studies

Anderson et al. (2007) reported that there are three critical aspects for computational biomechanics studies: verification, sensitivity analysis and validation. All of them are crucial for the acceptance of the results obtained from modelling in the medical and biomechanical communities.

A. Verification

Finite element model verification consists in the evaluation of numerical efficiency, i.e. how well the model replicates the solution of the equations that are behind it (Jones & Wilcox 2008). In this sense, the first verification that can be applied to the models is a convergence study and it should be done before validation (Noailly & Lacroix 2012a).

Mesh convergence

Finite element analysis consist in the integration of side by side equation solutions inside a simple geometry volume, called element. The constitutive law in the integration points of the element defines its behaviour (Noailly & Lacroix 2012a). Also, the density of the mesh regulates the efficiency of the simulation results, and the optimal mesh size can be obtained from a convergence study. In addition, mesh convergence usually address numerical and modelling issues that are well described in Noailly & Lacroix (2012a). Despite their importance, detailed convergence studies are rarely reported in the literature. As such, this aspect will be addressed in the Chapter 3.

B. Sensitivity analysis

The construction of an effective model and the interpretations of their outputs critically depends on how sensitive the model results are to the input parameters (Jones & Wilcox 2008). A sensitivity analysis can provide information about the accuracy of the input variable defined and how these variables might contribute to the overall error in the system. In addition, complex models usually need more exhaustive sensitivity analysis (Jones & Wilcox 2008). These kind of studies are vital in cases where the properties of the tissue are not well defined and when the simulations have complex coupled loads (Jones & Wilcox 2008). Sensitivity analyses are also particularly important when model validation cannot be done due to the lack of experimental data.

C. Validation

System validation shows that the model results are in agreement to the result in the real scenario (Jones & Wilcox 2008). Frequently, the validation of spine models is made comparing with experimental results. Such comparison does not warrantee that the model can represent the *in vivo* situation, since many *in vitro* models cannot replicate the *in vivo* conditions (Jones & Wilcox 2008). Nevertheless, the validation against *in vitro* experiment is a good first step. Also, it is suggested that there are two types of validation: direct and indirect (Jones & Wilcox 2008).

Direct validation

Direct validation consists in comparing the model calculations to an experimental test result when the model was created to replicate that experiment. As such, material properties and geometry of the model often come from the specimen of the experiment. With frequency, this kind of validation is done against experiment performed by the same or closely collaborating institution (Jones & Wilcox 2008). However, direct validation does not warrant that the model can be used for another purpose than the simulation of the reduced experimental system used for validation. As such, the whole concept of direct validation is therefore limited in the simulation of biological/complex systems.

Indirect validation

In the indirect validation, the model is compared to an experiment where it is unknown if the conditions of the experiment are the same used in the model. Most of the comparison with *in vitro* data reported in the literature, and also the comparison against historical medical data and clinical trial results are included in this type of validation (Jones & Wilcox 2008). In addition, the identification of mechanisms that might relate with measured evidences is the point of interest in this kind of validation. In this sense, interpretations, qualitative and comparative analyses become utmost important, in relation to model assumptions. At this point, sensitivity analyses are very relevant.

2.9 Intervertebral disc modelling approaches

2.9.1 Poro-hyperelastic models

The disc can be considered at the millimetric scale as a deformable continuous media, and simplifications that can be made in terms of disc material. For example, it can be considered a solid phase composed by macromolecules, e.g. elastine, proteoglycans and collagen, including cells, and a fluid phase composed by water and solutes. Therefore, in the biphasic mixture theory each part of the material is formed by two particles, fluid and solid (Mow et al. 1980). On the other hand, Biot poroeslastic theory considers each material part as a homogenized combination of solid and fluid (Biot 1941). Nevertheless, the two theories behave equal when it is assumed that fluid and solid component are incompressible (Simon et al. 1985; Huyghe & Janssen 1997).

The solid phase stiffness of the annulus and the nucleus in poroelastic models is that of a compressible drained porous skeleton, which can remarkably affect the prediction of disc mechanic (Malandrino et al. 2009). Porohyperelasticity considers the nonlinear effect of geometry that occurs under large deformations of the solid skeleton, and it is indeed an improvement of the poroelastic theory (Simon et al. 1998). The stress of the solid skeleton is derived from the strain energy function, and the Neo-Hookean formulation is the simplest form.

The anisotropy of the annulus is modelled by adding an anisotropic strain energy term. In addition, there are several forms of simulating fibre-matrix interaction (Caner et al. 2007; Reutlinger et al. 2014). The simplest one considers the fibres hyperelastic and perfectly linked to the matrix (Gasser et al. 2006). Another form considers the viscoelasticity of the annulus fibres (Schroeder et al. 2006; Schroeder et al. 2010)which is necessary to simulate short-term disc response under compression (Malandrino et al. 2015a).

The fluid phase affects the volumetric part of the total stress tensor, and it can be quantified by the pore pressure (Malandrino et al. 2015b). Also, to add the osmotic effect produce by proteoglycan describes in section 2.3.1, the pore

pressure is suggested to be the sum of a water chemical potential and an osmotic pressure gradient (Schroeder et al. 2006).

2.9.2 Electro-chemo mechanical models

The triphasic mixture theory describes the electro-chemical behaviour of the disc. A solute phase, e.g. nutrients and ions is added to the solid and fluid mixture. This theory assumes electrochemical equilibrium with the vascular osmolarity of disc outer boundary (Lai et al. 1991). In addition, the equations involved in the modelling of this theory are based on the equilibrium of linear momentum for the mixture and on the mass conservation of the phases or solutes (Malandrino et al. 2015b).

2.9.3 Cell nutrition and viability models

The simulation of indirect mechanotransduction requires the incorporation of the description of the anaerobic glycolysis to the models mentioned above. Bibby et al. (2005) gave one of the experimental bases for transport modelling. Additionally, previous studies found that: (a) lactate production was around twice the consumption of glucose, (b) lactate production and oxygen consumption were linked through pH and oxygen concentration, and (c) pH decreases with the concentration of lactate linearly (Bibby et al. 2005; Soukane et al. 2005). In terms of mechanical coupling, volume changes affect the distance of diffusion and the diffusive coefficients that are controlled by the porosity (Huang & Gu 2008; Malandrino et al. 2011). Nevertheless, a link between matrix degradation/production and tissue mechanical behaviour is missing. As such, the incorporation of matrix update would allow the further exploration of different processes related to disc degeneration.

The incorporation of cell death into the models was made firstly by Shirazi-Adl et al. (2010) and Jackson et al. (2011a). One major limitation of those models was the lack of time-dependency of cell viability, which allowed the resurrection of the cells when the solute concentrations increase above the critical values (Malandrino et al. 2015b). Later, Zhu et al. (2012) used the theoretical framework for microbial cell growth to define the rate of cell density change. This model eliminated the problem of resurrection but it did not consider the effect of

pH. Malandrino et al. (2014a) incorporate a constant death rate for the pH. The model predictions were in agreement with experimental findings (Malandrino et al. 2015a). Nevertheless, the effect of pH on cell death seemed nil compared to glucose deprivation, probably due to the low diffusion coefficient of the glucose. However, the influence of nutrient deprivation on disc mechanical behaviour that might be relevant for disc degeneration cannot be studied using the current mechano-transport coupling, indicating the need of a new approach to address such influence. Another point to consider, is the inclusion of the CEP composition in the mechano-transpot methodology, aspect that is important to evaluate the role of the CEP in disc degeneration.

2.10 Limitations of modelling

In disc poromechanical models, special care must be taken in the calculation of fluid pressures under velocities similar to the in vivo ones (Stokes et al. 2010). In addition, material parameters that come from optimizations can have no physical significance, e.g. negative values often do not have physical meaning (Noailly & Lacroix 2012a). On the other hand, the validation of transport and cell viability models is complicated since the experimental measurement of metabolic concentrations is a challenge and can produce data with noise (Bartels et al. 1998). Moreover, the experiment used to validate the cell viability model was done using nucleus cells only (Horner & Urban 2001), and the energy metabolisms of annulus and nucleus cells can be different (Salvatierra et al. 2011; Fernando et al. 2011). As shown in section 2.8.1.3, models are often validated against *in vitro* measurements that rarely can be extrapolated to *in vivo* scenarios, thus the models validation become even more difficult.

Malandrino et al. (2015b) reported that poromechanics-transport simulations can allow the study of complex scenarios, despite the models limitations mentioned above. For example, the changes in porosity produced by loading have been connected with the changes in the hydraulic permeability and with diffusivity changes. In addition, those changes were linked to the solute concentrations. The authors suggested the need of a sensitivity study of the mechano-transport model to parameter changes, since relevance of each

phenomenon is linked to the parameter values. Such sensitivity analysis will be addressed in the Chapter 4 of this thesis.

2.11 Modelling contributions in the study of disc degeneration

2.11.1 Poromechanical properties

The study of Malandrino et al. (2011) revealed that the load-dependency of the transport of solutes might come from: (a) changes in the effective solute diffusivity in the continuum, and (b) variations in the diffusion distance from the simulated supply. They showed that there is a competition between the two effects mentioned above. As such, whereas there is a limitation of diffusivity transport due to pore reductions of disc matrix, the decrease of the distance from the supply improves the diffusion. This last effect was predominant in healthy disc models but not in degenerated discs because the latter were simulated as more fibrotic and stiffer. Also, transport calculations were sensitive to changes in the osmotic pressure, porosity and initial cell density. Moreover, finite element simulations are valuable in the study of the anisotropy of disc nutrient transport and water content (Jackson et al. 2008). Indeed, water diffusivity, and the diffusion coefficients of ions, glucose and oxygen were shown to be anisotropic (Drew et al. 2004; Iatridis & Ap Gwynn 2004; Jackson et al. 2006; Jackson et al. 2008; Travascio & Gu 2007). The complex disc organization might be responsible of such anisotropic behaviour.

2.11.2 Tissue condition

Jackson et al. (2011a) and Zhu et al. (2012) studied the increment of matrix stiffness and other model changes so as to simulate degeneration effects, e.g. geometrical and biochemical changes, on cell viability calculations. They found that degenerated conditions generate a decrease of the glucose concentration that might produces local cell death. In addition, cell death started in the nucleus at the boundary nucleus-annulus and it propagated to the disc centre.

Glucose concentrations could not be improved by mechanical loads, in degenerated disc models, although disc height reduction was simulated the (Malandrino et al. 2011; 2014a). In this case, the positive effect of the diffusion

distance reduction was negligible compared to the effect of the strain dependent diffusivity which made worse the cell death. However, the reduction of the nutrient supply via CEP between 40% and 50% was needed to predict cell death. Hence, the relevance of nucleus and annulus conditions appears to be minimal in comparison to the effect that might have the nutrient supply via CEP.

2.11.3 Endplate

Strong heterogeneity of permeability and porosity values have been determined for the bony endplate (BEP) (Malandrino et al. 2014b). Such changes have a insignificant effect on solute distributions, and also a limited effect on the fluid velocities within the cartilage endplate (Malandrino et al. 2014b). In addition, the variation of the hydraulic permeability of the CEP did not alter the nutrition by diffusion or by advection (Malandrino et al. 2011). Nevertheless, the simulation of the CEP calcification has a negative effect on cell viability since there is a decrease in the porosity (Shirazi-Adl et al. 2010; Jackson et al. 2011b; Noailly et al. 2014). While models suggest that nutrient supply at the boundary vertebral-cartilage endplate regulates the cell death, the effect of damage and degenerative changes remains unclear and can be controversial (Rodriguez et al. 2011). The effect of CEP degeneration on disc nutrition will be explored in Chapter 6.

2.11.4 Load scenarios

Zhu et al. (2012) found that dynamic compressive loads have a positive effect on cell viability for models that consider degenerated disc properties. Such effect is due to the capacity of dynamic loads to limit the consolidation of the tissue, and the diffusivity of solutes though the tissue, therefore. Nevertheless, the positive effect of dynamic loads have on cell death prediction is negligible compared to the negative effect of sustained compressive loads (Malandrino et al. 2011). Most of the studies that explore disc nutrition and cell viability just consider axial compression. As such, to have a better idea of the effect of disc posture on nutrition, rotational loads needs to be added to the simulations.

2.11.5 Disc geometry

Patient-specific predictive models are the next step for disc explorations. Recently, Malandrino et al. (2015a) combined disc geometries obtained from MRI of patient that had distinct degeneration grades with a mechano-transport and cell viability simulations. They found that disc height mainly controls the prediction of cell death. Also, whereas disc models that were higher than 14 mm presented adverse nutrient and cell viability conditions in the nucleus, disc models with height around 10 mm the interface annulus-nucleus was the most affected area in terms of glucose content. Moreover, for large discs the effect of diffusion distance was stronger than the effect of strain-dependent diffusivity.

2.12 Conclusions

This Chapter described the biological frame of the intervertebral disc. The indirect mechanotransduction mechanism relates the mechanical loads with disc nutrition and cell viability. Moreover, the deprivation of nutrients activates catabolic processes that degrade the disc matrix, aspect that might be important in the understanding of disc degeneration. In this sense, the experiments can provide information about the processes mentioned above, but they fail in the integration of biological and physical information. However, the consideration of the disc as a biphasic material makes possible the study of its biomechanics using porohyperelastic finite elements models. In addition, the coupling of such mechanical models to transport models with cell viability criteria allow the exploration of the interaction between mechanobiological processes, e.g. between changes in tissue condition and the transport of nutrients that might be very relevant in the study of disc degeneration.

3 NUMERICAL STABILITY OF POROMECHANICAL INTERVERTEBRAL DISC MODELS

Numerical studies of the IVD are important to better understand the load transfer and the mechanobiological processes within the disc. Among the relevant calculations, fluid-related outputs are critical to describe and explore accurately the tissue properties. Porohyperelastic finite element models of IVD can describe accurately the disc behaviour at the organ level and allow the inclusion of fluid effects. However, results may be affected by numerical instabilities when fast load rates are applied. It is hypothesized that such instabilities would appear preferentially at material discontinuities such as the annulus-nucleus boundary and should be considered when testing mesh convergence. A L4-L5 IVD model including the nucleus, annulus and cartilage endplates was tested under pure rotational loads, with different levels of mesh refinement. The effect of load relaxation and swelling were also studied. Simulations indicated that fluid velocity oscillations appeared due to numerical instability of the pore pressure spatial derivative at material discontinuities. Applying local refinement only was not enough to eliminate these oscillations. In fact, mesh refinements had to be local, material-dependent, and supplemented by the creation of a material transition zone, including interpolated material properties. Results also indicated that oscillations vanished along load relaxation, and faster attenuation occurred with the incorporation of the osmotic pressure. It is concluded that material discontinuities are a major cause of instability for poromechanical calculations in multi-tissue models when load velocities are simulated. A strategy was presented to address these instabilities, and recommendations on the use of IVD porohyperelastic models were given.

The work developed in this chapter led to the publication Ruiz, C., Noailly, J., Lacroix, D., 2013. Material property discontinuities in intervertebral disc porohyperelastic finite element models generate numerical instabilities due to volumetric strain variations. J. Mech. Behav. Biomed. Mater. 26, 1-10.

3.1 Introduction

As shown in the previous Chapter, the IVD is the largest avascular tissue in the human body and provides the spine with flexibility and functional load support. In addition, all disc tissues, i.e. nucleus, annulus, and cartilage endplates, are highly hydrated and mechanically coupled (Urban et al. 2004; Setton & Chen 2004). According to its fibrous structure, the AF bears mostly tensile loads, even under compressive loads due to the hydrostatic fluid pressurization within the NP which generates annular bulging. The CEP are thought to be critical in regulating diffusion of nutrients and waste products to and from the IVD (Malandrino et al. 2014a; 2014b). They might also contribute to the intradiscal fluid pressurization by controlling the fluid exchanges between the discs and the adjacent vertebrae (Setton & Chen 2004; Ayotte et al. 2001).

Indeed, because of the poroelastic nature of the IVD, fluid flow and fluid contents are inextricably coupled to the deformations of the disc. A substantial volume of fluid is expelled from the disc during daily loading, and is subsequently reimbibed overnight during rest, helped by osmotic effects and possibly by the CEP composition/permeability (Riches & McNally 2005; Noailly & Lacroix 2012b). On one hand, changes in the extracellular matrix composition within the IVD contribute to alter substantially intradiscal pressurization, to decrease disc height, and to change the mechanics of the entire spine motion segment (Setton & Chen 2004). On the other hand, IVD poromechanics and biophysics are intimately related to each other. For example, disc ageing and degeneration have been related to changes in lumican, a small proteoglycan that was found to be regulated by exposure to interstitial fluid shear (Wang et al. 2011). This biophysical coupling is very important to understand both the maintenance and degenerative changes of disc tissues. Their exploration requires quantitative local assessments that are not easy to achieve experimentally (Hsieh & Twomey 2010), but these assessments can be provided alternatively by advanced numerical models in which fluid effects are explicitly considered (Noailly & Lacroix 2012a).

Accordingly, numerous finite element models including poroelastic disc formulations have been developed in the last years as a tool for a better understanding of both the disc biomechanics and the associated biophysics. For

example, important phenomena such as swelling and transport of solute could be simulated and explored (Laible et al. 1993; Ferguson et al. 2004; Malandrino et al. 2011). As a matter of fact, long lasting static loads are generally used in the models. However, cell experiments suggest that cells are also responsive to dynamic loads at about 1Hz (Benallaoua et al. 2006; Fernando et al. 2011), suggesting that simulations involving fast loads could be necessary for explicit mechanobiological coupling.

Actually, the disc experiences combinations of forces and deformations at a rate of 1 Hz along diurnal activities e.g. walking, and the disc load can increase from 100N to 1000N in one second (Rohlmann et al. 2008). The literature information is scarce about IVD numerical studies under this kind of loading velocity, but Stokes et al. (2010) reported that tissue poroelastic models may become unstable when rapid loads are simulated. Such an issue would largely hinder the mechanobiological explorations of the IVD in silico.

On the other hand, Schroeder et al. (2006) predicted unexpected peaks of compressive stress at the boundary between the annulus and nucleus when simulating the effect of a 1h compressive load upon a poromechanical disc model. The authors suggested that the discontinuity between two sets of different material properties could explain such peaks of stress although they did not verify such hypothesis (Figure 3.1). Moreover, in the finite element (FE) method, material interfaces are known as weak discontinuities. Those discontinuities occur in the derivatives of the solution variable. For instance, they would produce punctual increments of strain in bi-material structures. In consequence, poromechanical predictions obtained at the material interfaces in IVD models might be compromised.

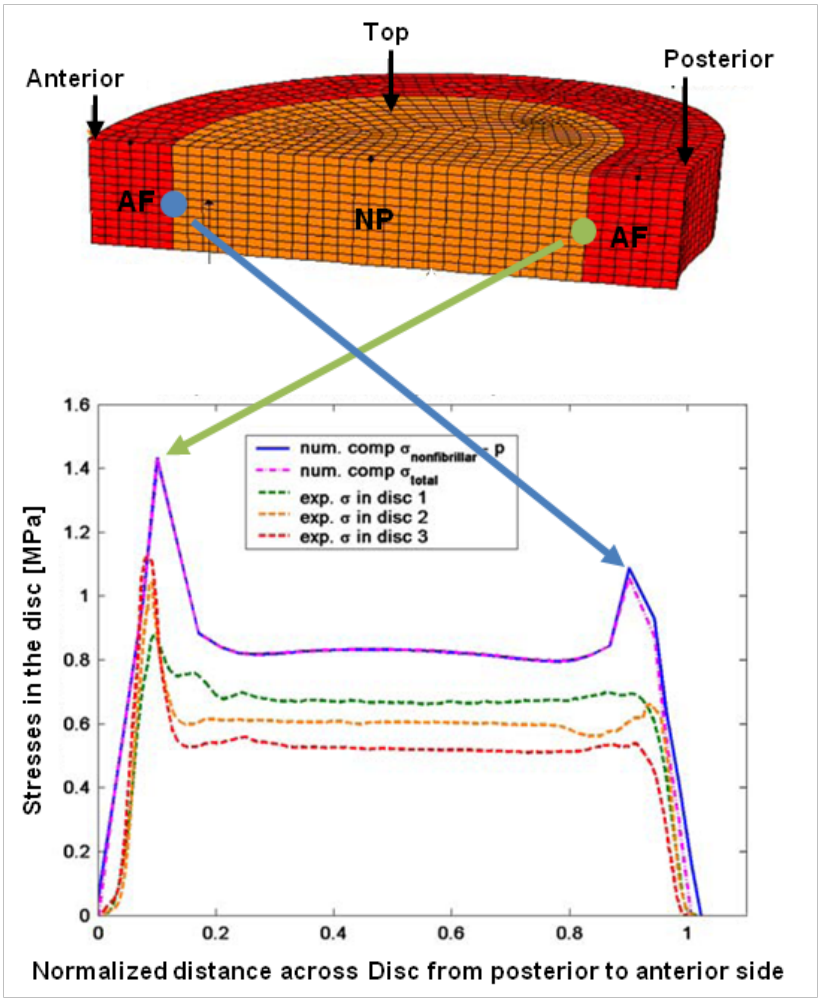

Figure 3.1: Peaks of stress at the AF-NP boundaries (adapted from Schroeder et al. (2006))

Thus, this Chapter aimed to evaluate whether the numerical convergence of an IVD porohyperelastic model can be reached under physiological load rates, and to find optimal mesh conditions for proper convergence. Particular attention was paid to the material transitions, since it is hypothesized that weak discontinuities, i.e. material property discontinuities could enhance the instability of finite element poromechanical calculations. As such, the ultimate objective was to evaluate both the mesh and simulated load conditions under which local poromechanical predictions could be locally reliable to allow further couplings to biophysical explorations.

3.2 Materials and methods

3.2.1 IVD models

An anatomical FE model of the L4-L5 intervertebral disc based on a validated L3-L5 bi-segment geometry was taken (Noailly et al. 2007). The IVD model included the AF, the NP and the CEP, as well as the superior and inferior bony endplates (BEP). Five different mean mesh sizes, Δh, were used to evaluate the model convergence: Δh= 3.04 mm (model 1), Δh= 2.76 mm (model 2), Δh= 1.72 mm (model 3), Δh= 0.86 mm (model 4) and Δh= 0.43 mm (model 5) (see Figure 3.2). The oriented collagen bundles of the annulus were excluded from the disc models so as to better focus on the convergence of the porohyperelastic elements of the ground substance. This point is further commented in relation to the results in the discussion of this chapter. All IVD tissues were considered as porohyperelastic materials where the pores were virtually saturated of an incompressible fluid (water) and had walls made of an incompressible solid matter (extracellular matrix). Such assumptions allowed expressing the total stress tensor, $\boldsymbol{\sigma}$, as the sum of a pore pressure component p and an effective stress $\boldsymbol{\sigma_{eff}}$:

$$\boldsymbol{\sigma} = \boldsymbol{\sigma_{eff}} - p\boldsymbol{I} \tag{3.1}$$

where $\boldsymbol{I}$ is the tensor identity and $\boldsymbol{\sigma_{eff}}$ is given by the followed expression:

$$\boldsymbol{\sigma_{eff}} = \frac{1}{J}\frac{\partial W}{\partial \boldsymbol{F}}\boldsymbol{F}^T \tag{3.2}$$

where $\boldsymbol{F}$ is the deformation gradient tensor, J is the determinant of $\boldsymbol{F}$ and W is the strain energy density of the drained porous skeleton given by

$$W = \frac{G}{2}(I_1 - 3) + \frac{K}{2}(J-1)^2 \tag{3.3}$$

where G is the shear modulus, I_1 is the first invariant the left Cauchy-Green strain tensor, and K is the bulk modulus.

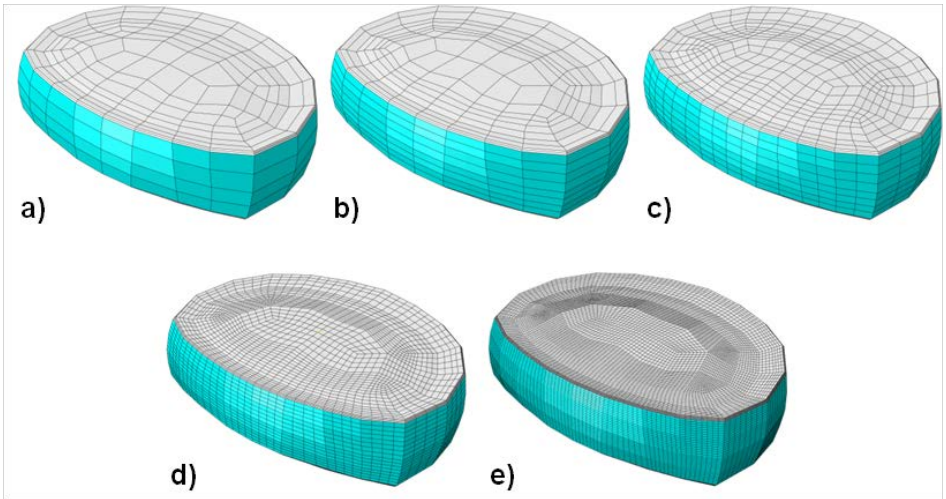

Figure 3.2: Mesh size (Δh) of the models used: a) model 1 (Δh= 3.04 mm), b) model 2 (Δh= 2.76 mm), c) model 4 (Δh= 1.72 mm), d) model 4 (Δh= 0.86 mm), and model 5 (Δh= 0.43 mm)

The pore pressure p was integrated from the Darcy's law that relates the fluid mass flow q to the spatial gradient of pore pressure ∇p, and to the hydraulic permeability κ:

$$q = -\kappa \nabla p \tag{3.4}$$

Also, the fluid flow can be expressed by:

$$q = v \cdot \varphi \tag{3.5}$$

where, v is the fluid velocity and φ is the fluid volume fraction, i.e. the porosity of the medium.

The material properties for all tissues were taken from the literature and are summarized in Table 3.1. A strain-dependent permeability was used (Mow et al. 1980; Argoubi & Shirazi-Adl 1996):

$$\kappa = \kappa_0 \left[\frac{e(1+e_0)}{e_0(1+e)}\right]^2 exp\left[M\left(\frac{1+e}{1+e_0} - 1\right)\right] \tag{3.6}$$

where κ_0 is the initial permeability, e is the void ratio which is the ratio of the current pore volume (i.e. fluid) to the current volume of the solid matrix, e_0 is the initial void ratio, and M is an empirical constant. The void ratio is related to the porosity of the tissue, n, according to the following expression:

$$e = \frac{n}{1-n} \tag{3.7}$$

Table 3.1: Material properties (Malandrino et al. 2011)

Material	G (MPa)	K (MPa)	Initial Void Ratio	Permeability (mm4/Ns)	M
Annulus fibrosus	0.28	0.37	3.08	0.0002*	1.18
Nucleus pulposus	0.17	0.22	4.88	0.0009*	8.5
Cartilage endplate	7.14	15.2	4	0.0025*	4.63
Bony endplate	4274	5051	0.05	26,800	-

*From Eq. 3.6

Sagittal extension and axial rotation were simulated as pure rotations corresponding to the intersegmental motions generated by 7.5 Nm moments in a lumbar spine model for which the ranges of motion predicted were verified against in vitro experiments (Noailly et al. 2007). The loads were applied in 1 s, in order to simulate a fast load rate. The condition of free fluid flow at the external boundaries of the model was simulated by applying a nil external pore pressure.

3.2.2 Numerical instabilities

The presence of possible numerical instabilities related to the poromechanical predictions was explored. Therefore, the preferential site for instabilities suggested by Schroeder et al. (2006), i.e. the boundary between AF and NP, was studied in terms of numerical issues. Then, different strategies were tested to stabilize the predictions whenever necessary. The evolution of the instabilities along tissue consolidation was also explored, as well as the influence of considering explicitly tissue swelling.

A. Stabilization strategies

- Local mesh refinement

According to the study of Stokes et al. (2010), the Vermeer and Verruijt criterion was used to avoid numerical pore pressure oscillations:

$$\Delta t \geq \frac{\gamma(3K+G)(\Delta h)^2}{54KG\kappa} \qquad \textbf{(3.8)}$$

Δh is the maximum mesh size to avoid pore pressure instabilities for a minimum time of mechanical load ramp, Δt, and γ is the specific weight of the interstitial fluid i.e. water at 37°C in this study.

- Material transitions

The relative effect of each material parameter discontinuity upon the instabilities at the AF-NP boundary was evaluated by homogenizing individually each material parameter from Eq. (3.1) to (3.4) across adjacent tissues, i.e. AF and NP. Thus, seven different cases of homogenization were studied: (1) shear modulus G; (2) bulk modulus K; (3) all hyperelastic parameters G and K (Eq. 3.2); (4) initial void ratio e_0; (5) initial permeability κ_0; (6) empirical constant M and (7) all the strain-dependent permeability parameters e_0, κ_0 and M (Eq. 3.6).

Thereafter, material transition areas were created at material discontinuities, to smooth the changes of material properties from one tissue to another. The width of the transition zone (TZ) was taken as the minimum space needed to obtain significant reductions of the instabilities. Within this space, different mesh refinements were combined to several types of interpolations (linear, logarithmic and exponential) for the most critical parameter(s) found in the sensitivity study. As for the local refinements associated to the material interpolations, the introduction of relatively finer meshes was tested alternatively from one material area to another, independently on the Vermeer and Verruijt criterion.

B. Time-dependent behaviour of numerical instabilities and swelling effect

The evolution of the numerical instabilities was tested for differently stabilized models along a stress relaxation period of 1 hour applied to the most critical rotational load case regarding the poromechanical instabilities. Moreover, the effect of simulating disc swelling on the time behaviour of the instabilities was assessed. For this, the rotational load case was preceded by a step of free swelling due to an initial gradient of osmotic pressure of 0.15 MPa (Johannessen et al. 2006). The swelling at the NP was applied by considering the pore pressure, in Eq. 3.1, as the sum of the water chemical potential u_w and a constant swelling pressure term $\Delta\pi$ as proposed by Wilson et al. (2005), and used in disc modelling by (Malandrino et al. 2011; Galbusera et al. 2011a):

$$p = u_w + \Delta\pi \quad \textbf{(3.9)}$$

Along this free swelling simulation, the lower BEP was fixed in terms of displacements and rotations, and the pore pressure around AF and BEP external surfaces was nil.

3.2.3 Calculations

All simulations were performed with ABAQUS v6.10-1 (Simulia, Providence, RI, USA). The strain energy density (SED), the pore pressure, and the fluid velocity (FV) were calculated for different node paths, respectively along (1) the mid-sagittal plane, (2) the disc circumference, and (3) the posterior and (4) anterior disc height (Figure 3.3). While SED results were used principally to perform a common assessment of the mesh convergence, numerical instabilities were studied through both pore pressure and FV predictions. Models 1, 2 and 3 calculations were performed with a high performance computational server (HP Proliant G2 Intel® Xeon®, 2 CPU, 3GHz, with 64 GB RAM) using 4 cores for each simulation, whereas model 4 and model 5 predictions were achieved with a supercomputer (SGI UV1000 Intel® Xeon®, 224 CPU, 2.66 GHz, with 6.14 TB RAM) using 4 and 8 cores, respectively.

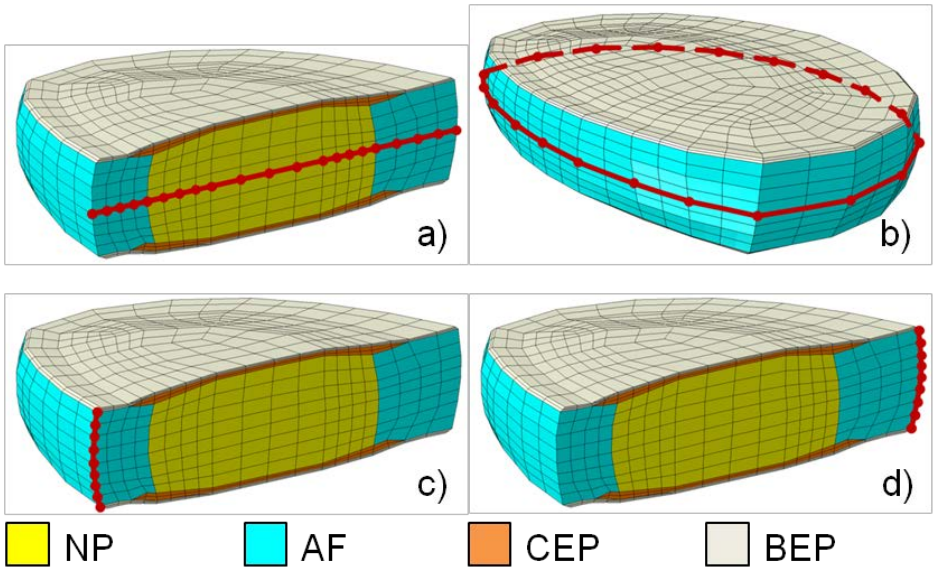

Figure 3.3: Paths studied (lines) on model 3 mesh: a) Path 1, b) Path 2, c) Path 3, d) Path 4

3.3 Results

3.3.1 Converge study

SED calculations showed that models 2, 3 and 4 led to similar results under extension (Figure 3.4a and 3.4b). However, under axial rotation, models 2, 3 and 4 results differed to the results obtained with model 5, along path 2 (Figure 3.4d). FV predictions led to similar model convergence along all paths studied under both extension and axial rotation. However, FV predictions presented spatial oscillations under both load conditions in the mid sagittal plane (Figure 3.5), though these oscillations had very small amplitudes under axial rotation (Figure 3.5b), and even disappeared for model 5. Conversely, they had large amplitudes under extension and curiously, these amplitudes increased with mesh refinement (Figure 3.5a).

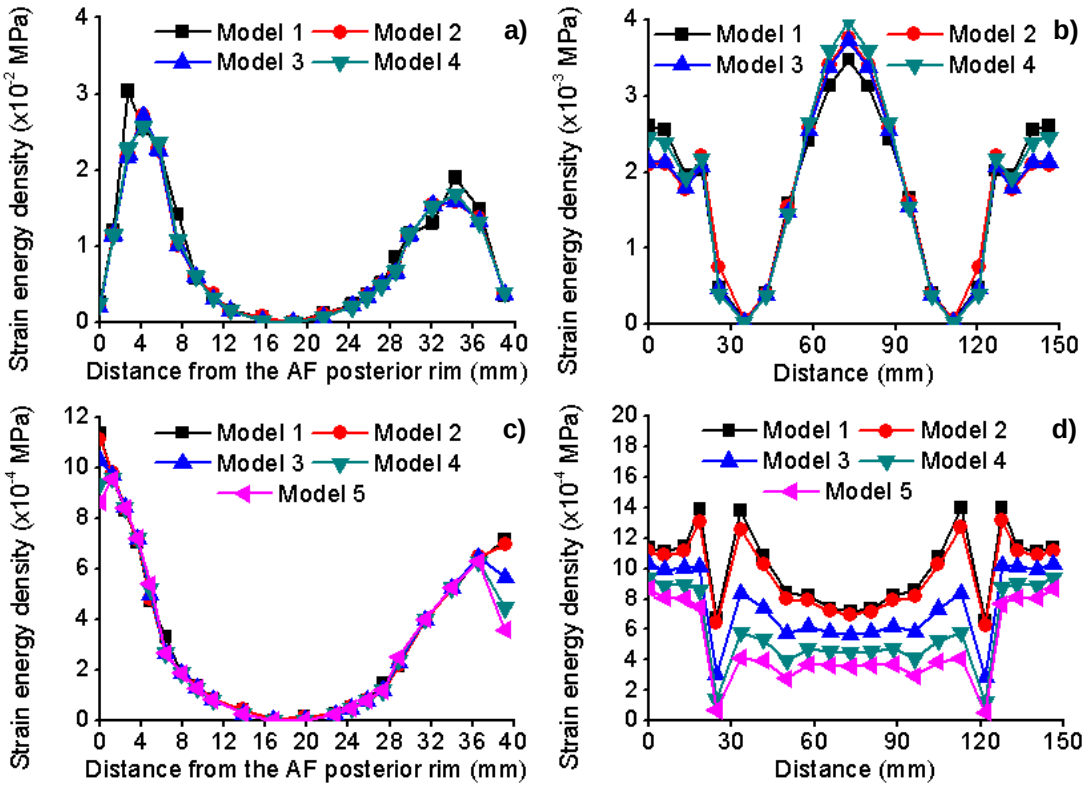

Figure 3.4: Strain energy density predictions a) under extension along Path 1, b) under extension along Path 2, c) under axial rotation along Path 1 and d) under axial rotation along Path 2

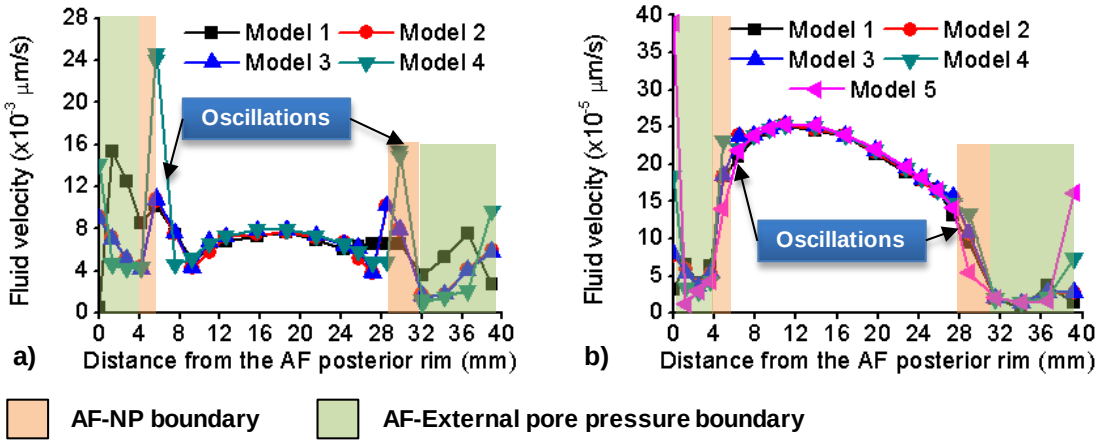

Figure 3.5: Fluid velocity oscillations predicted along the mid-sagittal plane path, a) under extension and b) under axial rotation

Table 3.2 presents the computational time given by all models under extension. Note that model 5 led to extremely high computational times. SED results of model 3 already converge to model 4 results under sagittal extension (Figure 3.4a). Also, model 3 led to manageable computational times (Table 3.2). As such, this model was selected to further study both the mesh convergence under axial rotation and the oscillations under sagittal extension (Figure 3.5a).

Table 3.2: Computational time for all models

Model	CPU	CORES/CPU	RAM	CPU time (s)
1	2 CPU @ 3 GHz*	4	147 MB	195
2	2 CPU @ 3 GHz*	4	291 MB	427
3	2 CPU @ 3 GHz*	4	0.9 GB	1,846
4	2 CPU @ 2.66 GHz**	6	16 GB	92,300
5	2 CPU @ 2.66 GHz**	6	37 GB	12,393,700

* HP Proliant G2 Intel® Xeon® with 64 GB RAM

** SGI UV1000 Intel® Xeon® with 6.14 TB RAM

3.3.2 Oscillations study

Simulations with and without material discontinuities showed that such discontinuities in the nonlinear IVD model were responsible for most of the numerical instabilities related to porohyperelasticity, i.e. FV oscillations. Among the strategies used to prevent FV oscillations, local refinements based on the Vermeer and Verruijt criterion did not allow stabilizing the FV predictions (Figure 3.6a). Surprisingly, homogenizing the shear modulus *G* over the NP and AF tissues eliminated completely the instabilities (Figure 3.7). The Darcy's law parameters analysis showed that variations of the pore pressure gradient along the sagittal plane path were mostly responsible for the FV oscillations (Figure 3.8). No instability was found in terms of pore pressure calculations at order zero, and the pore pressure values obtained were in the range of 0.06-0.12 MPa for the compressed annulus area. Instabilities were best reduced by using exponential interpolations (Figure 3.9). The creation of a material transition zone, refining more the AF area did not stabilize the FV calculations, whereas refining more the NP area led to significant improvements, although oscillations remained (Figure 3.6b). FV predictions within the outer AF were improved through a radial local refinement applied to model 3 (Figure 3.10a). Though not aiming at coping with the FV oscillations, a further tangential refinement was performed and allowed for the convergence of model 3 SED results to model 4 results under axial rotation (Figure 3.10b). This final mesh was used to explore the load relaxation and swelling effects on the poromechanical instabilities.

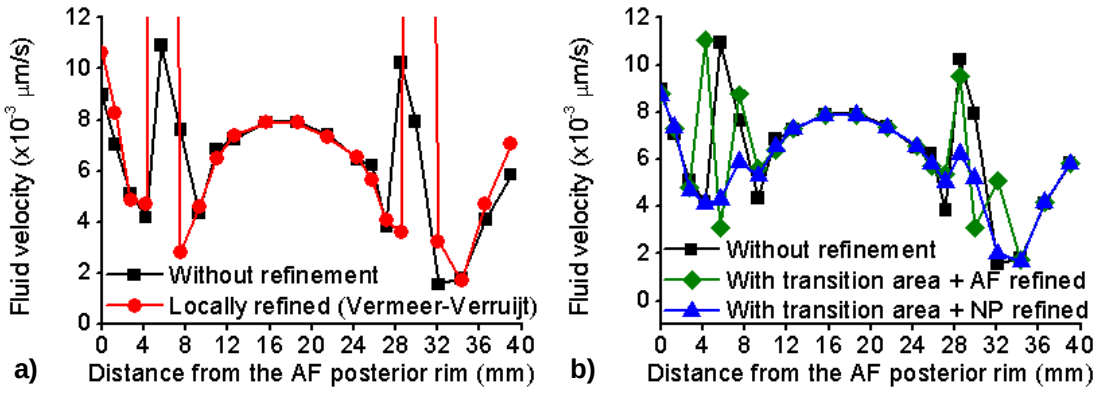

Figure 3.6: Oscillations strategies for model 3 along the mid-sagittal plane path, a) locally refined (dot line) and b) Material transition zone, refining more the AF (diamond line) and refining more the NP (triangle line)

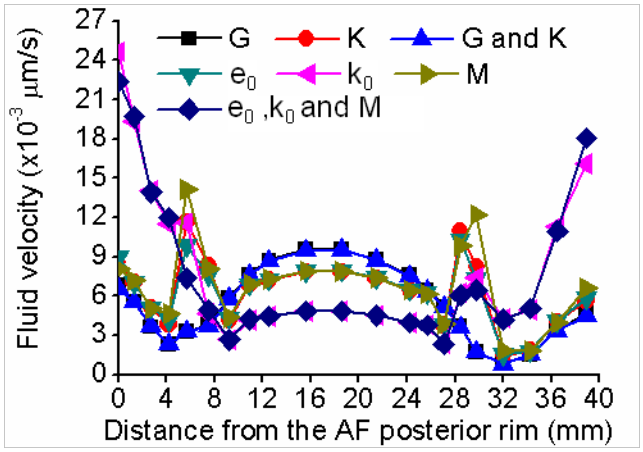

Figure 3.7: Fluid velocity sensitivity study for model 3 under extension along the mid-sagittal plane path, where G is the shear modulus, K is the bulk modulus, e_0 is the initial void ratio, k_0 is the initial permeability, and M is an empirical constant

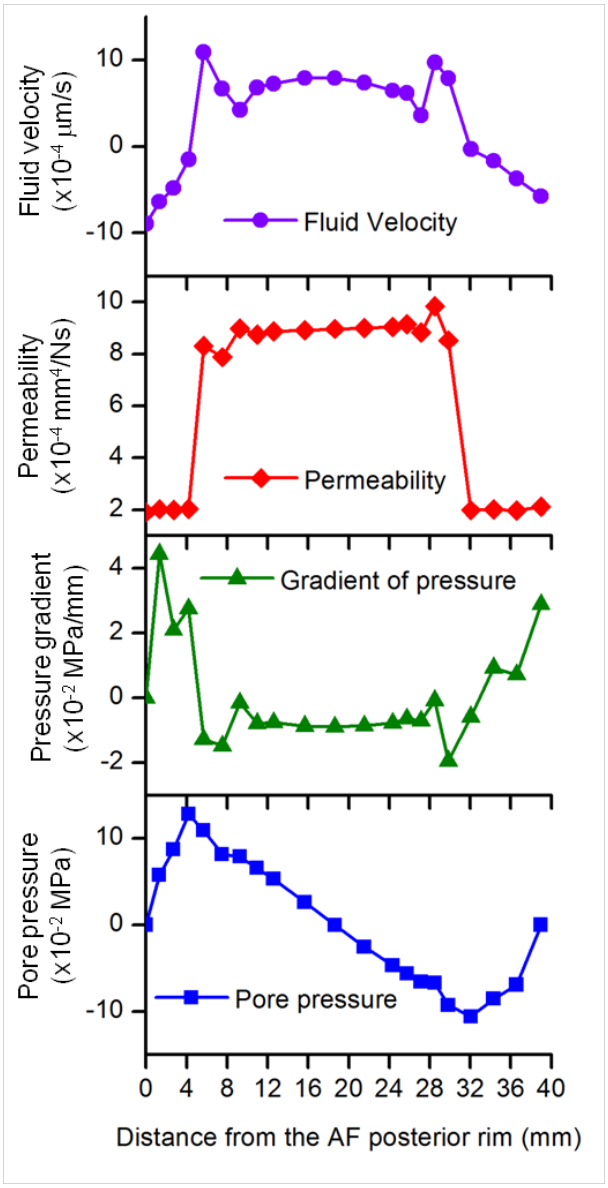

Figure 3.8: Relation between the oscillations at the fluid velocity with the gradient of pore pressure along the mid-sagittal plane path

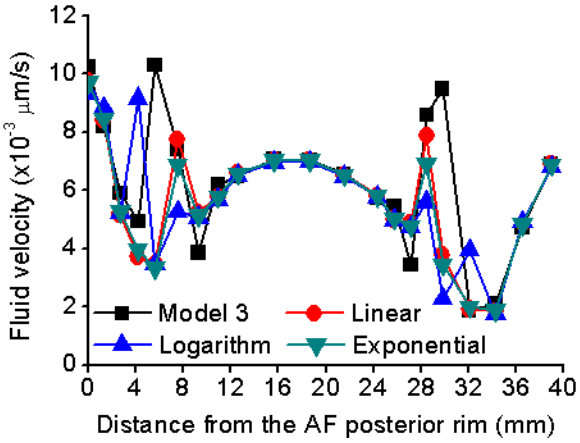

Figure 3.9: Effect of material parameter interpolations: linear, logarithm and exponential at the AF-NP boundary

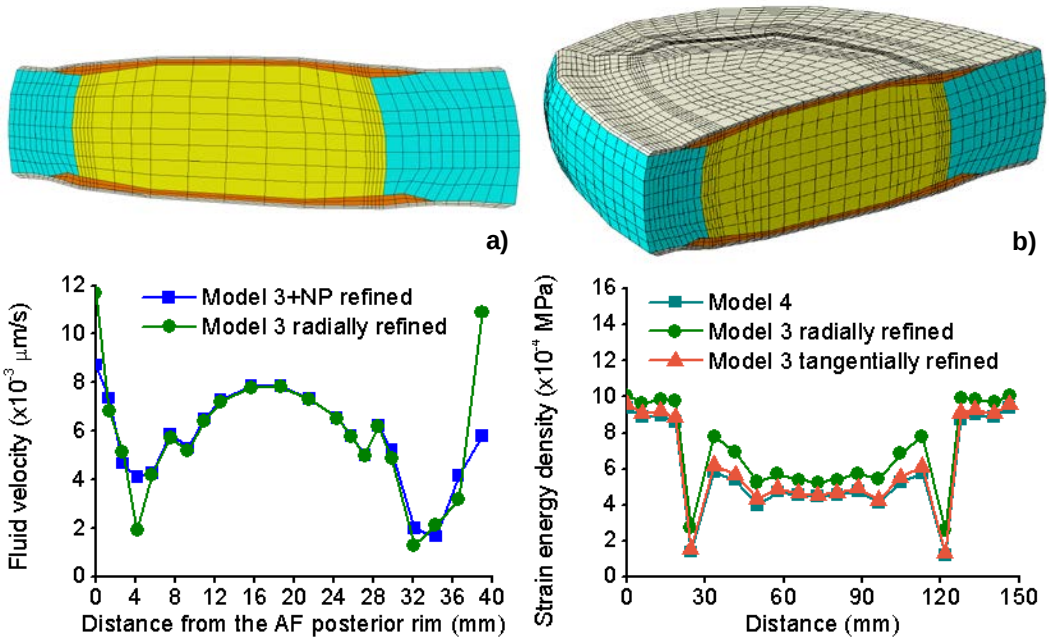

Figure 3.10: Predictions along the mid-sagittal plane path for: a) Fluid velocity in model 3 with local radial refinements at the AF-NP interface (computational time of 1h 30) and b) Strain energy density in model 3 optimized with an additional tangential refinement (computational time of 2h 30)

3.3.3 Load relaxation and swelling effect

After 15 minutes of stress relaxation, the FV oscillations almost disappeared, and they disappeared completely at some point between 30 minutes and 1 hour of relaxation (Figure 3.11a). Furthermore, FV oscillations were attenuated through the application of the osmotic pressure within the nucleus. In particular, the oscillations in the posterior part of the disc were eliminated, but

those in the anterior part remained (Figure 3.11b). The addition of the osmotic pressure to the load relaxation condition reduced to 10 minutes the time after which FV instabilities disappeared (Figure 3.11c).

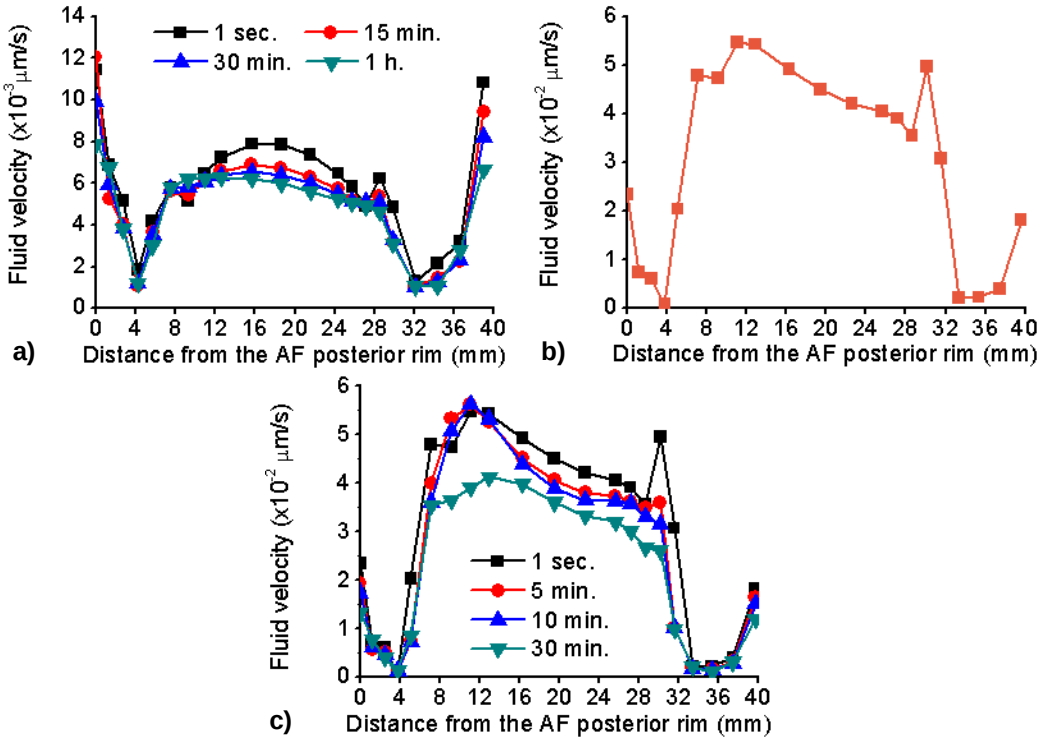

Figure 3.11: Fluid velocity behaviour along the mid-sagittal plane path: a) after 15 minutes, 30 minutes, and 1h of load relaxation, b) after 1 second incorporating of the osmotic pressure at the nucleus, and c) after 5 minutes, 10 minutes, and 30 minutes of load relaxation and osmotic pressure incorporated

3.4 Discussion

The aim of this Chapter was to analyse the convergence of an IVD porohyperelastic model under fast load rates representative of those involved in a load cycle of a 1 Hz dynamic physiological load, and identify possible numerical instabilities related to poromechanical calculations. The SED and FV were both evaluated along four different node paths under pure rotational motions of extension and axial rotation. Results indicated poor SED convergence under axial rotation, and numerical instabilities of the poromechanical predictions that appeared under the form of FV oscillations at the boundary between two different materials.

The poor convergence of SED results under axial rotation could be explained by analysing the strain components. The deviatoric strain had the greatest influence on the total strain, and in the less refined model, this strain quantity diverged by up to 500% (relative difference) from the value predicted in the most refined model. The corresponding relative divergence for the spherical strain, i.e. one third of the trace of the strain tensor, calculations were about five times lower. Maximum strain divergence was usually predicted in the postero-lateral AF. Under extension, since the volumetric strain was relatively small, it did not have any major effect upon the total strain and upon the mesh convergence. Overall, coarse elements are more resistant to shape changes than finer ones, and our shear strain divergence follows the well-known Poisson stiffening effect (Büchter et al. 1994; Bischoff & Ramm 2000). Thus disc model mesh convergence should be assessed under axial rotation rather than under other load cases for non-poromechanical predictions. It is worth to mention that the load cases presented in this Chapter are those for which the poorest convergence was obtained.

As for the poromechanical predictions, slight instabilities of FV calculations were present under axial rotation in the sagittal plane path, but could be suppressed through simple mesh refinement. Under extension, the scenario was very different, and strong FV oscillations occurred along the same path. However, FV instabilities were not found along paths 2, 3 and 4, where no material discontinuity was present.

The sensitivity analysis indicated that the shear modulus G had the greatest influence on the oscillations. Indeed, the confined NP behaved as mostly incompressible and tried to impose mostly deviatoric deformations to the AF. However, the AF restricted theses deformations, for it had a larger shear modulus than the NP. This restriction forced locally volumetric deformations at the periphery of the NP, which caused small spatial variations in these volumetric deformations (Figure 3.12b) and generated non-physical variations in the gradient of the pore pressure (Figure 3.8). It is worth to highlight that this is not only a problem of material discontinuity, but also a problem of confinement of a highly hydrated tissue model, i.e. the NP, that interacts numerically with a less permeable and stiffer confining tissue model.

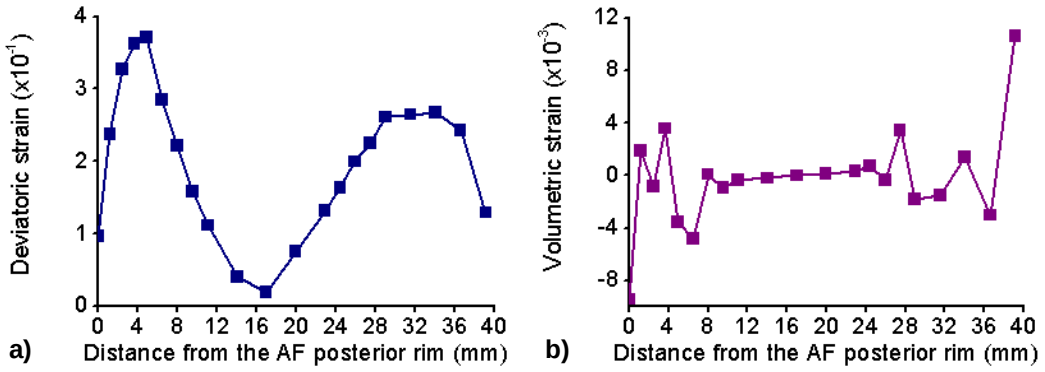

Figure 3.12: Strain components for model 3 along path 1, a) deviatoric strain and b) spherical strain

Analysing the FV instabilities along the spatial variation of the different parameters of Darcy's law, and comparing to the pore pressure distribution, revealed that zero-order pore pressure predictions were relatively stable. Hence, we could confirm that the spatial derivatives of the pore pressure variations were mostly responsible for the FV oscillations (Figure 3.8). Such outcome contrasts with the results obtained by Stokes et al. (2010) who found fluctuations of zero-order pore pressure between adjacent nodes. A reason for the difference between the above-mentioned results and the calculations obtained in this Chapter could be the presence of higher pore pressure due to the AF confinement effect, which may have stabilized the pressure predictions at order zero.

By using a single material model, Stokes et al. (2010) showed that numerical oscillations in pore pressure could be removed by the application of a global mesh refinement based on the Vermeer and Verruijt criterion (Eq. 3.8). In the present simulations, instability arose from the spatial derivative of the pore pressure. As such, the creation of smaller elements led to steeper gradients of pore pressure throughout the material discontinuities, and increased the magnitude of FV oscillations, though happening over a reduced length of the node paths. Indeed, oscillations occurred also along the sagittal axial path, at the NP-CEP boundary, and the oscillation amplitudes at this boundary were larger than at the AF-NP boundary. Though such issue can be partly due to higher fluid velocities throughout the CEP than throughout the AF, the reduced length of the elements over the NP-CEP boundary seems to confirm that simple mesh refinements are not appropriate to smooth out the pore pressure spatial derivatives across material discontinuities.

The weak discontinuities addressed in this Chapter might be avoided by using the extended finite element method (XFEM). Such method is based on a partition of unit (Melenk & Babuška 1996; Duarte & Oden 1996) and requires minimal remeshing (Belytschko & Black 1999). Although some studies with XFEM have considered hyperelastic materials, they addressed just cracked structures, i.e. strong discontinuities (Karoui et al. 2014; Zaafouri et al. 2015). In biomechanics, XFEM has been used to study the brain (Vigneron et al. 2012), hip fracture (Ali et al. 2014), and the cut of soft tissues (Courtecuisse et al. 2013). However, there is a lack of information about the use of XFEM in modelling multi-material porohyperelastic soft tissues. As such, the efficiency of the XFEM in addressing the fluid velocity oscillations studied in this Chapter needs to be explored.

Within the disc model, the fluid moved from a region of higher pressure and higher permeability to a region of lower pressure and lower permeability, i.e from the NP to the AF. Therefore, combining a material transition area and a refined nucleus area guided a progressive pressure change and the decrease in FV from the NP to the AF. Accordingly, oscillations were reduced by 91% when using an exponential interpolation (Figure 3.6b) that favoured the decrease of FV within the NP area, leading to an improved numerical stabilization of the transition area.

Interestingly, the transition zone created between the NP and the AF so as to improve poromechanical convergence exists in the IVD. Indeed, observations of the IVD biosynthesis identified three zonal differences: the annulus, the nucleus and a transition zone of thin fibrosus tissue (Guilak et al. 1999; Cassinelli et al. 2001; Chen et al. 2002). Morphology of the fusiform shape cells within the AF changes progressively in the radial direction into a spherical shape cells (nucleus like) at the AF-NP border (Bruehlmann et al. 2002). According to this change in cell phenotype, the interlamellar septae within the inner AF contain proteoglycan aggregates, with water imbibing properties and their random collagen and elastin structures resemble the NP (Bruehlmann et al. 2002). Modelling the transition zone in this study, not only provided an enhancement over FV oscillations, but also represented an improved approximation of the disc structure. Unfortunately, no quantitative information could be found about the width of such transition zone.

The FV oscillations in the current study produced a peak on the stress calculations in the compressed area of the disc (posterior part) at the boundary

AF-NP, which was in agreement with the results reported by Schroeder et al. (2006). Reducing the FV oscillation amplitudes in our study reduced the amplitude of this peak of stress, confirming therefore that material discontinuities are responsible for such numerical instabilities. Though the load cases studied were convenient for the purpose of exploring poromechanical instabilities, cyclic loads may have to be considered. Accordingly, up to 10 cycles of charge-discharge-charge extension were simulated at 1 Hz (Figure 3.13). The FV profiles obtained after different number of cycles remained very similar to that obtained after the first load at 1 s.

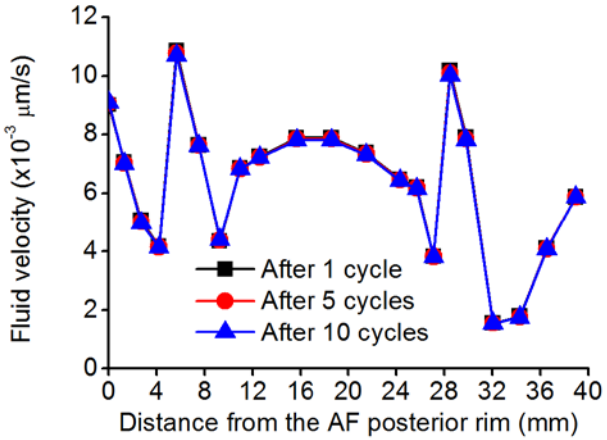

Figure 3.13: Fluid velocity after 1, 5 and 10 cycles of charge-discharge-charge extension at 1 Hz along the mid-sagittal plane path of the non-refined Model 3

Despite the positive outcomes in terms of FV stabilization, the present study has some limitations worth to mention. First of all, fibres of the AF were not included, in order to achieve a system sufficiently simple for proper interpretations of the results. In terms of mesh deformation and convergence, such a limitation is not expected to have any significant impact, since the displacement-controlled boundary loads imposed geometrical distortions that can be expected for a L4-L5 disc within a complete spine segment (Noailly et al. 2007). In terms of shear modulus discontinuity at the AF-NP boundary, the further inclusion of the collagen fibres increased the oscillations due to their influence on the effective deviatoric stiffness of the AF. The contribution of the fibres to numerical instabilities also depended on the type of modelling approach used, i.e. continuum, or structural. Whereas the use of a continuum approach for AF fibres based in the model of Gasser et al. (2006) would increase the oscillations, the inclusion of the structural approach for collagen fibres developed by Wilson et al. (2005) in the

final model did not alter the stabilization achieved. As a result, this latter approach was included in the AF for the simulation of the collagen fibres in the disc models of the following Chapters.

Also, the nodes used along the mid-sagittal plane path in models 4, 5 and in the locally refined model 3, corresponded to the nodes of the reference path defined in model 3. This strategy was selected to thoroughly compare the effective effects of both global (models 4 and 5) and local (model 3 tangentially refined) refinements at specific locations within the disc. Indeed, evaluating a node path by using all the additional nodes created by the local refinements led to a field of residual oscillations at the AF-NP transition zone between the nodes that were effectively studied. In any case, stabilization strategy at the tissue-scale for further calculation of local events can focus on very specific nodes where the results can be reasonably picked up.

The values obtained with the incorporation of the osmotic pressure suggested that simulating swelling effects at the NP tissue selectively attenuated the oscillation of pore pressure gradient in the compressed areas of the disc (Figure 3.9b). The added osmotic pressure seemed to act similar to a penalty factor which restricted the spatial gradients of volumetric deformation and made the oscillation of the volumetric strain disappear, eliminating the FV oscillations. Naturally, this mechanism did not achieve a full stabilization in the anterior part of the disc because of local axial tractions. However, results under load relaxation with the osmotic pressure indicated that the oscillations at the anterior part of the disc disappeared after 10 minutes, i.e. a reduction of 20 minutes with respect to the stabilization achieved without osmotic pressure. Such results suggest that porohyperelastic models can be used to study long-term load effects, i.e. diffusion phenomena. According to the time required to achieve FV stabilization under creep, additional calculations revealed that the sagittal FV profile required load rates reduced to the order of min^{-1} to start to change.

Overall the poromechanical issues identified in the present Chapter would persist for load events, e.g. application rate, charge-discharge cycles, creep, that can encompass time frames of up to several tens of minutes. Interestingly, the slight FV oscillations that remained in the stabilized model were eliminated when a compression load of 1000 N was added to the extension load (Figure 3.15 – to be

compared with Figure 3.10a), corroborating nicely the above-mentioned effect of swelling pressure.

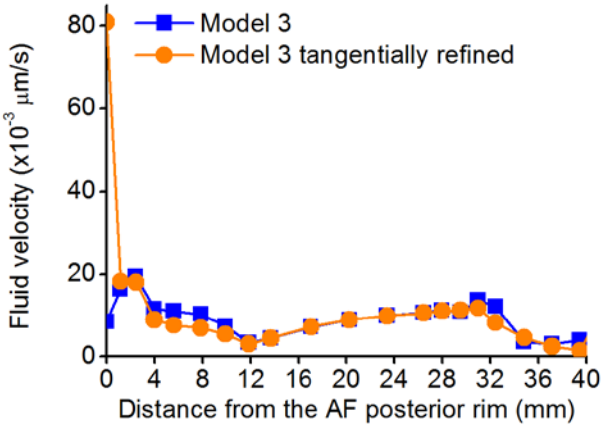

Figure 3.14: Fluid velocity under combined extension-compression loads along the mid-sagittal plane path

3.5 Conclusions

This study showed that material discontinuities create oscillations in IVD porohyperelastic models when fast load rates are simulated. At the AF-NP boundary, the creation of a material transition zone, with a gradient of material properties and local mesh refinements, removed the oscillations partially and is, indeed, more representative of the true configuration of the disc. This improvement should allow the use of the local tissue predictions of the model to generate inputs for lower scale biophysical / mechanoregulation simulations.

As such, local biophysical processes related to the maintenance or to the degenerative changes of the disc tissues should be explored only after a thorough convergence study for which the present Chapter can provide the main guidelines. Truly, the effect of additional combinations of load frequencies and number of cycles might be necessary to assess the effective persistence of the poromechanical instabilities when specific physical activities, e.g. walking, are simulated. In the meantime, it can be concluded that porohyperelastic models used to simulate long lasting loads may not be affected by oscillations, minimizing the possible biases when linking local tissue biomechanics to slow phenomena such as solute/nutrient diffusion. As a results, the model developed in this Chapter can be coupled to a transport models for the study of nutrient diffusion phenomena under sustained compressive loads, as it will be shown in the next Chapters.

4 DEVELOPMENT OF A COMPOSITION-TRANSPORT-CELL VIABILITY INTERVERTEBRAL DISC MODEL

Altered nutrition in the intervertebral disc can affect cell viability and generate catabolic cascades contributing to extracellular matrix (ECM) degradation. Such degradation is expected to affect couplings between disc mechanics and nutrition and accelerate the degenerative processes. However, the relation of ECM changes to major biophysical events within the loaded disc remains unclear. A L4-L5 disc finite element model including the nucleus (NP), annulus (AF) and cartilage endplates (CEP) was used and coupled to a transport-cell viability model. Solute concentrations and cell viability were evaluated along the mid-sagittal plane path. A design of experiment (DOE) was performed. DOE parameters corresponded to AF and NP biochemical tissue measurements in discs with different degeneration grades. Cell viability was not affected by any parameter combinations defined. Nonetheless, the initial water content was the parameter that affected the most the solute contents, especially glucose. Calculations showed that altered NP composition could negatively affect AF cell nutrition. Results suggested that AF and NP tissue degeneration are not critical to nutrition-related cell viability at early-stage of disc degeneration. However, mild ECM degenerative changes may alter significantly disc nutrition under mechanical loads. Coupling disc mechano-transport simulations and enzyme expression studies could allow identifying spatiotemporal sequences related to tissue catabolism.

The work developed in this chapter led to the manuscript Ruiz Wills, C., Malandrino, A., Lacroix, D., Ito, K. and Noailly, J. (2014) Simulating the sensitivity of cell nutritive environment to composition changes within the intervertebral disc. Submitted in the *Journal of the Mechanics and Physics of Solids*.

4.1 Introduction

The mechanical and biophysical functions of the disc are determined by both the biochemistry and the ultrastructure of the extracellular matrix (ECM) (Setton & Chen 2004). The NP has a high concentration of negatively charged proteoglycans. On one hand, these proteoglycans lead to tissue swelling, which stretches the fibres of the surrounding AF. Both the mechanical resistance of the latter and the pressurization of the interstitial fluid of the NP provide the IVD with a unique balance of flexibility and mechanical strength (Setton & Chen 2004). On the other hand, the concentration of proteoglycans in the NP affects the rate at which molecules can diffuse through the tissue (Urban et al. 2004), while it also depends on disc deformations. More generally, the disc ECM, i.e. a collagen network embedded in a dense proteoglycan gel, acts as a selective physical barrier to the diffusion of molecules into the disc and controls the diffusive exchange of molecules with the surrounding tissues.

The IVD has a very low density of cells in comparison to other tissues; only 1% of the disc volume is occupied by cells (Roberts & Urban 2011). Nevertheless the continuing activity of cells largely controls the fate of the disc. On one hand, cells produce the macromolecules that keep the disc tissues functional with the passage of time (Roberts & Urban 2011). On the other hand, they are able to trigger catabolic processes that may accelerate the depletion of ECM components. The ECM balance that results from these processes affects directly the biomechanical function of the IVD as well as numerous biochemical processes.

In particular, essential solutes such as oxygen and glucose are supplied to the IVD from the blood vessels located at the margins of the organ (Urban et al. 2004). The further transport of these solutes to the cells relies mainly on diffusion within the fluid phase that saturates the disc ECM (Urban et al. 2004). Disc cells consume oxygen and glucose and produce lactic acid (glycolysis). While the lack of glucose can be a strong trigger of catabolic cell responses (Neidlinger-Wilke et al. 2012), the lack of oxygen was reported to alter the proteoglycan production (Horner & Urban 2001). At the same time, acid lactic needs to be removed in order to avoid any drop of pH in the extracellular medium. The local balance of these

important chemical entities is governed by the properties of both the ECM and the solutes (Urban et al. 2004).

In the indirect mechanotransduction phenomenon mentioned in Chapter 2, it is intuitive to anticipate that tissue compaction, i.e. consolidation, and the resulting changes in both diffusion distances and fluid fractions affect solute diffusion. With disc degeneration, proteoglycan depletion is the most important biochemical change. In consequence, the osmotic pressure falls and the disc becomes less able to maintain hydration when loaded mechanically (Urban & Roberts 2003). Tissue fibrosis might happen concurrently, contributing to increase the relative amount of solid phase at the detriment of the fluid phase. Addressing the difficulty to explore experimentally the effect of these alterations on disc cell nutrition at the organ level, different finite element (FE) studies have been proposed.

Malandrino et al. (2011) studied the coupling between disc poromechanics and metabolic transport. They found that mechanical loads and tissue properties might affect significantly the distribution of oxygen and lactate when large and prolonged volume changes are involved. Also, the simulation results obtained by Galbusera et al. (2011) suggest that water loss inside the disc can induce cell death because of a reduced diffusion of nutrient and waste products. For a given disc geometry, a predominant impact of tissue consolidation on nutrition-related cell death was further reported based on the calculations results obtained by Malandrino et al. (2014a). Interestingly, Zhu et al. (2012) found that dynamic compression might limit nutrition-related cell death when degenerated disc properties were simulated, whilst earlier reported simulations suggested that dynamic loads limit the mechanically-induced water loss from the disc (Schmidt et al. 2010). However, none of the reported mechano-transport models incorporated explicit information about ECM composition, e.g. proteoglycan, collagen and water content, and the precise influence of ECM composition changes on IVD cell viability remains unaddressed.

In order to clarify the relationships between ECM composition, disc degeneration, nutrition, and cell viability, a comprehensive analysis is needed with explicit consideration of degeneration-dependent changes in proteoglycan, collagen and water. Schroeder et al. (2007) have reported an

osmoporoviscoelastic constitutive model for the AF and NP disc tissues, the parameters of which depended on the biochemical composition and organization of these tissues. For the first time, such a model allowed describing the internal mechanical conditions of the disc as a function of assessable ECM characteristics, through the FE method.

Accordingly, this Chapter aims to combine the respective assets of mechano-transport simulations and composition-based tissue modelling in the IVD, in order to study how degenerative changes in disc composition may affect cell nutrition under mechanical loads. The biochemical changes explored were based on previous measurements of collagen, proteoglycan and water contents in healthy and mildly-moderately (Pfirrmann grade III) degenerated discs. Numerical explorations were based on a systematic parametric analysis of the variation of these composition parameters, and metabolic transport results were extrapolated to the possible occurrence of nutrition-induced cell death.

4.2 Materials and methods

4.2.1 Composition-based disc model

A L4-L5 IVD model including the NP, the AF, the TZ and the CEP was used (Figure 4.1) (See Chapter 3). For the NP, the TZ, and the AF, tissue constitutive models described the poromechanical interactions between a hyperelastic porous matrix, saturated by intra and extra-fibrillar fluid, a swelling pressure simulated the Donnan osmotic effects, and viscoelastic collagen fibres (AF only) (Roberts & Urban 2011; Schroeder et al. 2007). The total stress tensor, $\boldsymbol{\sigma}$, was given by the sum of a pore pressure component p and the effective stress of the porous solid skeleton, $\boldsymbol{\sigma_{eff}}$:

$$\boldsymbol{\sigma} = \boldsymbol{\sigma_{eff}} - p\boldsymbol{I} \quad \textbf{(4.1)}$$

where $\boldsymbol{I}$ is the identity tensor and where the pore pressure, p, is the sum of the water chemical potential, u_w, and a swelling pressure term $\Delta\pi$ (Schroeder et al. 2007):

$$p = u_w + \Delta\pi \quad \textbf{(4.2)}$$

The macroscopic stress-strain response of the solid matrix was controlled by a small strain shear modulus (G_m), an initial solid fraction ($n_{s,0}$) and by the current deformation of the homogenised poroeleastic continuum. A modified neo-Hookean model was used to describe the finite strain behaviour of the material (Schroeder et al. 2007):

$$\boldsymbol{\sigma_{eff}} = -\frac{1}{6}\frac{Ln(J)}{J}G_m\boldsymbol{I}\left[-1+\frac{3\left(J+n_{s,0}\right)}{\left(-J+n_{s,0}\right)}+\frac{3JLn(J)n_{s,0}}{\left(-J+n_{s,0}\right)^2}\right]+\frac{G_m}{J}\left(\boldsymbol{B}-J^{2/3}\boldsymbol{I}\right) \qquad \textbf{(4.3)}$$

where J is the determinant of the deformation gradient tensor $\boldsymbol{F}$, $\boldsymbol{I}$ is the first invariant the left Cauchy-Green strain tensor $\boldsymbol{B}$.

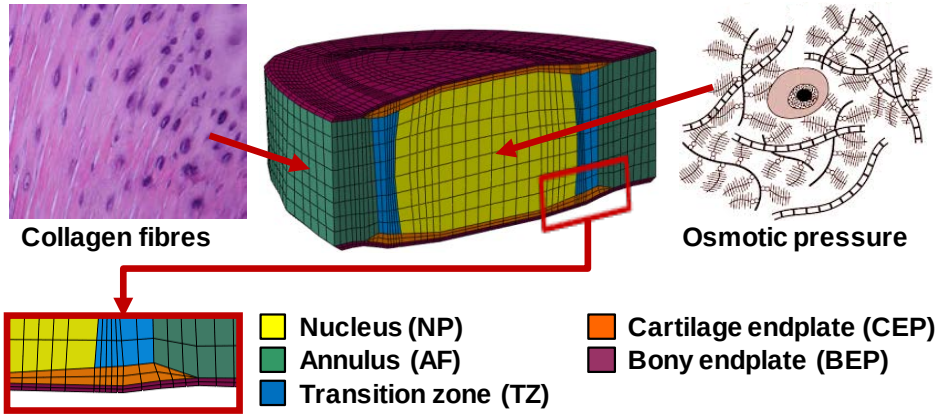

Figure 4.1: L4-L5 finite element disc model with all sub-tissues: nucleus pulposus (NP), annulus fibrosus (AF), transition zone (TZ), cartilage endplates (CEP) and bony endplates (BEP). Donnan osmotic pressure is included at the nucleus and the collagen fibres reinforcement in the annulus.

In Eq. 4.2, u_w was related to the velocity of the interstitial fluid through the permeability, by applying Darcy's law. As for the osmotic pressure gradient $\Delta\pi$, it was given by the expression (Schroeder et al. 2007):

$$\Delta\pi = \phi_{int}RT\left(\sqrt{c_{F,exf}^2+4\left(\frac{\gamma_{ext}^{\pm}}{\gamma_{int}^{\pm}}\right)^2 c_{ext}^2}\right)-2\phi_{ext}RTc_{ext} \qquad \textbf{(4.4)}$$

where ϕ_{int} and ϕ_{ext} are the internal and external osmotic coefficients respectively, γ_{int} and γ_{ext} are the internal and external activity coefficients, c_{ext} is the external concentration of salt and $c_{F,exf}$ is the effective proteoglycan fixed charge density that depends on both the extra-fibrillar water (n_{exf}) and the apparent fixed charge density c_F that is expressed in mEq/mL of the total fluid, according to the expression:

$$c_{F,exf} = \frac{n_f c_F}{n_{exf}} \tag{4.5}$$

with,

$$c_F = c_{F0}\left(\frac{n_{F0}}{n_{F0} - 1 + J}\right) \tag{4.6}$$

where c_{F0} and n_{F0} are the initial fixed charge density and initial water content respectively and J is the volumetric deformation of the tissue. The extra-fibrillar water is given by:

$$n_{exf} = n_f - \varphi_{ci}\rho_{c,tot} \tag{4.7}$$

where n_f is the total fraction of water, φ_{ci} is a parameter that defines the intrafibrillar water per unit of collagen mass, and $\rho_{c,tot}$ is the collagen content with respect to the total wet weight. The strain-dependent hydraulic permeability of the tissue, κ , is considered that depends on the extra-fibrillar water according to the expression (Schroeder et al. 2007):

$$\kappa = \alpha\left(1 - n_{exf}\right)^{-M} \tag{4.8}$$

where α stands for an initial permeability at zero strain, and M is a positive constant.

The collagen fibres in the AF were considered to have a unidirectional viscoelastic mechanical response, simulated with a Zener rheological model that was modified in order to account for finite strains through two nonlinear springs (Schroeder et al. 2007).

4.2.2 Transport and cell viability model

The composition-based disc model was coupled to the transport model developed by Malandrino et al. (2011; 2015a). The model considers the diffusion-reaction of oxygen, lactate and glucose:

$$\frac{\partial}{\partial t}\begin{pmatrix} C_{O_2} \\ C_{lact} \\ C_{gluc} \end{pmatrix} - \begin{pmatrix} D_{O_2} & 0 & 0 \\ 0 & D_{lact} & 0 \\ 0 & 0 & D_{gluc} \end{pmatrix} \nabla^2 \begin{pmatrix} C_{O_2} \\ C_{lact} \\ C_{gluc} \end{pmatrix} = \begin{pmatrix} R_{O_2} \\ R_{lact} \\ R_{gluc} \end{pmatrix} \tag{4.9}$$

where C_i, D_i and R_i are the concentrations, tissue diffusion coefficients, and the reactions of oxygen ($i = O_2$), lactate ($i = lact$) and glucose ($i = gluc$) respectively.

Tissue deformations and interstitial fluid flow were linked to the reactive transport of these solutes through integration of the mechanically-induced changes in porosity and fluid velocity, as calculated through the poromechanical equations. Moreover, the diffusion coefficients of the solutes were assumed strain dependent (Mackie & Meares 1955):

$$\boldsymbol{D}_{solute} = \left(\frac{n_f}{2 - n_f}\right)^2 D_{water}\boldsymbol{I} \tag{4.10}$$

where $\boldsymbol{D}_{solute}$ is the tissue diffusivity, n_f is the update water content of the tissue, D_{water} is the diffusivity of the tissue in water, and $\boldsymbol{I}$ is the first invariant of the left Cauchy-Green strain tensor $\boldsymbol{B}$.

As for the metabolic reactions, the model included the system of reactions reported by Bibby et al. (2005):

- Oxygen cell consumption

$$R_{O_2} = -n_f \frac{7.28\rho_{cell}}{S_{O_2}}\left(\frac{C_{O_2}(pH - 4.95)}{1.46 + C_{O_2} + 4.03(pH - 4.95)}\right) \tag{4.11}$$

- Lactate production (per unit of fluid volume)

$$R_{lact} = \rho_{cell} exp\left[-2.47 + 0.93pH + 0.16C_{O_2} - 0.0058\left(C_{O_2}\right)^2\right] \tag{4.12}$$

- Glucose consumption

$$R_{gluc} = -\frac{1}{2}R_{lact} \tag{4.13}$$

where R_{O_2} is in kPa/h, R_{lact} is in nmol/(mLh), R_{gluc} is in nmol/(mLh) , ρ_{cell} is the cell density of the tissue, C_{O_2} is the oxygen concentration in kPa. The pH was linked to the lactate concentration, C_{lact} (in nmol/mL), by the expression (Mokhbi Soukane et al. 2009):

$$pH = 7.4 - 0.09C_{lact} \tag{4.14}$$

which is a linearization of experimental results of pH decay with lactate accumulation (Bibby et al. 2005).

The cell viability was considered as the ratio $\rho_{cell}/\rho_{cell,0}$, being $\rho_{cell,0}$ the initial cell density, before any cell death occurs with tissue-specific values taken from the literature (Bibby & Urban 2004) (Table 4.1). Cell density change over

time was based on the experimental study of Horner & Urban (2001), where cells in wells start to die exponentially without glucose and when the pH is acid. Thereby, the cell density was given by this expression:

$$\rho_{cell} = \rho_{cell,0}\exp(-\alpha_i t) \quad \textbf{(4.15)}$$

where the death rate for pH (α_{pH}) is constant and equal to $3.43 \times 10^{-6}\ s^{-1}$, and the rate for glucose (α_{gluc}) is $9.28 \times 10^{-6}\ s^{-1}$. These constants were directly derived by curve fitting, from the experiment of cells performed by Horner and Urban (2001) and ensured an accurate representation of the spatiotemporal cell death patterns for cell density values relevant to the IVD, i.e. $4x10^6$ cells/mL and $8\ x10^6$ cells/mL (Malandrino et al. 2015a). The viability criteria were taken from previous studies (Bibby & Urban 2004), where exponential decays start when: a) the glucose concentration decreases below 0.5 nmol/mL, b) the pH value is below 6.8 and c) both glucose and pH are below their critical values.

4.2.3 Boundary conditions

A day cycle of 8 hours of rest under 150 N compressive load and 16 hours of activity under 800 N in compression was repeated for three days (Wilke et al. 1999). The load was applied at the upper bony endplate while the lower bony endplate was fixed. External pressure was nil. Oxygen, lactate and glucose concentrations were applied at the outer surfaces of the CEP and of the AF (Figure 4.2a), and literature-based values (Maroudas et al. 1975; Urban & Maroudas 1979; Holm et al. 1981) were used (Table 4.1). Before simulating the effect of any mechanical load, the transport model was initialized to achieve steady state solute concentrations throughout the IVD model. Transport parameters and cell viability were evaluated along the mid sagittal plane path: NP centre, anterior and posterior AF (Figure 4.2b).

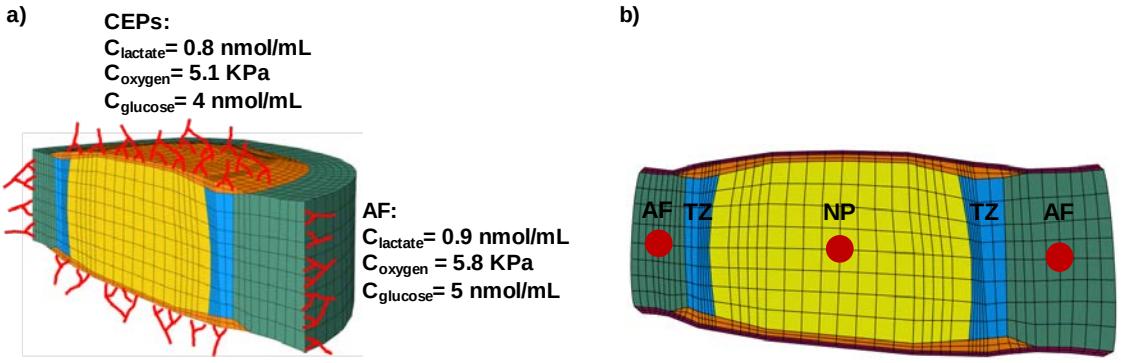

Figure 4.2: a) Solute boundary conditions applied at the surfaces of the AF and CEP and b) Points selected for nutrition-cell viability evaluation: posterior annulus centre (left side), nucleus centre and anterior annulus centre (right side)

Table 4.1: Transport-cell viability parameters applied: oxygen concentration (C_{O_2}), lactate concentration (C_{lact}), glucose concentration (C_{gluc}) and cell density (ρ_{cell})

Tissue	Boundary conditions at the edge			Initial condition
	C_{O_2} (kPa)	C_{lact} (nmol/mL)	C_{gluc} (nmol/mL)	ρ_{cell} (10^6 cells/mm^3)
CEP	5.1	0.8	4	0.0135
AF	5.8	0.9	5	0.00555

4.2.4 Design of experiment

A design of experiment (DOE) using a fractional factorial statistical method was performed, and variations were defined for the following biochemical parameters of the composition-based AF and NP models (Eqs. 4.4, 4.5, 4.6 and 4.7): initial water content (n_{F0}), initial fixed charge density (c_{F0}) and collagen content ($\rho_{c,tot}$) (Table 4.2). For each parameter, variations in the DOE consisted in a switch between an upper level and a lower level parameter value. While upper level values corresponded to the composition data measured for Pfirrmann grade I IVDs, lower level values corresponded to grade III IVDs (Pfirrmann et al. 2001). Both the biochemical analysis and the grading of the IVD have been performed in a parallel study according to standard methods (Dao et al. 2014).

Table 4.2: Design of experiment parameters and values: annulus initial water content (n_{F0} AF), annulus collagen content ($\rho_{c,tot}$ AF), nucleus initial water content (n_{F0} NP), nucleus initial fixed charge density (c_{F0} NP) and nucleus collagen content ($\rho_{c,tot}$ NP)

Level	n_{F0} AF (*)	$\rho_{c,tot}$ AF (**)	n_{F0} NP (*)	c_{F0} NP (mEq/mL)	$\rho_{c,tot}$ NP (**)
Grade I	0.75	0.65	0.80	0.30	0.15
Grade III	0.70	0.78	0.76	0.23	0.28

* Fraction of wet weight ** Fraction of dry weight

A fractional factorial analysis of $2^{5-1} = 16$ runs was used, representing a resolution V. In fractional factorial designs, such a resolution allows thorough identification of the main effects, without any confusion with multiple factor interactions. The significance of each parameter effect was analysed statistically (Minitab Inc.) using an analysis of variance (ANOVA) with a significance threshold $\alpha = 0.05$. The standardized effect T_1 was calculated using the following equation:

$$T_1 = \frac{COEFF_1}{COEFF_{SE}} \quad \textbf{(4.16)}$$

where $COEFF_1$ is the effect coefficient of the parameter and $COEFF_{SE}$ is the standard error of the coefficient.

4.2.5 Convergence analysis and model validation under creep

The mesh convergence of the model was verified based on a comprehensive convergence study performed for the mesh template of the IVD model, including assessment of the stability of the poromechanical predictions (Chapter 3). However, the transport model was sensitive to the time step selected for the calculations. As such, an additional convergence study was performed for the time discretisation of the transport model, so as to obtain the best compromise between accuracy of the results and computational cost at the different time points selected for the DOE. In order to validate the composition-based model under compression, calculated disc height reductions achieved after creep were

compared to measurements reported in the literature after the experimental boundary conditions were simulated.

4.3 Results

After 900 s of creep under 500 N compressive load, a disc height reduction of 1.27 mm was calculated with the material properties representative of a grade I IVD (Figure 4.3). This result was within the range of 1 and 1.35 mm measured experimentally by Heuer et al. (2007) under similar load conditions. After 4 hours of creep under body weight, the same model predicted a height loss of 1.91 mm (Figure 4.3), in agreement with the range of values reported by Adams & Hutton (1983).

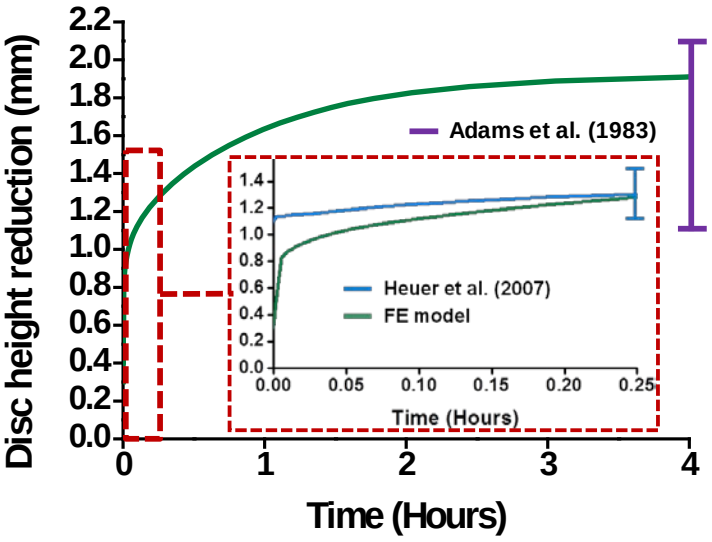

Figure 4.3: Predictions of disc height reduction performed with the composition-based model under 500 N of axial compression up to 4 hours (Adams et al. 1983). The zoom area represents the same results, from 0 to 900 s, according to the experiments reported by Heuer et al. (2007)

In terms of the convergence of the transport model, the simulation results for oxygen, at the NP centre, in the 16h of creep under 0.54 MPa of compression were very sensitive to the seize of the time increments. In order to find the best relation computational time-accuracy of the results, different approaches were tested: by dividing the 57600 second, i.e. 16 hours in:

A) 2 initial increments of 5 seconds followed by 10 increments of 5759 seconds each,

B) 2 initial increments of 5 seconds followed by 26 increments of 2215 seconds,

C) 2 increments of 2 seconds, 5 increments of 118 seconds and 10 increments of 5700,

D) 2 increments of 5 seconds, 5 increments of 118 seconds, 8 increments of 1425 and 10 increments of 4560 seconds, and

E) 2 increments of 5 seconds, 5 increments of 188 seconds and 103 increments of 550 seconds.

The Figure 4.4 shows that the Test E led to the best representation of solute evolution. However, the time of calculation for this case to simulate one day was higher than 72h. Since the transport outcomes will be evaluated at the end of the each day simulated, the Test C was selected to perform all transport simulations since it took less than 10 hours to simulate three loading days, and the relative difference of the outcomes between Test C and E was less than 0.003% at the end of one day simulated. In addition, the range solute concentrations obtained after the initialization of the transport model in the NP were: 2.3-4.5 kPa for oxygen, 1.3-3.2 nmol/mL for lactate and 2.5-3.7 nmol/mL for glucose.

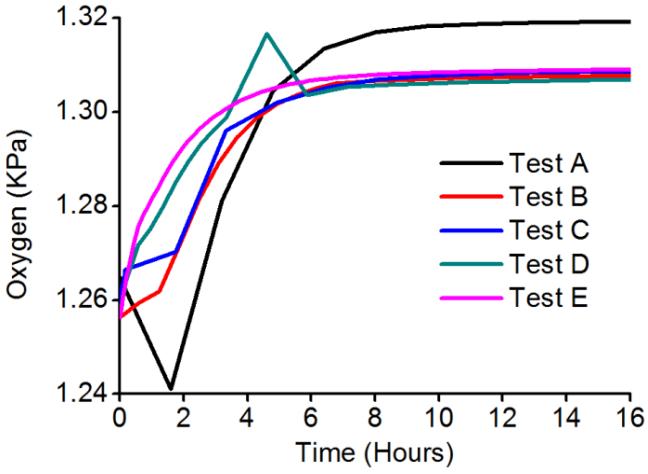

Figure 4.4: Oxygen concentration results at the NP centre along 16h of creep under 800N of compression for different test of time increment: test A) 2 increments of 5 seconds followed by 10 increments of 5759 seconds, test B) 2 increments of 5 seconds followed by 26 increments of 2215 seconds, test C) 2 increments of 2 seconds, 5 increments of 118 seconds and 10 increments of 5700, test D) 2 increments of 5 seconds, 5 increments of 118 seconds, 8 increments of 1425 and 10 increments of 4560 seconds, and test E) 2 increments of 5 seconds, 5 increments of 188 seconds and 103 increments of 550 seconds

None of the biochemical parameter variations defined, or combinations thereof, affected cell viability. As a result, 100% of cells remained alive during the three days simulated, for all the simulations that resulted from the DOE. In terms of solute distributions, using any (combination of) lower level (i.e. degenerated) parameter values always led to decreased levels of oxygen and glucose and increased levels of lactate. Also, DOE results showed that the biochemical composition parameter that affected most the transport of all disc solutes, in a particular tissue region, was the local initial water content. In terms of oxygen reduction, the NP centre was the most affected region with a standardized effect of 206, followed by the anterior AF with 87 and finally the posterior AF with 83 (Figure 4.5a). Similar results were obtained for the increase of lactate; however, standardized effects were lower than for the oxygen (Figure 4.5). In terms of glucose, the most affected zone was the anterior AF with a standardized effect of 455, followed by the posterior AF with 218 and the NP centre with 215 (Figure 4.5c).

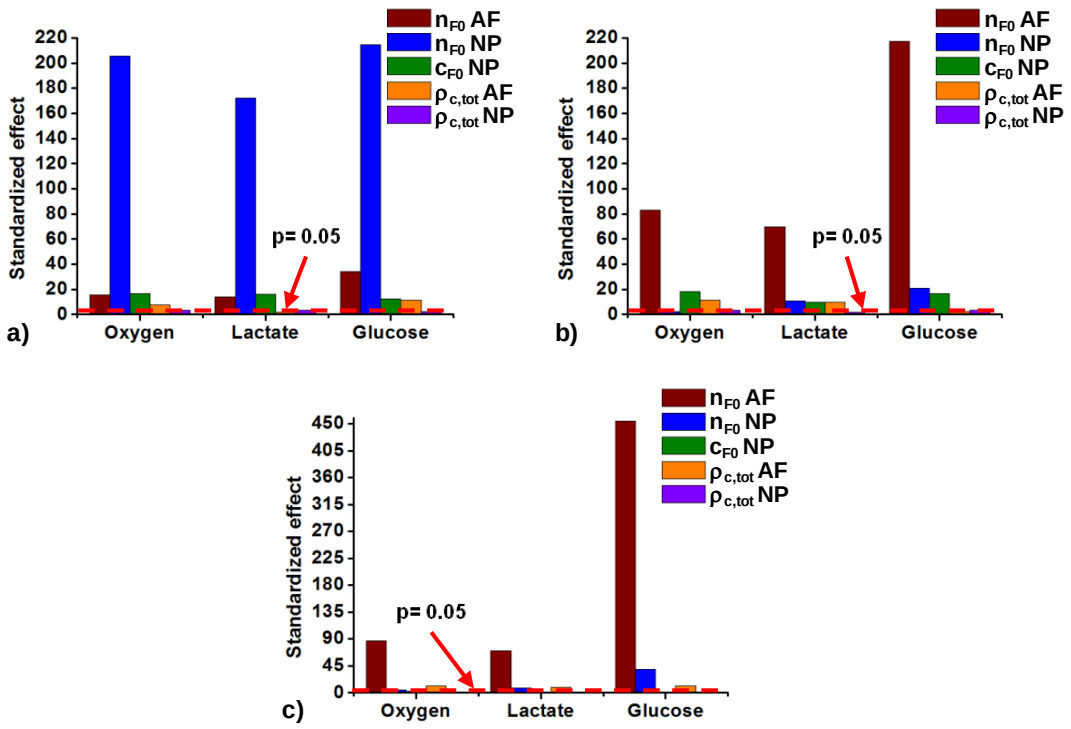

Figure 4.5: Standardized effect of disc composition parameters variation from grade I to grade III, after 3 days of simulation, on oxygen, lactate and glucose concentrations at: a) NP centre, b) posterior AF and c) anterior AF (Dashed horizontal line is the threshold of significance)

Analysing the solute distributions along the mid-sagittal plane after three days, the 16 created models led to a reduced number of groups of results in terms of regional solute concentration (Figure 4.6). In the AF, four groups were unequivocally defined (Figure 4.6a) according to different combinations of initial water contents in the different IVD tissues, e.g. per order of decreasing glucose concentrations:

- Group 1: n_{F0} AF and n_{F0} NP representative of grade I
- Group 2: n_{F0} AF representative of grade I and n_{F0} NP representative of grade III
- Group 3: n_{F0} AF representative of grade III and n_{F0} NP representative of grade I
- Group 4: n_{F0} AF and n_{F0} NP representative of grade III

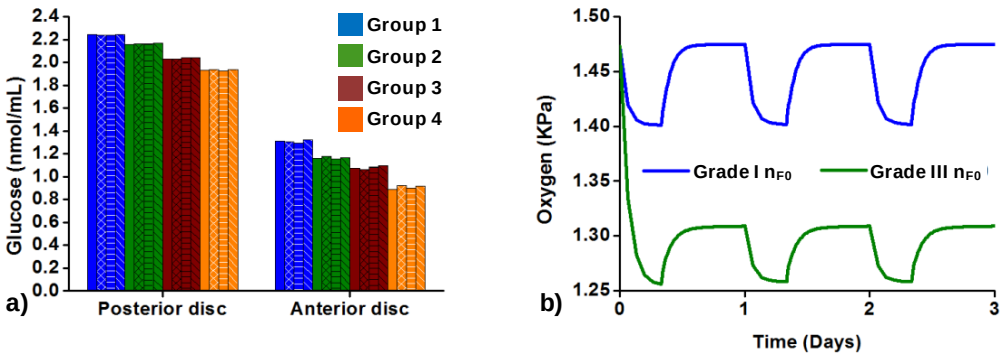

Figure 4.6: Effect of initial water content (n_{F0}) variations on IVD solute concentrations: a) glucose at the sagittal plane (day 3). The figure shows the groups of results formed according to the initial water contents of the tissues; group 1: both n_{F0} AF and n_{F0} NP of grade I, group 2: n_{F0} AF of grade I and n_{F0} NP of grade III, group 3: n_{F0} AF of grade III and n_{F0} NP of grade I and group 4: both n_{F0} AF and n_{F0} NP of grade III and b) oxygen at NP centre along three days of simulation. Two groups of results are identified; one with high oxygen content corresponding to simulations with n_{F0} NP of grade I and another group with lower oxygen content corresponding to the results with n_{F0} NP of grade III

In the NP, two groups of results were identified, as illustrated in Figure 4.6b in terms of evolution of the oxygen content over three days at the centre of the tissue. The group with high oxygen concentration corresponded to simulations with a NP initial water content representative of grade I, i.e. simulations from the Groups 1 and 3 defined above. In contrast, the group with lower oxygen concentrations gathered the simulation results with NP initial water content representative of grade III (Groups 2 and 4).

In addition to the direct effects of local composition changes, the ANOVA results also showed that the glucose content in the anterior AF was strongly influenced by the initial water content of the NP (Figure 4.7a). However in the posterior AF, the glucose distribution was significantly affected by both the initial water content and the fixed charge density of the NP, and the effect of the local collagen was relatively limited (Figure 4.7b).

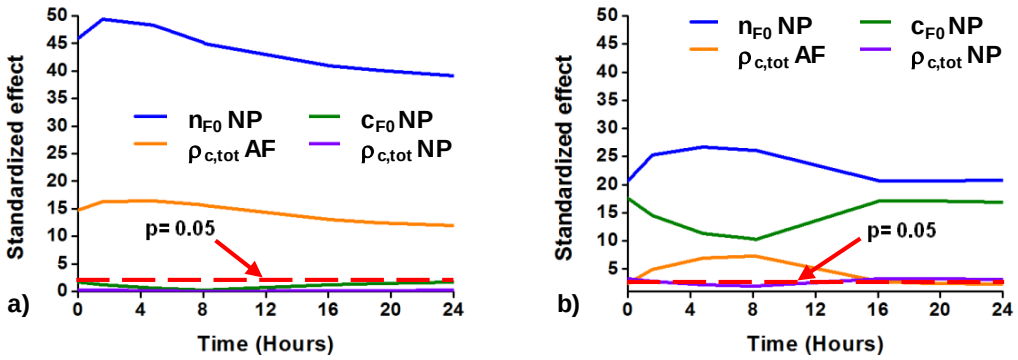

Figure 4.7: Evolution of the effect of composition parameter variation of the nucleus (n_{F0} NP, c_{F0} NP and $\rho_{c,tot}$ NP) and annulus ($\rho_{c,tot}$ AF) on glucose concentration during a day at: a) the anterior AF and b) the posterior AF. (Dashed horizontal line is the threshold of significance)

All the biochemical changes simulated in this study affected the diurnal height loss after three days. Both at the NP centre and in the posterior AF, the initial fixed charge density of the NP was the parameter that influenced most the disc height (Figure 4.8). For the anterior AF, the AF initial water content was the most relevant parameter followed by the initial fixed charged density of the NP.

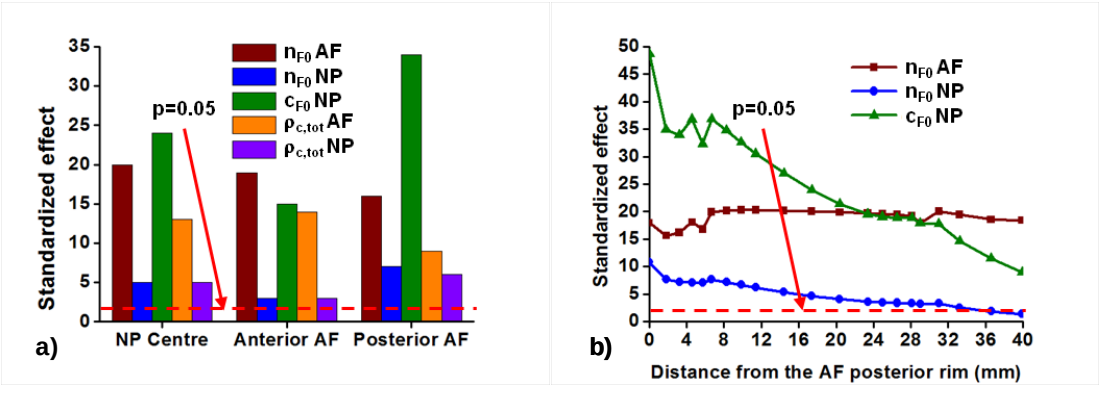

Figure 4.8: Effect of disc composition parameters (annulus initial water content (n_{F0} AF), annulus collagen content ($\rho_{c,tot}$ AF), nucleus initial water content (n_{F0} NP), nucleus initial fixed charge density (c_{F0} NP), and nucleus collagen content ($\rho_{c,tot}$ NP)) variation on daily disc height: a) after 3 days simulated and b) at the sagittal plane (day 3). (Dashed horizontal line is the threshold of significance)

4.4 Discussion

The osmo-poroviscohyperelastic formulation used in this study was duly verified against thermodynamical consistency (Huyghe et al. 2009). At the tissue level, the model was also validated, with parameter values that represented healthy tissues (Schroeder et al. 2007). In terms of organ validation, the amount of creep measurements available in the literature is limited. In the report of their experimental study, Adams & Hutton (1983) mentioned that the used compressive boundary load corresponded to the body weight, but they did not give any specific value. Hence, it was taken a generic value of 500 N of compressive load (Wilke et al. 1999) in order to simulate their creep experiment. Assuming that this approximation is acceptable, our results showed that the healthy model extrapolated up to 4 hours the behaviour obtained from the simulation of 15 minutes of creep, validated against the measurements reported by Heuer et al. (2007).

As for the validity of the degenerated models, this study did not aim to simulate a degenerated disc, but aimed to identify those composition changes that might affect the nutrition of the cells along degeneration, based on biochemically measured quantities. Hence, the variations of phenomenological tissue model parameters such as the stiffness moduli and the permeability were not taken into account. This approximation allowed focusing the design of experiments on the composition, and was supported by a previous sensitivity analysis reported by Malandrino et al. (2011): by using a similar mechano-transport model, the authors showed that the porosity and the osmotic pressure were the osmo-poromechanical parameters that mostly affected the nutrient transport, being the effect of the stiffness and the permeability parameters negligible. This outcome was confirmed through a previous sensitivity analysis that included α and G_m, according to Eqs 4.8, and 4.3, respectively (results not shown). Hence, the exploration of the effect of composition changes on the transport of nutrients effectively targeted those tissue model components, i.e. the porosity and the osmotic pressure, most relevant to the metabolic transport calculations.

Solute contents were always decreased with degenerative composition changes, but the minimum glucose and pH values were 0.76 nmol/mL and 6.90

respectively, which did not exceed the critical values that would lead to cell death (Horner & Urban 2001). Accordingly, cell viability remained 100% for all the simulations performed during the three days simulated. Glucose and pH thresholds used for cell viability were taken from *in vitro* experiments (Horner & Urban 2001). It is difficult to know whether these thresholds are valid *in vivo*, since no related investigations have been reported so far. However, these criteria have been already used in many numerical studies that have explored the possible role of nutrition in disc degeneration. Malandrino et al. (2014a) used a 3D mechano-transport model to study the mechanical effects on cell viability via transport variations, depending on simulated CEP calcification, AF and NP tissue degeneration, and disc height reduction. Though their tissue constitutive modelling was different from this study, their results supported our findings that moderate AF and NP degeneration only is unlikely to lead to critical glucose levels under physiological load magnitudes and for generic disc geometries.

The calculations of Malandrino et al. (2014a) suggested that simulating CEP calcification (50%) was necessary in order to predict cell death, the latter occurring because of an increased lack of glucose in the inner AF. These results were qualitatively similar to those achieved by Zhu et al. (2012) with a slightly different cell viability function, in which pH was not an explicit trigger of cell death and where cell death rate (i.e. α_{gluc} in Eq. 4.15) was a nonlinear function of the current glucose concentration. The studies of Shirazi-Adl et al. (2010) and Jackson et al. (2011a) reported loss of cell viability due to changes in disc composition. Both studies simulated CEP calcification to observe cell death. The first study reduced by 40% the CEP permeability, and the second study reduced by 50% CEP water content. In this Chapter the CEP composition was not changed in order to focus on the AF and NP degeneration that, as mentioned before, lead to critical glucose concentrations. The effect that changes in CEP composition have on disc nutrition will be explored in Chapter 6. In all the studies mentioned above, the experiment-based critical glucose concentration of 0.5 mM was the most important assumption for cell death predictions, and all results suggested that nutrition-induced cell death might not be linked to AF and NP degeneration. While this study used a similar assumption, and led to a similar outcome, the new model

allowed a refined control of the specific degeneration changes that may alter cell nutrition in the different tissue.

Supporting these results, several simulation reports pointed out that the glucose concentration in inner AF is easily affected by any simulated degenerative change (Galbusera et al. 2011b; Zhu et al. 2012; Malandrino et al. 2014a). This phenomenon was largely attributed to the strong local consolidation of the TZ regions, due to the lateral pressure exerted on the fibre-reinforced AF by the lateral expansion of the NP under mechanical loads (Chapter 3). Among the different mechano-transport cell viability studies published, our full 3D simulations can be compared directly to the work reported by Malandrino et al. (2011; 2014a), with the same model geometry. Whilst using a porohyperelastic constitutive model with a fixed osmotic pressure in the NP, these authors always identified the inner anterior AF as the disc region where glucose concentration was mostly reduced. In contrast, it was predicted that the cumulated effect of water and proteoglycan loss within the NP was particularly critical to the availability of glucose in the posterior AF. Interestingly, this issue seemed to arise from the particularly high impact of NP proteoglycan loss on disc height reduction and increased tissue consolidation in the TZ of the posterior AF area. Acknowledging that limited glucose can trigger inflammatory and catabolic responses by disc cells (Neidlinger-Wilke et al. 2012), it may be inferred that early NP degeneration might contribute to weaken biochemically the posterior AF due to local nutrition issues. Confirmation of this possible non-mechanical weakening would require, however, experimental data about disc cell catabolic activity for different glucose contents between 0.5 and 5 mM.

The composition-based model reproduced the expected disc height reduction under compression changes due to ECM degeneration, but it was not considered permanent disc height loss. Such a consideration could have modified slightly the computed influence of the diffusion distances (Galbusera et al. 2011b; Malandrino et al. 2011). However, this issue is not expected to have a major impact on the current study, since the influence of tissue consolidation is probably predominant, for our particular disc model geometry, as suggested by Malandrino et al. (2011) and further discussed in the next paragraph. Endplate sclerosis was not considered either. Whereas Zhang et al. (2008) considered that this condition

rarely appears in grade III discs, Benneker et al. (2005) reported that sclerosis in grade III discs is frequently found. As mentioned earlier, several authors of numerical studies have simulated CEP sclerosis, but the way to do it is not clear, especially for a specific grade, and exploring such simulation hypothesis is beyond the scope of this Chapter.

Overall, the initial water content is the parameter of disc composition that affected most the transport of solute at the end of the three days simulated. The most affected solute was glucose, especially in the anterior AF. This trend did not change when an ANOVA was performed at the end of each simulated day. The predominant influence of water content is supported by earlier sensitivity studies where a decrease in porosity was reported to affect the transport of oxygen and lactate, more than any other poromechanical parameters did (Malandrino et al. 2011). Simulated composition changes led to disc height reductions in the mechanically loaded disc models, which reduced the effective diffusion distances. However, our results revealed that without any initial disc height reduction in an unconsolidated state, the possible benefits for diffusion of the mechanically induced height reduction are largely countered by increased tissue consolidation, i.e. decreased current porosity. Though a similar outcome was suggested by Galbusera et al. (2011b) through a parameterization of the porosity and of diffusion coefficients, our diffusion coefficients were porosity-dependent and obeyed to a Mackie-Meares diffusivity law (Malandrino et al. 2011). According to this law (see Eq. 4.9), the porosity reduction due to consolidation decreased the diffusivity of all solutes. This effect combined to the fact that the diffusion coefficient of glucose was about three times lower than oxygen, might explain why glucose was the most affected solute. Hence, our approach was physically reasonable especially due to a likely effect of constrictivity (Holzer et al. 2012), which depends on the ratio between the diameter of the particle that diffuses and the pore diameter. Nevertheless, other laws have been proposed (Zhu et al. 2012), and their relative effects might have to be assessed.

As anticipated earlier, the simulated degenerative changes in the NP may affect the AF nutrition. In the anterior AF, the effect of n_{F0} in the NP was 39 at the end of one simulated day. This standardized effect was higher than the separate effect of each NP parameter on the glucose concentration in the posterior AF, i.e.

21 for n_{F0}, 17 for c_{F0} and 3 for $\rho_{c,tot}$. However, combining the respective effects of all NP parameters at the posterior AF gave a cumulative effect of 41, slightly higher than the global effect of NP alterations on the anterior AF. According to measurements (Iatridis et al. 2007), NP desiccation and proteoglycan depletion would be concomitant in mildly to moderately degenerated discs, and our findings suggest that such a situation exposes particularly the posterior AF. According to the hypothesis of possible biochemical AF weakening made earlier, such impact of NP alteration on the AF may contribute to explain mechanistically why radial tears in the posterior AF mostly appear in moderately to severely degenerated discs (Osti et al. 1992). Interestingly, calculations indicated that NP dehydration alone affected both the posterior and anterior AF. Here, it becomes worth to mention the possible effect of any early loss of CEP functionality that might contribute to reduce the NP water content by altering the balance of water in-flow and out-flow along daily loading (Ayotte et al. 2001). Hence, assuming that early NP dehydration is possible, our simulations raise the question whether nutrition issues could play a role in the occurrence of circumferential tears, already present in both the anterior and posterior AF of normal to moderately degenerated discs (Osti et al. 1992).

This study has the following limitations: first, the three days chosen for the simulations might not be enough for reaching a steady-state cell viability; although it was found that the simulation of two days was enough to observe cell death with a calcified CEP (data not shown) (Malandrino et al. 2014a). Second, dynamic load variations were not simulated around the mean load value chosen for daily activity. These loads might limit the loss of water (Schmidt et al. 2010) and could favour the transport of nutrients (Zhu et al. 2012). However, simulating dynamic loads would have increased the computational cost, and earlier studies (Zhu et al. 2012) suggest that it would not have changed our interpretations. Third, no local variations in proteoglycan concentration and in total amount of collagen were considered within each modelled tissue. Though such a variation could have better informed the suggested sensitivity of the posterior AF in relation to the anterior AF, our model was based on degeneration-specific composition measurements, made available for this study. Finally, the effect of other important factors related to disc nutrition, e.g. inflammatory factors (Lotz & Ulrich 2006) was not

considered, while necessary to assess whether the local nutrient deprivation calculated can weaken the tissues.

4.5 Conclusions

This chapter presented a composition-based model coupled to a transport-cell viability model as a tool to explore the influence of measured ECM changes on disc nutrition and cell viability. This study suggested that small degenerative ECM changes may produce significant solutes alterations. While these changes between grade I and grade III degeneration did not seem relevant to nutrition-related cell viability, they allowed identifying possible mechanisms related to known AF alterations along degeneration. The computational approach developed here provides a powerful tool to achieve improved understanding of disc degenerative mechanisms. Furthermore, the results suggest that NP dehydration can significantly reduce the availability of nutrient to cells in particular disc regions, independently on any degeneration-related proteoglycan depletion. Should such reduced availability of nutrients be sufficiently high to trigger catabolic cell activity, early NP dehydration should become a primary target in disc. Also, changes in solute concentrations affects the proteoglycan content, which will alter the indirect mechanotransduction phenomena, such aspect will be study in the next Chapter. The simulations performed in this Chapter could also be highly relevant for the design of biomimetic IVD implants or scaffold materials in disc regenerative therapies (Noailly et al. 2014).

5 MODELLING OF THE EVOLUTION OF PROTEOGLYCAN DISC CONTENT WITH AGEING

In Chapter 4, it was found that the local water content of disc tissues was the main responsible for alterations in disc nutrition. Whereas nucleus dehydration affected the nutrition of all annulus regions, the nucleus proteoglycan depletion particularly affected posterior annulus nutrition. In the present chapter a new formulation is developed, implemented and tested for the proteoglycan content. It takes into account the synthesis and breakdown of the proteoglycans. This formulation aims to explore how disc nutrition can affect the proteoglycan content, which in consequence, can produce alterations in disc nutrition and cell viability. The composition-transport model described in Chapter 4 was modified in this Chapter. This former mechano-transport model was solved sequentially, and the transport analysis required a previous complete mechanical analysis to obtain the fully history of global and local deformations. This approach did not permit to see how the changes in disc nutrition may affect disc mechanical behaviour. In the present Chapter, an iterative coupling of the mechano-transport simulations allowed to observe both the effect of changes in composition in the transport of nutrient, and the effect of changes in solutes transport on the disc mechanical behaviour. The results revealed that nutrition affected the proteoglycan content in the NP. Whereas the reduction of proteoglycan alters disc mechanical behaviour, it did not affect disc nutrition. However the addition of NP dehydration altered disc nutrition, possibly activating catabolic enzyme expression within the NP. The results showed a possible path to understand the role of nutrition in disc degeneration.

The work developed in this chapter led to the manuscript Ruiz Wills, C., Malandrino, A., Lacroix, D., and Noailly, J. (2014) Simulating proteoglycan turnover and cell viability in the intervertebral disc: a numerical exploration of nutrition-induced changes along degeneration.

5.1 Introduction

The proteoglycan loss in the nucleus is reported as the most important biochemical change that occurs in disc degeneration (Urban & Roberts 2003). The underlying paradigm is that the loss of proteoglycans reduces nucleus swelling capability, which threatens disc hydration. In consequence, the shape and volume of the disc change, affecting the effective absorption and distribution of loads (Cassinelli et al. 2001; Urban & Roberts 2003). Also, the water loss would influence the exchange of solutes through the disc boundaries, and would alter disc cell nutrition, therefore (Urban & Roberts 2003). The likeliness of the relation between disc cell nutrition and disc hydration was confirmed by the simulations performed in Chapter 4.

Previous studies suggested that the fall in nutrient supply is one of principal causes of the catabolism of the proteoglycans (Rinkler et al. 2010; Neidlinger-Wilke et al. 2012). Neidlinger-Wilke et al. (2012) found that low solute concentrations activate the expression of enzymes, e.g. matrix metalloproteinase (MMP), especially MMP-3 that breakdown the disc matrix. Although this evidence arose from *in vitro* experiment, it is unclear whether it holds true for the whole disc organ *in vivo*. Moreover, the fall in nutrient supply produces a reduction of the oxygen concentration inside the disc, and low oxygen levels reduce the proteoglycans synthesis, especially by nucleus cells (Ishihara & Urban 1999). Additionally, when the levels of pH and glucose decreased below some critical values the disc cells start to die (Horner & Urban 2001; Bibby & Urban 2004).

Hence, two interconnected processes can be identified. On one hand, the proteoglycan loss associated with degeneration could affect disc cell nutrition. On the other hand, lack of nutrients can activate the expression of enzymes that breakdown the proteoglycans. In consequence, both processes might forms a vicious cycle with occurrence of cell death from further nutrition reduction, along with an increment in the rate of reduction of matrix synthesis when loads increase. However, it is still unclear whether the lack of nutrition is a main cause for disc degeneration, as represented by proteoglycan depletion, or whether it only accelerates degeneration once the latter has already initiated.

Understanding the possible paths between disc degeneration and disc nutrition requires a comprehensive analysis. It is known that it is difficult to study disc degeneration experimentally because there is a lack of good animal models, also there are many anatomical differences between humans and the animals used in the lab as models (Alini et al. 2008; Sun et al. 2013), and integrated mechanisms are difficult to identify because of a limited capacity to perform local in situ measurements . Therefore, finite element (FE) models are frequently used to complement experimental studies, providing information that help to understand degeneration mechanisms and disc nutrition issues. For example, Zhu et al. (2012) used a 3D disc model and found that dynamic loads did not alter the cell viability in healthy disc representations, but increased cell survival in degenerated disc models. Malandrino et al. (2014a) used a mechano-transport 3D model to show that mechanical deformations increase cell death at the inner annulus zone, and that such effect was accentuated in degenerated disc. In Chapter 4, by using a composition-transport-cell viability disc model, it was found that degenerative changes in disc extracellular matrix alters solute concentrations. Although those studies provide valuable information about the effect of degeneration on disc nutrition and cell viability, they do not consider how nutrition might affect disc degeneration. Thus, this Chapter aimed to explore the effect of the loss of proteoglycans on cell viability via disc nutrition by using an iteratively coupled composition-transport-cell viability FE disc model that includes a novel formulation for the content of proteoglycans.

5.2 Materials and methods

5.2.1 Iterative composition-transport disc model

The L4-L5 IVD composition-transport model developed in Chapter 4 was used (Figure. 4.1). In this model transport simulations were sequentially coupled to a mechanical model, the behaviour of which was controlled by tissue composition, e.g. water, proteoglycans and collagen.

The solid matrix and transport phenomena were modelled using the same formulation presented in Chapter 4 (from Eq. 4.1 to Eq. 4.14). Composition parameters for a mature healthy disc, i.e. for a disc of a person between 25-30

years old, were taken from the literature (Table 5.1)(Dao et al. 2014). The values for the transport model were taken from Table 4.1 of Chapter 4. Solute concentrations and cell viability were evaluated along the mid-sagittal plane path.

Table 5.1: Material properties for a full mature human disc

Parameter	Tissue	
	Nucleus	**Annulus**
Matrix shear modulus (MPa)	1	1
Initial fixed charge density (mEq/mL)	0.3	0.20
Initial water content (% of wet weight)	80	75
Collagen content (% of dry weight)	15	65
External salt concentration (mEq/mL)	0.15	0.15
α (mm^4/N.s)	0.00016	0.00016
Constant M	1.2	1.2

The mechano-transport simulation workflow presented in Chapter 4 was modified in order to capture the evolution of time-related changes of the ECM in the nucleus (Figure. 5.1). The mechanical analysis provided the current initial water content and deformations in the transport analysis. Within the transport analysis, oxygen, lactate, pH and glucose concentrations were updated including the cell density. And integrated mechanisms are difficult to identify because of a limited capacity to perform local in situ measurements Then, the initial fixed charge density (c_{F0}) was updated by considering the levels of oxygen and cell density, and the new value was used to reinitialize the mechanical model, closing the cycle, and initiating a next iteration.

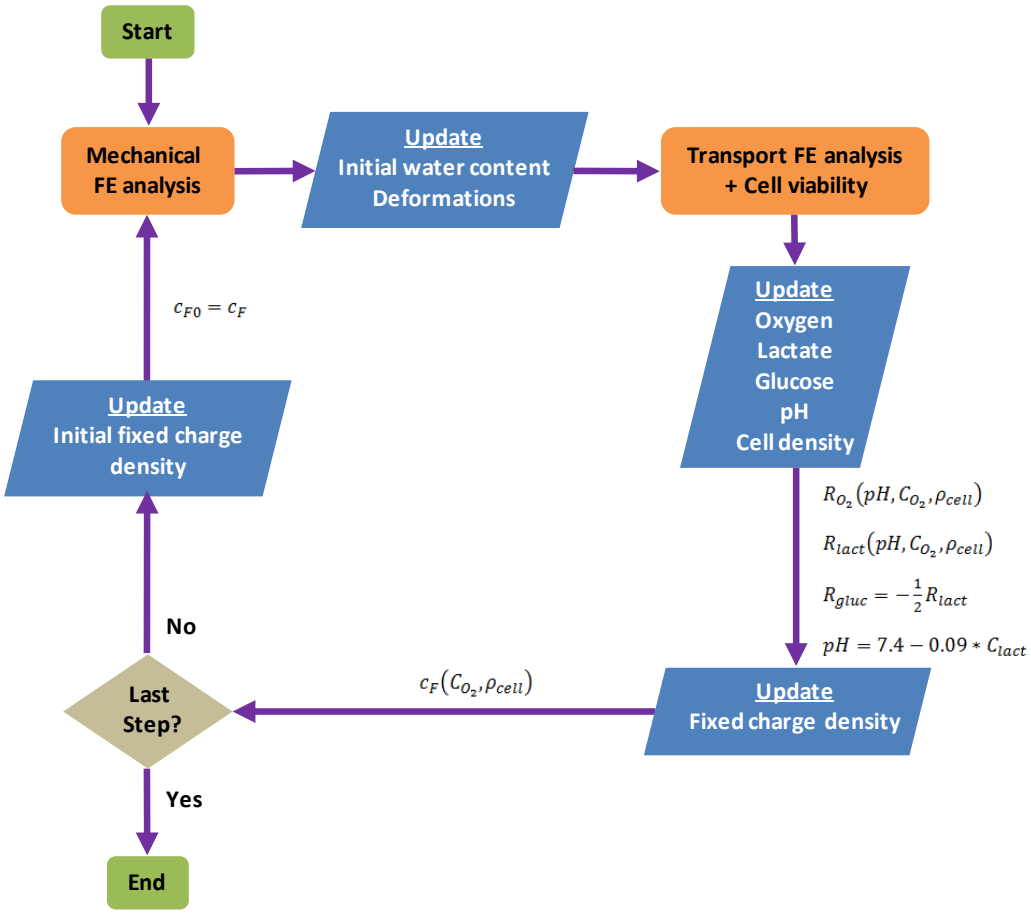

Figure 5.1: Scheme of the iterative composition-transport analysis: it starts with the mechanical analysis that provides the initial water content and deformations that the transport-cell viability analysis needs to update the consumption/production of solutes and cell density. Later, the updated oxygen concentration and cell density is used to update the initial fixed charge density (c_{F0}) needed by the mechanical analysis completing the cycle

5.2.2 Proteoglycan formulation

The initial fixed charge density (c_{F0} - related to the proteoglycans content) of the NP was updated inside the transport model (Figure 5.1). The total content of proteoglycans was expressed as the sum of two terms, one related to the half-life and another that considered production. Proteoglycan decay due to half-life was described by the following expression:

$$c_{F0,half-life}(t) = c_{F0,t-1} \cdot \exp(-\lambda * \Delta t) \quad \textbf{(5.1)}$$

where $c_{F0,t-1}$ is the initial fixed charge density of the previous increment, Δt is time increment defined by the convergence of the transport analysis and λ is the decay constant and is given by:

$$\lambda = \frac{Ln(2)}{t_{1/2}} \quad \textbf{(5.2)}$$

where $t_{1/2}$ is the half-life of disc proteoglycans (12 ± 2 years according to Sivan et al. (2006b)

The production of proteoglycans by cells was also taken into account, as shown in the following expression:

$$c_{F0,production}(t) = k_{prod} \cdot C_{viability} \cdot \Delta t \quad \textbf{(5.3)}$$

where k_{prod} is the production rate of proteoglycan, $C_{viability}$ is the cell viability considered as the ratio $\rho_{cell}/\rho_{cell,0}$ (Eq. 5.6) where $\rho_{cell,0}$ is the initial cell density before any cell death occurs (Horner & Urban 2001), and Δt is the increment of time defined by the convergence of the transport analysis.

Combining Eq. 2 and Eq. 4 gave:

$$c_{F0}(t) = c_{F0,half-life}(t) + c_{F0,production}(t)$$

$$c_{F0}(t) = c_{F0,t-1} \cdot \exp(-\lambda * \Delta t) + k_{prod} \cdot C_{viability} \cdot \Delta t \quad \textbf{(5.4)}$$

All parameters of Eq. 5.4 were known except the production rate of proteoglycans (k_{prod}). To find this term, a hypothetic homeostatic state (internal equilibrium) was considered: the partial derivative of Eq. 5.4 over time was set equal to zero, considering that 100% of cells are alive ($C_{viability} = 1$):

$$\frac{\partial c_{F0}}{\partial t} = -\lambda \cdot c_{F0,t-1} \cdot \exp(-\lambda * \Delta t) + k_{prod} = 0$$

$$k_{prod} = \lambda \cdot c_{F0,t-1} \cdot \exp(-\lambda * \Delta t) \quad \textbf{(5.5)}$$

The rate shown in Eq. 5.5, switches between two levels depending on oxygen concentration according to the findings of Horner & Urban (2001). Whereas high oxygen levels lead to a full rate, at low levels this rate decreases a 20%.

5.2.3 Cell viability criteria

The effect of pH and glucose on cell density was considered by assuming that cells start to die when: a) glucose level was below 0.5 nmol/mL, and/or b) pH level decreased below 6.8 (Horner & Urban 2001; Razaq et al. 2003; Bibby &

Urban 2004; Guehring et al. 2009). The experimental curve for cell viability was taken from a previous study (Horner & Urban 2001), where cell density decreased exponentially according to the following expression:

$$\rho_{cell} = \rho_{cell,0} \cdot \exp\left[-\left(\alpha_{glucose} + \alpha_{pH}\right)t\right] \quad \textbf{(5.6)}$$

where ρ_{cell} and $\rho_{cell,0}$ are the current and initial cell density respectively, the death rate (α_{pH}) due to low pH was constant and equal to $3.43 \times 10^{-6} s^{-1}$ according to the cell experiment of Horner & Urban (2001).

In Chapter 4, the death rate (α_{gluc}) due to low glucose concentrations was considered constant. In this Chapter the α_{gluc} was updated according to the formulation presented by Zhu et al. (2012) who considered that α_{gluc} depends on the glucose concentration (C_{gluc}) as shown in the following expression:

$$\alpha_{gluc} = \left(\frac{C_{gluc} - 0.5}{C_{gluc} + 0.2} - \frac{\left|C_{gluc} - 0.5\right|}{C_{gluc} + 0.2}\right) \quad \textbf{(5.7)}$$

5.2.4 Boundary conditions

Three cycles of daily loads were simulated, each cycle consisting in 8 hours of rest under 0.11 MPa of compression followed by 16 hours of activity under an average load of 0.54 MPa of compression (Wilke et al. 1999). The load was applied at the surface of the upper BEP and the lower BEP was fixed. External pore pressure was considered nil. Oxygen, lactate and glucose concentrations were applied at the CEPs and the AF surfaces (Figure 4.2a).

The effect of punctual increases of pressure that corresponded to punctual activities, e.g. standing from a chair, going up and down stairs, was evaluated by simulating 9 peaks of pressure of 1.1 MPa along the 16 hours of activity of the daily cycle (Figure 5.2) (Wilke et al. 1999).

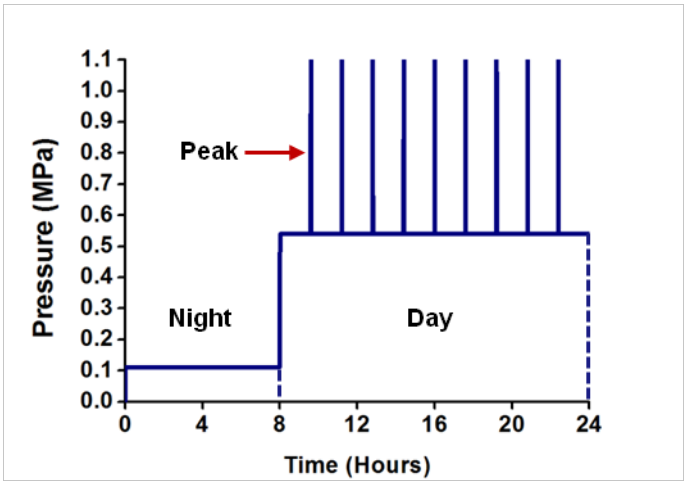

Figure 5.2: Daily load cycle with 9 peaks of 1.1 MPa included at the 16 hours of activity

5.2.5 Macroconsolidation study

The simulation of proteoglycan turnover, e.g. 14 years, would have a high computational cost. In order to reduce this cost, time-scale conversion within the transport model was needed. It was assumed that a macro-consolidation would represent the cumulative effect of shorter consolidations repeated over time. Should this assumption be valid, it would give a simple way to make the time scale conversions: the results obtained for few days could be used in substitution of a simulation of years, thus reducing the computational cost and allowing to cover the 14 years needed to study of the proteoglycan turnover. In order to verify the applicability of this rational for time-scale conversion, a consolidation study was performed. The axial displacements obtained after the simulation of 4 cycles of daily loads were compared with those obtained after the simulation of the cumulative effect of each part of the 4 days: a single day was simulated considering a rest component equivalent to the sum of the time of rest for 4 days (32h in this case) under 0.11 MPa, followed by an activity component of 64h under 0.54 MPa that corresponded to the sum of the hours of 4 days of activity.

5.2.6 Update of the initial water content

The turnover of the proteoglycans implicitly includes a reduction of the water content. Nevertheless, with ageing, additional processes of dehydration might occur in the NP. The causes of such process remain unclear but as shown in Chapter 4, alterations the water content has an important effect on the transport

of solutes. Hence, depending on the result obtained from the turnover of proteoglycans, an update of the water content would be needed. This new water content will be selected in an educated way in proportion of the values presented in the Table 4.2 of Chapter 4.

5.3 Results

5.3.1 Macroconsolidation

The results obtained for both simulations performed for the consolidation study were similar at the end of the time simulated, i.e. 4 days (Figure 5.3). In fact, the relative difference between the axial displacements at the top of the upper BEP was less than 0.01%. Based on this result a conversion of the time scale was performed inside the transport model. Such conversion consisted in a simulation of three days of transport, changing the time of days into years to be included in Eq. 5.4.

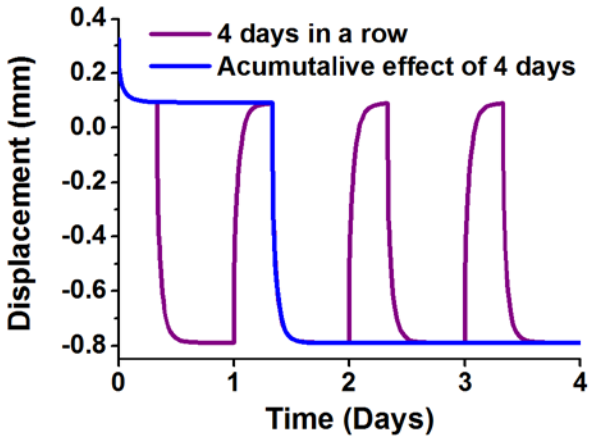

Figure 5.3: Axial displacement obtained simulation of 4 cyles of daily loads (purple line), and accumulative effect of 4 days of rest followed by 4 days of activity (blue line)

5.3.2 Proteoglycan turnover study

After a simulated period of 14 years the disc NP presented two different zones in terms of proteoglycan concentration. The NP had a zone at the top and bottom where the c_{F0} was around 0.3 mEq/mL (healthy condition), and another zone at the mid-height of the NP where the c_{F0} was lower (Figure 5.4). The disc starts is considered to degenerate after the beginning of disc maturation. Hence,

this point was selected as star point to evaluate the evolution of the two proteoglycan zones mentioned above until the half-life of proteoglycans (14years) (Figure 5.5). Whereas the c_{F0} of NP top and bottom decrease 2% only (Figure 5.5a), in the NP mid-height the c_{F0} was 0.25 mEq/mL; representing a reduction of 14% (Figure 5.5b).

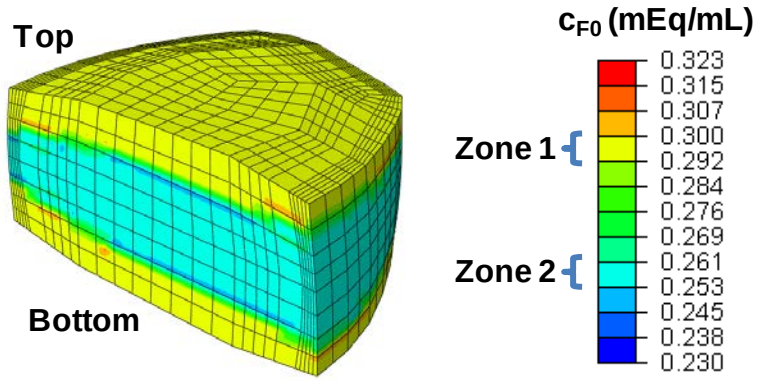

Figure 5.4: Nucleus initial fixed charge density (c_{F0}) zones after the simulation of 14 years: the top and bottom zone, i.e. the yellow area, has a high fixed charge density and the mid-height zone, the cyan one, has low fixed charge density

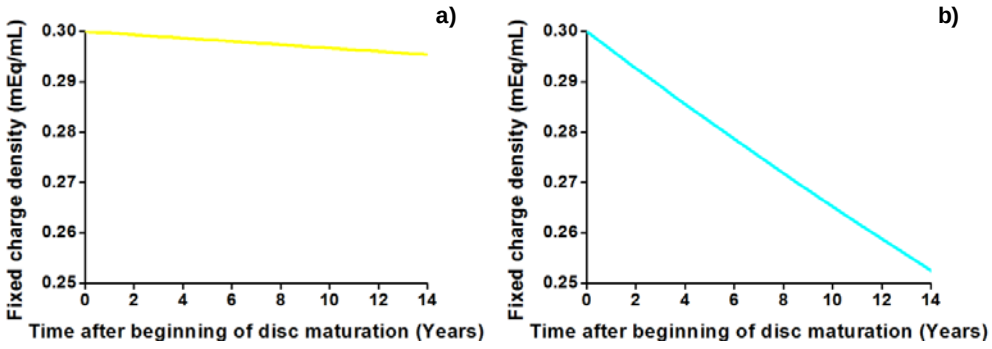

Figure 5.5: Initial fixed charge density evolution up to 14 years after the beginning of disc maturation until proteoglycan half-life at: a) the top of the nucleus and b) the mid-height of the nucleus

5.3.3 Effect of the reduction of the initial fixed charge density

The reduction of the c_{F0} affected the osmotic pressure at the NP centre after one day simulated. Indeed, the value obtained for the osmotic pressure was 0.21 MPa, which was 20% lower than the value obtained for a healthy disc (Figure 5.6a). Disc height was slightly reduced, with a relative difference of 1% (Figure 5.6b).

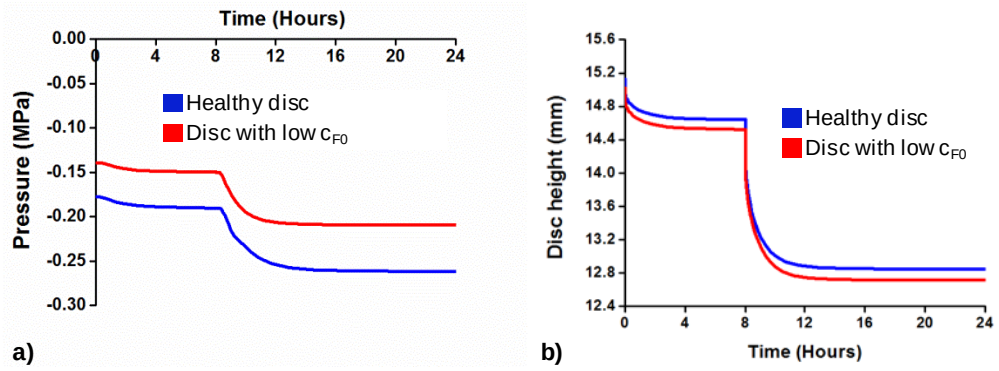

Figure 5.6: Disc mechanical behaviour when low initial fixed charge density is simulated: a) osmotic pressure at the nucleus centre and b) disc height

After the three days simulated, none of the solute concentrations were significantly affected by the reduction of the c_{F0}. In the case of the glucose, the relative difference with the healthy disc was of 0.5%. This result indicated that a further reduction of the initial water content, n_{F0}, was needed in order to observe of possible alterations in disc nutrition. The boundary anterior AF-TZ was the zone with the lower solute concentrations (Figure 5.7). Hence this zone was taken for the analysis of the evolution along time of the solute concentrations.

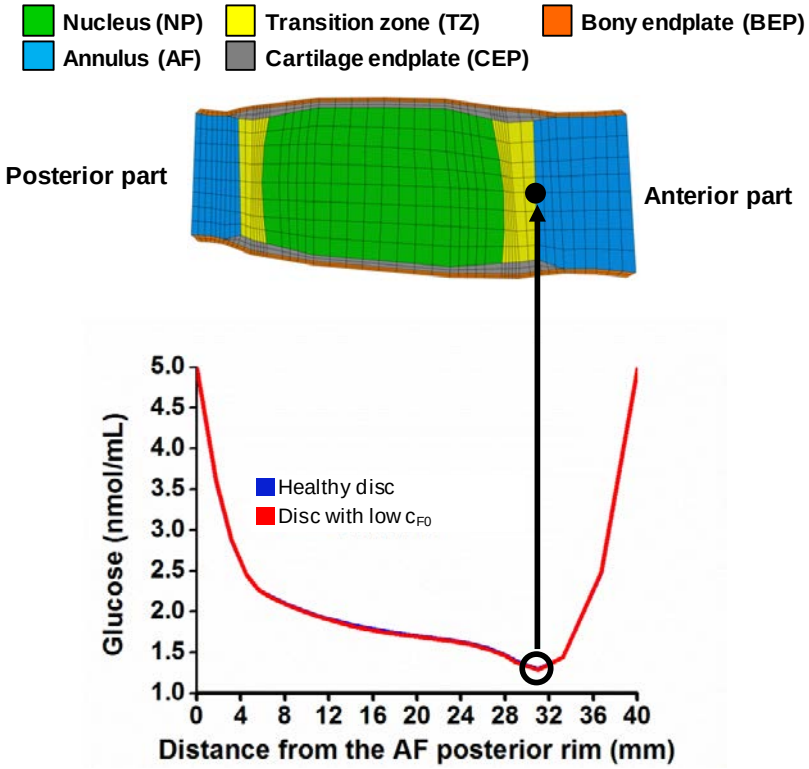

Figure 5.7: Glucose content along the mid-sagittal plane path after 3 days simulated

5.3.4 Effect of combined initial fixed charge density and initial water content reduction

Based on the values reported in the Table 4.2, a n_{F0} of 77% was selected for the c_{F0} of 0.25 mEq/mL obtained in the section 5.3.2. The combination of c_{F0} and n_{F0} reductions also changed the mechanical behaviour of the disc: the osmotic pressure in the NP centre was 0.20 MPa after one simulated day, representing a decrease of 21% (Figure 5.8a). The disc height was slightly affected. In fact, the disc height computed at end of the day was 13.25 mm, which was 1.25% lower than the value obtained for a disc with healthy properties (Figure 5.8b).

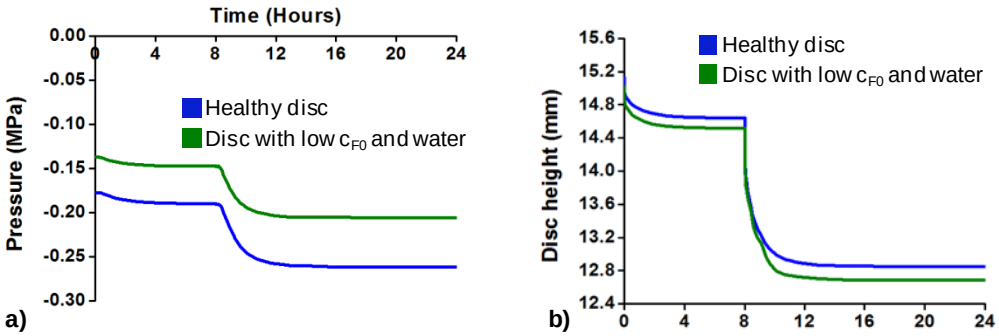

Figure 5.8: Disc mechanical behaviour when low c_{F0} and n_{F0} are simulated: a) osmotic pressure at the nucleus centre and b) disc height

The glucose concentration at the boundary anterior AF-TZ was affected by the combined c_{F0} and n_{F0} reduction. In fact, after the simulation of three days, the glucose concentration obtained was 1.06 nmol/mL; indicating a reduction of 13% (Figure 5.9b). Oxygen and lactate values obtained were not significantly different from the values obtained for a healthy disc. Also, there were no major changes in pH levels, i.e. relative difference in the pH values was less than 0.5% (Figure 5.9a).

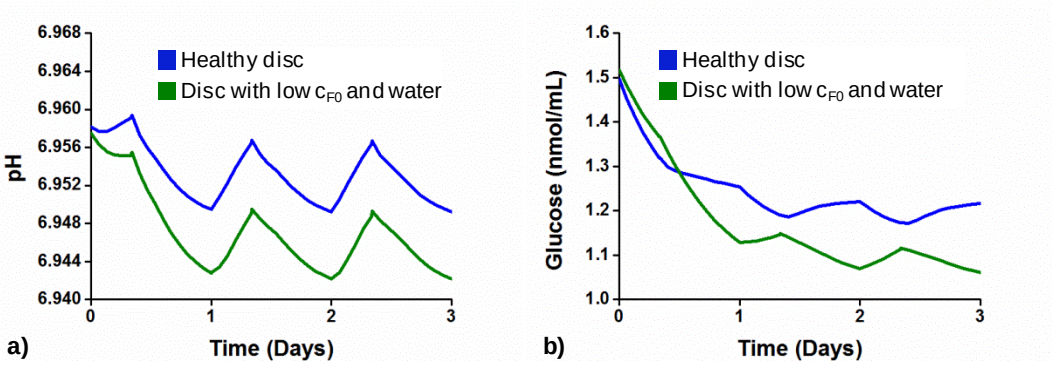

Figure 5.9: Solute concentration during the three days simulated at the boundary anterior AF-TZ: a) pH, and b) glucose

5.3.5 Effect of the peaks of pressure

The consideration of peaks of pressure with a disc with low c_{F0} and n_{F0} did not affect significantly the disc mechanical behaviour. Indeed, compared to a daily cycle with no peaks, the osmotic pressure at the NP centre and disc height only varied by 0.2% and 0.01% respectively. Similar outcomes were obtained in terms of transport of nutrients, where the solutes concentrations were not altered by the application of peaks of pressure. In addition, all disc cells remained alive after the three days simulated for the two load scenarios, regular daily load and daily load with peaks (Figure 5.10).

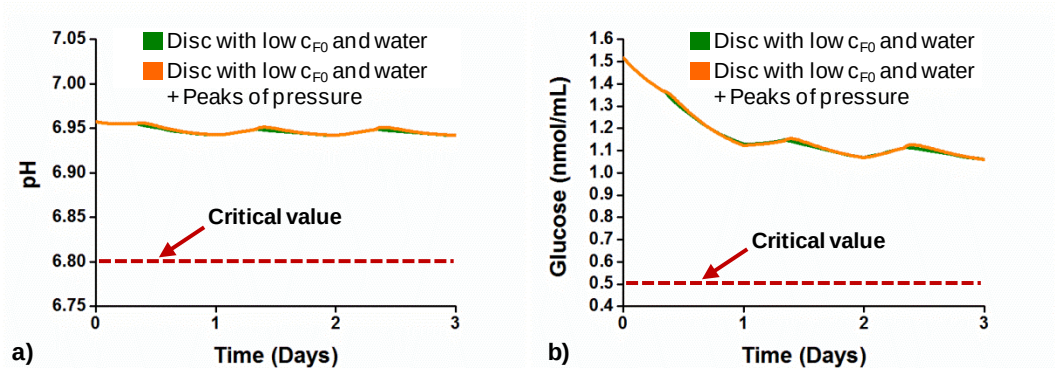

Figure 5.10: Solute levels at the boundary anterior AF-TZ after three days simulated when peaks of pressure are simulated: a) pH and b) glucose. The dot line corresponds to the critical values for cell viability

5.4 Discussion

Both simulations performed in the macroconsolidation study led to similar outcomes in terms of axial displacement. These results suggest that the effect of consolidation, e.g. porosity reduction, for a simulation of years in a row can be equivalent to simulate a single day that considers the sum of rest and activity time of those years. Thus, the hypothesis was confirmed that a time scale conversion in the transport model can be used to simulate 14 years of proteoglycan turnover. Therefore, three days of simulation in the transport model were equivalent to 14 years in terms of proteoglycan phenomena. Hence, the oxygen and cell viability predictions obtained in the transport model were use in Eq. 5.4 to describe years of proteoglycan changes.

Two zones were identified at the NP in terms of proteoglycan regulation after the simulation of 14 years. In this sense, the mid-height of the NP has a large

non-homeostatic area (Figure 5.5b), indicating that proteoglycan half-life term in Eq. 5.4 had a predominant effect. The low rate of proteoglycan production in this NP zone was due to reduced oxygen levels. Conversely, a quasi-homeostatic area was found at the top and bottom of the NP (Figure 5.5a), where the production rate of proteoglycan compensated better the half-life effect. In this zone, the oxygen level was high due to its proximity to the nutrient supply, and the production rate of proteoglycan was full.

In order to evaluate the further evolution of the initial fixed charge density a new time-scale conversion was set. The time of three days of simulation in the transport model was equal to 28 years in the proteoglycan phenomena. After approximately 21 years simulated, the initial fixed charged density obtained from Eq. 5.4 was 0.23 mEq/mL (Figure 5.11). This value corresponded to a grade III degenerated disc, according to the values reported in Chapter 4. Considering that at the beginning of the simulation the disc was fully mature, i.e. characteristic of a 25-30 year old patient, the model predicted that a grade III disc would be achieved for a 45-50 year old person. This result was in agreement with previous studies which reported that about 35-38% of humans around that age might have disc with grade III of degeneration (Antoniou et al. 1996; Boos et al. 2002). Also, the fixed charge density presented in Figure 5.11 decreases nonlinearly with time; this outcome is in agreement with the experimental study of Rodriguez et al. (2011).

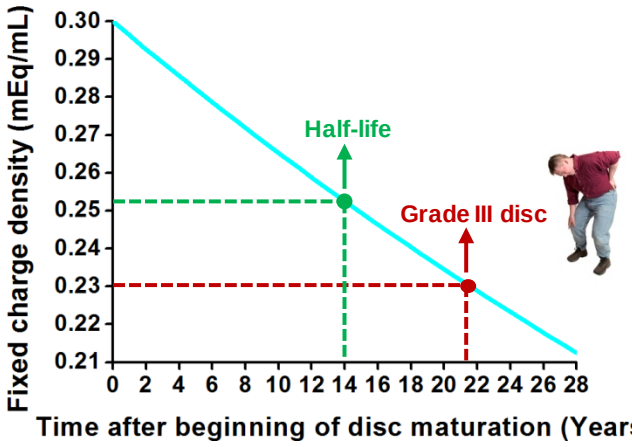

Figure 5.11: Initial fixed charge density evolution from the beginning of disc maturation up to 28 years later. The green point represents the fixed charge density for the half-life of the proteoglycans and the red point corresponds to the fixed charge density of a grade III disc (Chapter 4)

The specific loss of proteoglycan calculated in the centre of the disc produced a significant reduction in the osmotic pressure, in agreement with the literature (See Chapter 2, section 2.3.1). In fact, Zhu et al. (2014) found a reduction in the fluid pressure and water content at the NP when disc degeneration was simulated using a model that considered the changes in the proteoglycan content. Nevertheless, they did not mention if such water reduction was linked to the proteoglycan content. Also, they used a constant proteoglycan synthesis rate which might produce an overestimation in their predictions. Although the loss of proteoglycans might affect the water content and hence the disc height, this effect was not significant when reduced c_{F0} was simulated. This result suggests that the NP dehydration might be a consequence of other completely independent process apart of the proteoglycan loss.

The decrease of the osmotic pressure during disc degeneration might affect the propagation of pre-existing crack within the AF. Wognum et al. (2006) showed that the reduction of the fixed charge density has a large effect on the crack opening. They also found that the crack tip was subjected to a concentration of stress when the fixed charge density decreases. In addition, the high concentration of strain in the crack restricts the AF cell capacity of adaptive reorientation. Such restriction generates stretch-induced apoptosis that might contribute to the cell death (Abbott et al. 2012).

Disc height was slightly more affected by the combination of c_{F0} and n_{F0} reductions at the NP. This result confirms the link between water reduction and disc height loss mentioned previously. The osmotic pressure slightly decreased as well. On the other hand, solute concentrations were affected by the combined effect of c_{F0} and n_{F0} reduction. Glucose concentration was the most affected whereas the rest of the solute concentrations remained almost unaltered. The fact that glucose content was affected only when a reduced n_{F0} was considered can be explained in terms of the porosity-dependant diffusivity law used in the transport model (see Eq. 4.9, Chapter 4). As such, the loss of the water content reduces glucose diffusivity and hence its concentration. Also, the diffusion coefficient of glucose is about three times lower than oxygen. On the other hand, the solute distribution profiles obtained along the mid-sagittal plane path were in agreement with the profiles reported by Malandrino et al. (2011). It is worth to highlight that,

as shown in Chapter 4, the possible benefit of the reduction of the diffusion distance produced by the disc height loss was negligible compared to the effect of further consolidation, i.e. reduction of the water content.

Malandrino et al. (2015b) reported that the interface AF-NP was a critical area for disc nutrition due to local consolidation. In this Chapter, it was found that the boundary anterior AF-TZ was the area of the disc that presented the lowest glucose content, which was the zone with the highest local consolidation. Interestingly, if a 40% of reduction in the water content is simulated, i.e. n_{F0} of 72%, the critical point moves to the NP area (Figure 5.12). Such movement can be explained in terms of the porosity-dependant diffusivity earlier discussed.

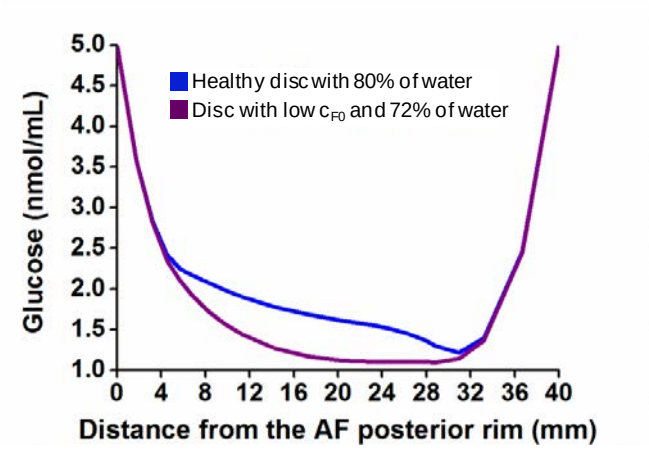

Figure 5.12: Glucose distribution along the mid-sagittal plane path for a disc with low c_{F0} and 72% of water conten

The inclusion of increments of pressure in the load cycle did not alter the osmotic pressure, disc height and the solute concentrations after the three days simulated. A possible explanation is the duration of each pressure increment. Nine peaks were applied in which the total time for charge and discharge was one minute for each peak. Although large changes in the deviatoric strain occurred instantly when the pressure increased, changes in the volumetric strain required more time to appear. In consequence, there was not enough time for consolidation, i.e. porosity reduction. There was a transient disc height reduction due the peak of pressure, but, as discussed previously, such reduction has no significant effect on solute transport compared to the reduction of the porosity.

The levels of solutes obtained in all transport simulations for the load scenarios simulated, i.e. with and without peaks of pressure, never achieved the glucose and pH thresholds to induce cell death (Figure 5.10). In fact, in the case of

glucose concentration, the minimum value obtained was approximately twice as large as the critical value. In terms of pH levels, the minimum values also remained above the critical level, but not in the same proportion than for the glucose.

Gu et al. (2014) simulated proteoglycan and water content reductions due to degeneration. They found that cells started to die after 5 days simulated. The reduced glucose values at the boundary NP-CEP at the beginning of the simulation combined to a large time simulated might explain the activation of the cell viability in that study. In this Chapter, both glucose and pH minimum values were obtained at the anterior AF-TZ boundary, and for the low c_{F0} and low n_{F0} condition. This result suggests that the proteoglycan loss does not have an effect on the nutrition-controlled cell viability. In addition, specific disc geometries might contribute to cause cell death. Although a recent experimental study found that changes in disc height do not affect the amount of disc cell (Boubriak et al. 2013), the study of Rodriguez et al. (2011) reported an inverse correlation between cell density and disc height. Moreover, disc geometry changes may involve larger diffusion distances, affecting disc nutrition and hence the cells (Malandrino et al. 2015a).

The values of pH and glucose obtained for combined c_{F0} and n_{F0} reductions at the NP might be low enough to activate catabolic processes within the disc. In the case of glucose, a concentration of 0.5 nmol/mL led to the gene expression of matrix metalloproteinase (MMP), especially MMP-3 that degrades the proteoglycans (Rinkler et al. 2010; Neidlinger-Wilke et al. 2012). The minimum computed glucose value obtained in this Chapter was 1.06 nmol/mL, which might trigger the expression of MMP-3. As for the pH levels, the computed value of 6.93 might also stimulate the expression of MMP-3. Nevertheless, the expression of MMP-3 reported by Neidlinger-Wilke et al. (2012) at pH 6.5 and pH 6.8 were not significant different from the expression at a normal pH of 7.2. This result suggests that combined c_{F0} and n_{F0} reduction might activate the expression of MMP-3 due to glucose reduction, that would possibly lead to disc degeneration via matrix degradation. In fact, degenerated disc presents high concentrations of MMP-3 and other enzymes, e.g. cathepsins and aggrecanases that can breakdown the molecules of the matrix (Crean et al. 1997; Weiler et al. 2002). However, it is unknown if the amount of MMP-3 expressed for the glucose and pH environment computed in this study may produce a considerable damage to the disc

extracellular matrix. As such, more experimental studies are needed to verify the relevance of MMP-3 expression under such nutritive environment. The present study has some limitations. Firstly, not all components of disc extracellular matrix were considered. However, a previous study has revealed that proteoglycan, collagen and water content are the most relevant component for disc mechanical behaviour (Schroeder et al. 2007). Secondly, only global proteoglycan and collagen content were considered. Thirdly, as shown earlier, tissue consolidation is the process that most influence nutrition. Hence the effect that could have the solute concentrations on the proteoglycan turnover can be explored simulating days instead of years. Also, the inclusion of grown factors, such as IGF-1, in the proteoglycan approach developed in this Chapter is needed to be considered, since a recent numerical study reported that IGF-1 receptors downregulated proteoglycan biosynthesis (Asfour et al. 2015). Finally dynamic compression was not simulated. Although cycle loads have been shown to enhance the cell viability under degenerated conditions (Zhu et al. 2012), sustained static compression have most considerable effect of disc nutrition and cell death (Malandrino et al. 2011). Hence, only this kind of loads were considered.

5.5 Conclusions

In this Chapter a novel formulation for the update of the proteoglycan content was included to the composition-based-transport-cell viability model developed in Chapter 4 to study the influence of the proteoglycans loss on disc nutrition and cell viability. The results showed that limited oxygen diffusion to the disc centre combined to cell nutrition might explain natural ageing. Additionally, the proteoglycan loss affected the osmotic pressure but not the solute concentrations. The addition of NP dehydration slightly altered the disc height and reduces the glucose concentration. Although all cells remained alive for any case simulated, the reduction of glucose and pH due to NP proteoglycan depletion and dehydration might trigger the release of MMP-3 that would breakdown the disc matrix, revealing a possible path to understand the role of disc nutrition in disc degeneration. Another disc tissue that might influence disc degeneration is the CEP. Indeed, the CEP has a gradient of composition which role in disc nutrition is still unknown. This aspect will be addressed in the next Chapter.

6 DEVELOPMENT OF A FORMULATION FOR THE GRADIENT OF COMPOSITION PERMEABILITY IN THE CARTILAGE ENDPLATE

The effect of the decrease of proteoglycans and dehydration in the nucleus on disc nutrition was studied on Chapter 5. Although the proteoglycan loss reduced the osmotic pressure, it needed to be combined to tissue dehydration to alter disc nutrition. Another structure that might have an influence on disc nutrition is the cartilage endplate (CEP), since it has the ability to control solute diffusion and most importantly disc hydration. However, all simulations performed in the previous Chapters did not consider any alterations in the CEP, i.e. it was simulated as a healthy tissue.

The CEPs stand for a major path for the diffusion of nutrients from the peripheral disc vasculature to the nucleus. Hence, some experimental and numerical studies have explored the CEP. In particular, numerical studies have paid special attention to the effect of CEP calcification. As simulated calcification effects impaired disc nutrition, but studies did not consider the degeneration, ageing, and specific composition of the CEP that might influence the exchange of fluid and disc degeneration. Moreover, it is unclear whether this calcification occurs in early/mild disc degeneration. In this Chapter, a novel composition-dependent CEP model was developed, so as to take into account tissue heterogeneity and ageing effects on the disc model poromechanics and simulated cell nutrition. The results showed that CEP permeability increased with disc degeneration. Moreover, CEP degeneration generated NP dehydration, and also reduced solute concentrations. The cell viability was activated when all disc tissues were simulated as degenerated. The results allowed to propose an alternative path for disc degeneration.

The work developed in this chapter led to the manuscript Ruiz Wills, C., Foata, B., Lacroix, D. and Noailly, J. (2015) Alterations of cartilage endplates composition generate dehydration at the nucleus pulposus: a novel finite element approach for the composition gradient of the cartilage endplate.

6.1 Introduction

The carry of solutes such as oxygen, lactate and glucose is regulated by the bone marrow contact channels that cross the bonny endplate (BEP). Nevertheless, the study of Malandrino et al. (2014b) suggested that BEP morphological changes due to degeneration had a negligible effect on the solute transport, quantitatively. Those result led to highlight the possible importance of the CEP in disc degeneration. Indeed, an *in vitro* study performed by Nachemson et al. (1970) suggested that CEP calcification might interfere with the supply of nutrient. Moreover, it has been reported that the calcification within the endplates occurs in scoliosis, affecting sometimes the whole CEP thickness leading to a reduction of the nutrient transport through the vertebral endplate path (Bernick & Cailliet 1982). Also, the CEP possesses a sharp gradient of composition from the NP to the BEP (Roberts et al. 1989), which main function is still unclear.

The disc fluid can be exuded and imbibed during a day cycle. This fluid recovery during the rest is suggested to be due the direction-dependant flow constriction in the CEP that would act like a valve (Ayotte et al. 2000). This flow constriction produces a large exudation resistant during flow inhibition, aspect that is important to avoid disc dehydration during daily load cycles. In addition, Ayotte et al. (2001) demonstrated that CEP resistance to flow was highly direction dependent, which favoured the restoration of the water loss produced by daily loads, once mechanical loads are relieved. Also, in Chapter 5 it was shown that the addition of NP water loss affected disc nutrition, but the cause of such loss is not clear. However, alterations at the CEP composition might be a possible cause of such water loss.

In vivo and *in vitro* local explorations of disc nutrition are difficult to perform. Because of that numerical models have risen as a tool to complement the experimental results. Riches & McNally (2005) used a theoretical model to study the influence of CEP permeability reduction on disc mechanical behaviour. They found that CEP permeability will affect the fluid movement and improve convective nutrition when CEP permeability is lower than disc tissue permeability. Mokhbi Soukane et al. (2009) and Jackson et al. (2011a) showed that CEP calcification led to a reduction in the solute concentration, specially glucose, and

the NP was the most affected part of the models. Shirazi-Adl et al. (2010), Galbusera et al. (2011b) and Malandrino et al. (2014a) revealed that simulating CEP calcification led to the reduction of disc cell viability. Based on the fact that when the CEP is calcified it acts like a barrier to solute transport, affecting disc nutrition (Nachemson et al. 1970; Roberts et al. 1996), those models simulated CEP calcification by reducing 40-50% the CEP water content or by reducing the tissue diffusivity. Nevertheless, there is no consensus about the way to simulate CEP calcification.

On the other hand, Chapter 4 showed that the consideration of composition changes in the AF and the NP affected disc nutrition. As mentioned above, the composition of the CEP is not uniform; instead it presents a chemical gradient which might have influence on the transport of solutes as well (Roberts et al. 1989). In addition, the study of Rodriguez et al. (2011) showed that endplate porosity and permeability increase with degeneration and ageing. Noailly & Lacroix (2012b) used an axisymmetric 2D model to simulate a mechanistic distribution of the CEP intrinsic permeability based of the proteoglycan content of the tissue. They confirmed the direction-dependency effect of the CEP for mechanistic permeability gradients and pointed out the importance of CEP composition in the study of disc dehydration. From this result and the ones presented in Chapter 4, it is highly relevant to consider composition changes of the poromechanical properties of the CEP in the simulation of the transport phenomena. Hence, this work proposes to use a novel modelling approach to study the effect of CEP composition on disc nutrition and cell viability.

6.2 Materials and methods

6.2.1 Modelling spatial CEP heterogeneity

An axisymmetric FE model was created, representing a central plug of the CEP, and NP tissue up to the IVD centre in order to simulate a reserve of water within the disc; the BEP was also included (Figure 6.1). The CEP and the NP were both modelled as osmo-poro-hyperelastic materials with explicit consideration of the proteoglycan fixed charge density (c_F), total water content (n_F), and collagen

content ($\rho_{c,tot}$) (Schroeder et al. 2007). The BEP was considered as a linear poroelastic material (Malandrino et al. 2011). NP composition corresponded to that of a healthy disc, and was taken from Table 5.1. As for the CEP, it was considered either a varying composition from the NP to the BEP (Roberts et al. 1989) or a virtually homogenized composition.

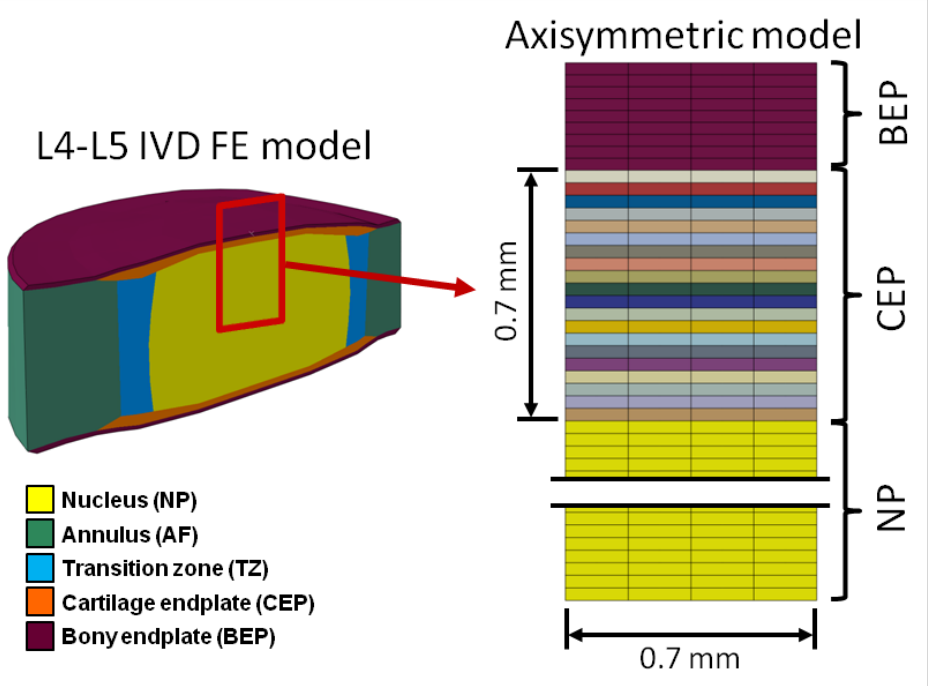

Figure 6.1: Axisymmetric cartilage endplate (CEP) FE model with surrounding tissues: bony endplate (BEP), and nucleus (NP)

6.2.2 CEP composition permeability approach

Motivated by experimental evidences and by a previous pilot numerical study (Comper & Lyons 1993; Noailly & Lacroix 2012b), a new composition-dependent permeability formulation was established in order to fully capture the effect of tissue composition on the effective fluid permeation through the CEP. A pre-existing strain-dependent permeability model was further developed and

incorporated the effect of collagen and proteoglycan, assuming that higher contents in these macromolecules will give an increased tortuosity effect (Eq. 6.1):

$$\kappa_{CEP} = A \cdot exp\left(B \cdot c_F + C \cdot \rho_{c,tot}\right) \cdot \left(\frac{1 - n_{F0}}{1 - n_F}\right)^M \quad \textbf{(6.1)}$$

where κ_{CEP} is the tissue hydraulic permeability in m^4/Ns, and A is a zero strain permeability value, for a reference composition defined by parameters B and C. B and C respectively rule the proteoglycan- and collagen-dependence. n_{F0} is the initial water content at zero strain, and M is a previously reported model parameter that controls the rate of permeability change along tissue consolidation.

To determine A, B, and C, a similar dependence of κ_{CEP} upon composition for both the CEP and the NP was assumed and used two sets of matching composition/permeability values available for the NP (Table 6.1). These data were coupled to a constrained numerical optimization, looking for the parameter triplet that minimizes the difference between mean κ_{CEP} values (i) based on reported collection of values used in modelling (Malandrino et al. 2009), and (ii) calculated with mean composition data (Roberts et al. 1989).

Table 6.1: Data used to find the parameters A, B, and C from Eq. 6.1 though constrained optimization

Property	**Constraints**		**Criteria for constrained optimization**
	Nucleus		Cartilage endplate
	Healthy	Degenerated	Mean composition
Fixed charge density (mEq/mL)	0.3	0.23	0.17
Water content (fraction of wet weight)	0.8	0.76	0.66
Collagen content (fraction of dry weight)	0.09	0.285	0.24
Permeability (mm4/Ns)	0.0009	0.0045	0.0025-0.015

6.2.3 3D composition-transport-cell viability disc model

A L4-L5 3D disc model was taken the previous Chapters, e.g. tissue distribution and mesh density from Chapter 3, and constitutive equations and composition parameters from Chapter 4. As described in Chapter 4, the model includes all disc tissues, i.e. AF, NP, TZ, CEP and BEP (Figure. 4.1).

The CEP permeability was considered composition-dependent using Eq. 6.1. AF and NP permeability were strain-dependent according to Eq. 4.8. The viscoelastic fibres of the annulus were also included. As for the solid matrix of the CEP, a composition-based formulation used for the AF and the NP (Eq. 4.3) was adopted. The disc model was fully coupled to the transport model presented in Chapter 4 (From Eq. 4.9 to Eq. 4.14). The cell viability criteria was taken from Chapter 5 (Eq. 5.6 and 5.7).

6.2.4 Boundary conditions

In the 2D model, sequences of rest and day activity were approximated through 1h and 2h of 0.26 MPa and 0.78 MPa compressive loads, respectively. Activity load was either static or dynamic (1Hz). All loads were applied on the BEP. The bottom of the NP was fixed and impermeable. The model was laterally confined, in terms of both lateral displacements and fluid velocities. Fluid mass loss was calculated as the integration of the fluid velocity along the time. Both mass loss and fluid velocity were evaluated at different points: NP area, boundary NP-CEP and CEP area (Figure 6.2a)

In the 3D model, three days of daily load, i.e. 8 hours of rest under 0.11 MPa of compression followed by 16 hours of activity under an average pressure of 0.54 MPa (Wilke et al. 1999), were simulated. The lower BEP was fixed in all directions, and the pressure was applied at the upper BEP. The external pressure was considered atmospheric. Solute concentrations were applied at the edges of the AF and CEP. All tissue composition and solute concentrations were taken from the literature (Tables 6.2 and 4.3) (Roberts et al. 1989; Dao et al. 2014; Chapter 4).

Table 6.2: Material properties for disc tissues of the 3D model

Parameter	Tissue					
	Nucleus*		Annulus*		Cartilage endplates**	
	Healthy	Degenerated	Healthy	Degenerated	Healthy	Degenerated
Matrix shear modulus (MPa)	1	0.8	1	0.7	1	0.8
Initial fixed charge density (mEq/mL)	0.30	0.23	0.20	0.20	0.17	0.13
Initial water content (% of wet weight)	80	76	75	70	66	60
Collagen content (% of dry weight)	15	28.5	65	78	24	35
External salt concentration (mEq/mL)	0.15	0.15	0.15	0.15	0.15	0.15
α ($mm^4/N.s$)	0.00016	0.00045	0.00016	0.00045	0.0017	0.044
Constant M	1.2	0.9	1.2	0.9	8.5	8.5

* Nucleus and annulus healthy and degenerated properties taken from Chapter 4.

** Cartilage endplates shear modulus taken from nucleus values in Chapter 4, initial fixed charge density from Eq. 6.1, and composition parameter from Fields et al. (2014).

The effects of different endplate conditions were explored: a) healthy CEP, b) grade III (degenerated) CEP (Pfirrmann et al. 2001) and c) grade III NP, AF, and CEP. For each simulated condition, cell viability, mass flow and solute concentrations were evaluated at the mid sagittal plane (Figure 6.2b).

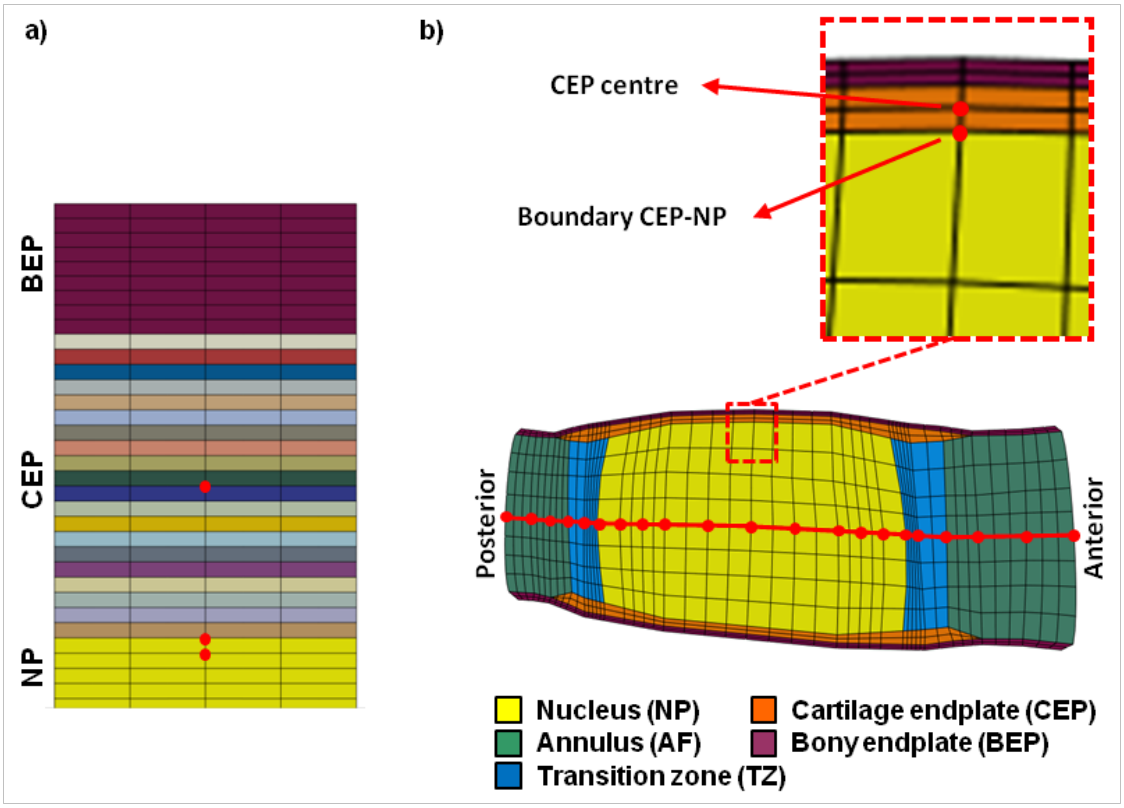

Figure 6.2: a) Points of study for the 2D model: cartilage endplate (CEP) centre, boundary cartilage endplate (CEP)-nucleus (NP) and nucleus (NP), and b) Sagittal path in the 3D model and point for the mass loss calculations: CEP centre and boundary CEP-NP

6.3 Results

6.3.1 Composition-dependent CEP parameters

The parameters found for composition-dependent permeability formulation are summarized in Table 6.3. The parameters B and C obtained had negative values, the absolute value of the former being much larger than that of the latter. Using these parameters in Eq. 6.1 and adding a gradient of composition parameters from NP to CEP led to the CEP permeability distribution shown in Figure 6.3, where the permeability increases from the NP to the BEP. The maximum value obtained for the permeability was 0.036 mm^4/Ns.

Table 6.3: Cartilage endplate composition-dependant permeability parameters for Eq. 6.1

Parameter		
A (mm^4/Ns)	B (mL/mEq)	C
0.891	-22.99	-0.00012

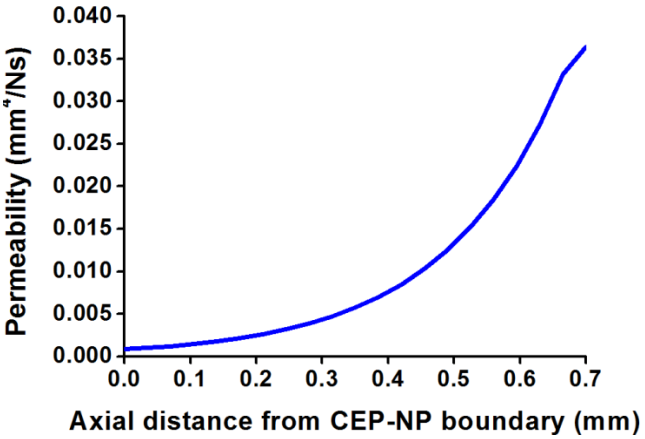

Figure 6.3: Cartilage endplate permeability variation in the 2D FE model, beginning at the boundary CEP-NP and ending at the boundary CEP-BEP

The permeability values obtained by using a mean CEP composition determined from the experimental study of Roberts et al. (1989) along the parameters from Table 6.4 was 0.017 mm^4/Ns for a healthy CEP. Also, using the composition values for a degenerated CEP the permeability was 0.044 mm^4/Ns, representing an increment of a 59%. Both values, i.e. healthy and degenerated, were used as initial (i.e. low strain) homogeneous CEP permeability (Eq. 4.7) for the 3D model simulations.

6.3.2 Axisymmetric study

The gradient of permeability reduced the fluid velocity in the 2D model at the beginning of the load application at the NP (Figure 6.4). In fact the velocity was up to 54% lower than the value obtained for a constant permeability. Also, the decay of the velocity after the load application was slightly lower with the gradient

of permeability. On the other hand, the mass loss in the NP decreased by 5% at the end of 2 hours of activity (Figure 6.5).

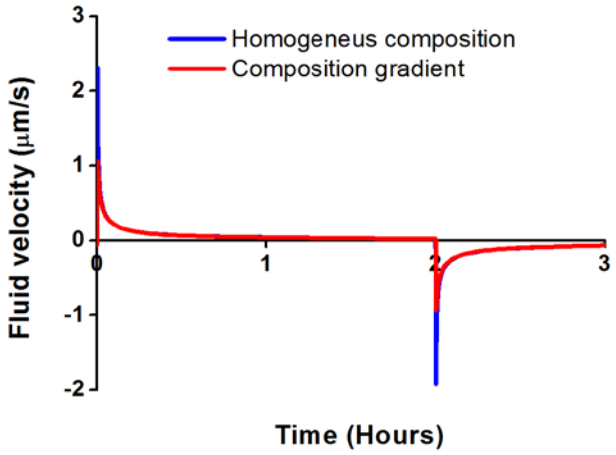

Figure 6.4: Fluid velocity obtained by the 2D model at the nucleus after the 3 hours simulated

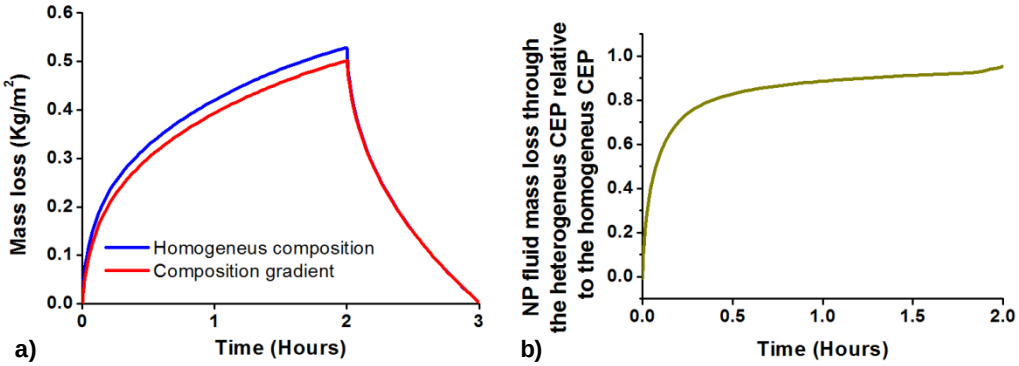

Figure 6.5: a) Effect of the gradient composition permeability on the mass loss at the nucleus, and b) Nucleus fluid mass loss calculated through the heterogeneous CEP along days load, relative to the mass loss calculated in the model with homogeneous CEP

The simulation of cyclic load in the 2D model led to an increase of fluid velocity at the NP. The use of a composition gradient permeability still reduced by up to 57% the fluid velocity at the beginning of the load application (Figure 6.6a). Also, it largely reduces the fluid velocity variations along a dynamic load cycle. On the other hand, the mass loss at the nucleus was reduced by 42% with this load scenario after the 2h of activity (Figure 6.6b). Compared to a mean homogenized composition, the CEP composition gradient did not significantly affect the water balance achieved at the end of the load-unload periods (Figure 6.6c).

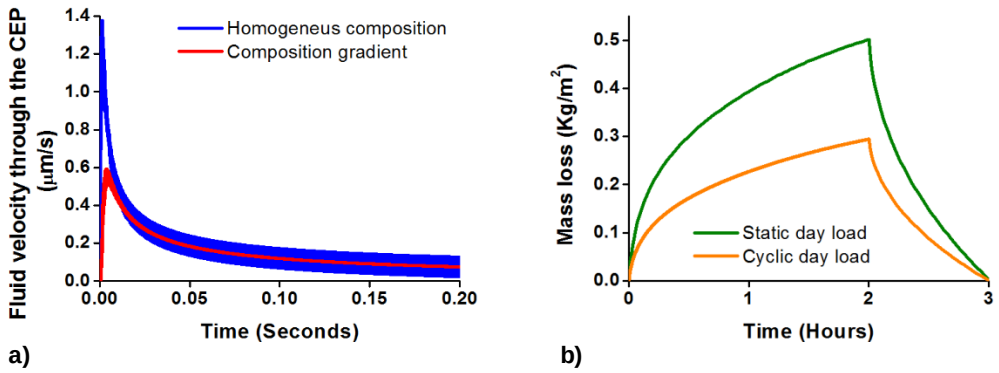

Figure 6.6: a) Effect of the type of day load on the mass loss calculated through the cartilage endplate (CEP) for the first 0.2 seconds of simulation, b) Effect of CEP composition gradient on the fluid velocities calculated during the day period under cyclic loads, and

6.3.3 3D simulations

The mass loss found at the CEP centre at the end of one day simulated for the 3D model was 2.55 kg/m^2 when the CEP properties are degenerated (Figure 6.7a). This value was 39% higher than the values obtained for healthy disc properties. For the disc with all tissue properties degenerated, the mass loss was 2.09 kg/m^2 which represented an increase of 14% compared to the healthy disc. At the CEP-NP boundary, the outcomes were similar. In fact, the mass loss increases by 56% when the CEP was degenerated and by 18% when all tissues were degenerated (Figure 6.7b). Moreover, the mass loss at the CEP-NP boundary was lower than at the CEP centre.

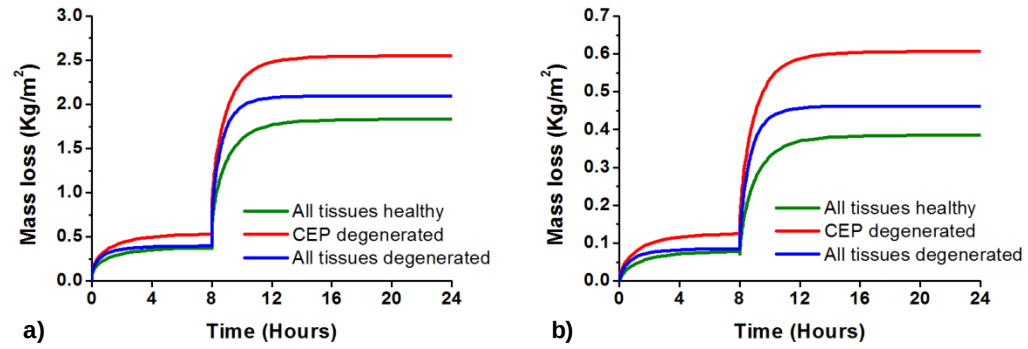

Figure 6.7: Mass loss calculation obtained with the 3D model for the three different tissue conditions at: a) CEP centre, and b) Boundary CEP-NP

The mean fraction of water content (porosity) at the end of one day simulated under 0.54 MPa computed within the NP volume was 0.7723 ± 0.0061 when the CEP was healthy. For the same time and load condition and a degenerated CEP, the mean water content at the NP was 0.7257 ± 0.0051 and when all disc tissues were degenerated the NP mean water content was 0.7255 ± 0.0051 (Figure 6.8). A two-way ANOVA revealed that NP water contents were statistically significantly different when the healthy and degenerated CEP effects were compared. Also, the NP mean water content was statistically significantly different between the CEP healthy condition and the condition when all tissues are degenerated.

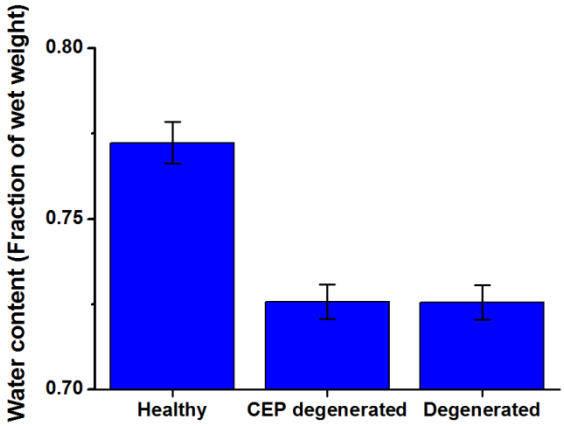

Figure 6.8: Mean water content obtained within the NP volume with the 3D model for the three tissue conditions at the end of the 16h of activity under 0.54 MPa for one day simulated

The 3D transport simulations revealed that all solute concentrations decreased when the CEP composition was that of a tissue considered as degenerated (Figure 6.9). In fact, the glucose concentration was reduced by 16% and the pH level was decreased by 2.4%. The minimum values obtained were 0.77 nmol/mL and 6.90 for glucose concentration and pH respectively, at the anterior AF-TZ boundary (Figure 6.9c and 6.9d). For a disc model with all tissues degenerated, the reduction of solute concentration was higher: the glucose concentration decreased by 55% and the pH decreased by 9%, with minimum values of 0.41 nmol/mL and 6.86 respectively (Figure 6.9c and 6.9d).

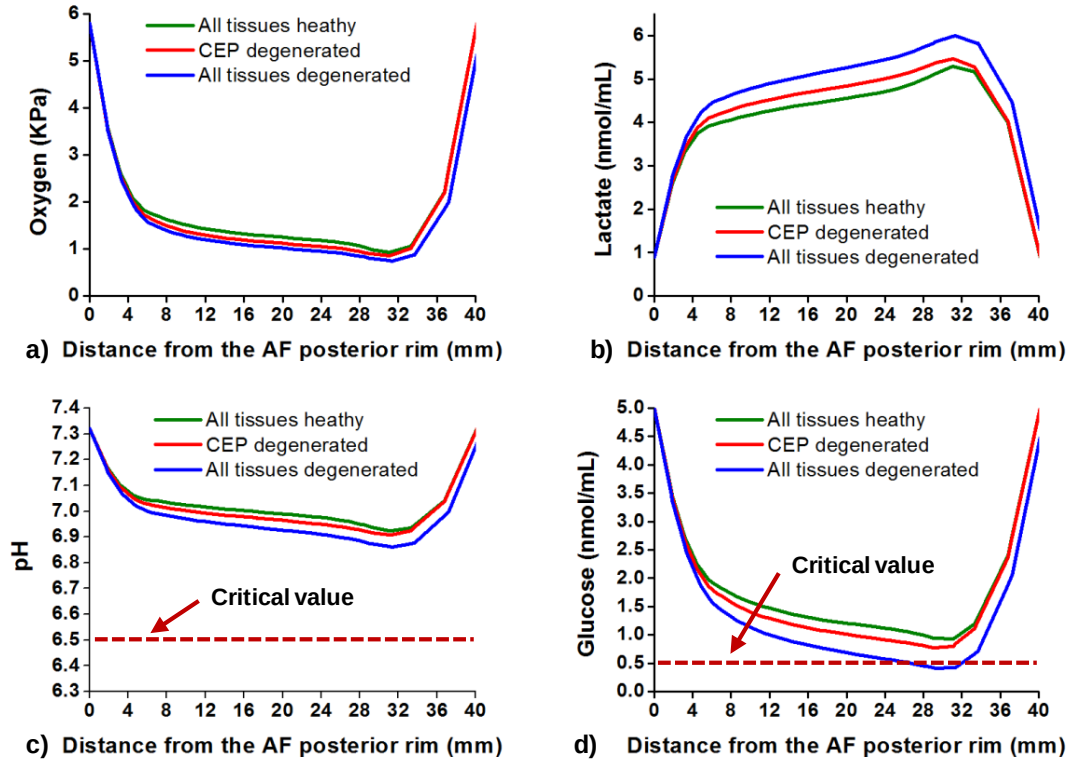

Figure 6.9: Solute concentrations distribution along the sagittal path of the 3D model after three days simulated: a) Oxygen, b) Lactate, c) pH (dot line is the critical value for cell viability), and d) Glucose (dot line is the critical value for cell viability)

All disc cells remained alive after the three days simulated when only the CEP was degenerated. However, the simulation of a disc with all tissue degenerated activated cell death. Indeed, the cells started to die between the simulated days 1 and 2. At the end of the third day 70% of the cell remained alive (Figure 6.10).

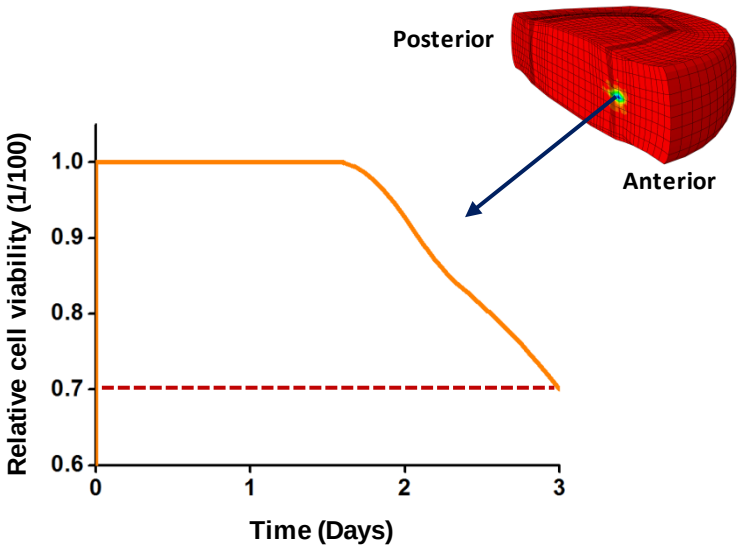

Figure 6.10: Cell viability at the anterior annulus along the three days simulated for a disc with all tissue degenerated

6.4 Discussion

The permeability value of 0.017 mm^4/Ns obtained using Eq. 6.1 for mean healthy composition values was in agreement with the mean value measured by Accadbled et al. (2008) on central endplate samples. Since the cartilaginous part of the endplate has the strongest hydraulic resistance, this comparison supports the validity our approach for the new composition-dependent CEP permeability model. In addition, the negative sign obtained for the parameters B and C (see Table 6.3) are in agreement to the correlation found by Williamson et al. (2001) for bovine articular cartilage, where it was reported that the hydraulic permeability presented a negative correlation with the proteoglycan and collagen content. Also, the relatively large B parameter value suggested that proteoglycans mostly control the effective CEP permeability. This result illustrates nicely the fact that proteoglycan aggregates control the amount of bounded water, and the effective flow through the matrix for a given water content value. Moreover, this result is in agreement to the finding of Comper & Lyons (1993), who showed that the frictional water resistant to water of the articular cartilage is controlled by the proteoglycans. Additionally, whereas Williamson et al. (2001) found a negative correlation between articular cartilage permeability and the proteoglycan content of the tissue, Mahmoodian et al. (2011) found no significant correlation; a possible explanation is the limited number of samples used in the latter study, i.e. two samples in total.

The use of degenerated composition for the CEP led to an increase in the permeability value. This result was in agreement with the study of Rodriguez et al. (2011), who found that the permeability of the CEP and BEP tended to increase with degeneration. Interestingly, their findings were against the general idea that CEP permeability decreases with degeneration because of possible calcification. However, the effect of the calcification nodules identified by Benneker et al. (2005) on disc nutrition at the CEPs remains unknown. Nevertheless, according to the results from Chapter 4 and 5, the present study infers on the likely effect of CEP degeneration on disc hydration. Also, the CEP permeability approach in this study leads to an increment of permeability when CEP composition changes due to degeneration, e.g. from grade I to grade III.

The gradient of permeability reduced the maximum fluid velocity at the NP area in the 2D model. Also, the constant flow that enters the CEP is limited by the gradient of permeability thereby increasing the effective relaxation time of the fluid velocity. The consolidation is high in the CEP layers with low permeability, i.e. nearest to the NP. As such, these layers both damped and added impedance to the overall hydraulic system, explaining the increment in the relaxation time of the velocity. In addition, the gradient of permeability did not change the recovery of water at the end of a cycle. However, it reduced the exchanged water due to the time considered along the transient poromechanical response of the model.

When simulating the effect of dynamic loading on the 2D model, it was found that cyclic compressive loads always limited NP dehydration through the CEP compared to static load effects (Figure 6.6a). This outcome supported the idea that long-lasting static loads might be prejudicial to the disc. In fact, Schmidt et al. (2010) suggested that constant compression might affect the function and injury of the lumbar spine. Also, Jackson et al. (2008) found that the water content decreases around 4% and 8% when the disc is under 10% and 20% of compression respectively, and as showed in the Chapter 4 and 5 a reduction of the water content affects the transport of solutes. Compared to a mean homogenized composition, the CEP composition gradient did not significantly affect the water balance achieved at the end of the load-unload periods. However, it largely limited the fluid velocity peaks in the CEP, as well as the instantaneous fluid loss when mechanical loads are applied (Figure 6.6b and 6.6c). Additionally, Mawatari et al. (2010) found a decreased in the production of aggrecan and type II collagen when the fluid flow increases due to mechanical loads in articular cartilage. This result indicates that the effect of mechanical loads on fluid flow might influence the balance in catabolic and anabolic processes within a cartilaginous tissue such as the CEP.

The calculated exchange of fluid mass thorough the CEP was affected by the simulated degeneration of the tissue (Figure 6.7). In fact the mass loss obtained when only the CEP was degenerated was the highest of all. This result contrasted with the study of Riches & McNally (2005) who found that the CEP permeability decreased with degeneration and that the exchanged volume of fluid

was reduced. Nevertheless, our results might explain what is happening during the ageing of the tissue since the CEP permeability increases when the tissue degenerates (Rodriguez et al. 2011). In consequence, the CEP allows the fluid to move fast producing a large exchange of volume that leads to a faster poromechanical consolidation of the rest of the disc tissues.

The influence of the degeneration of the CEP was evaluated by calculating the water content within the NP. The amount of water inside the nucleus was decreased by 6% when the CEP was considered degenerated. Such reduction in the NP water content certainly would affect the transport of solutes, since it was shown in Chapter 4 that a reduction of 4% in NP water content, i.e. when change from a grade I to a grade III condition, reduced solute concentrations. The same reduction of water was obtained when all disc tissues were degenerated. This result suggests that the CEP controls the water content of the NP. In addition, the water content found at the mid-height NP level was higher than the one at the boundary NP-CEP. Thus, the degenerated CEP had a major effect on the dehydration of the nucleus as shown previously using the 3D model. Also, the restriction of water due to CEP degeneration might influence the diffusion of solutes in and out the disc, aspect that might contribute to disc degeneration.

All solute concentrations were affected by the degeneration of the CEPs. In fact, oxygen and glucose decreased and lactate increased. Moreover, glucose was the most affected solute at the anterior AF-TZ boundary (Figure 6.9d). This zone also presented low water content. As mentioned before, the CEP is the disc tissue that mostly regulates the fluid exchange through the disc boundaries. Furthermore, Chapter 4 showed that a reduction in the water content has a major effect on disc nutrition. The results of the current Chapter showed that CEP degeneration facilitated the outflow of water under mechanical loads, which produced a strong tissue consolidation that decreases the solute diffusivity. Moreover, the level of reduction of pH and glucose were lower than the effect of independent or combined AF and NP degeneration as saw in Chapters 4 and 5. The fact that the CEP had stronger effect on the solutes confirms the importance of this tissue in disc metabolic transport. Most of the CEP studies in the literature highlight the CEP as a path for nutrition, also indicate that its calcification have a

lager influence on solute concentration (Urban et al. 2004; Ferguson et al. 2004; Mokhbi Soukane et al. 2009). The results obtained in this Chapter suggest that CEP degeneration produces NP dehydration, which affect disc nutrition. This last statement leads to propose that disc degeneration might affect the metabolic transport and the CEP degeneration plays a key role in this event. Overall, this is the first simulation that quantifies the effect of CEP degeneration on disc nutrition.

The CEP degeneration did not activate cell death along the three days simulated in the 3D model. On the other hand, the cells started to die when all disc tissues were considered degenerated. The anterior TZ was the location where the cells were affected. The increment of tissue consolidation presented in this area might be a consequence of the CEP degeneration. In addition, the cell viability results obtained differed from other studies that suggested that a calcification of the CEP is needed to observe cell death (Roberts et al. 1996; Shirazi-Adl et al. 2010; Malandrino et al. 2014a). Although calcification might interrupt the fluid flow through the endplate, this condition appears in late stages of disc degeneration. Also, the study of Rodriguez et al. (2012) suggested that there is no correlation between disc degeneration and sclerosis. In addition, Chapter 5 showed that the simulation of natural ageing corresponds to a reasonable disc degeneration, e.g. grade III Pfirrmann scale. In this Chapter, such tissue condition led to observe cell death. As such, this study is the first numerical study that suggests that it is not necessary to have CEP calcification to activate catabolic processes within the intervertebral disc.

Disc cell nutrition was suggested to be affected by CEP calcification, ageing, scoliosis and degeneration (Buckwalter 1995), and CEP calcification has been proposed as a major cause of the fall in nutrition (Roberts et al. 1996). Overall, the results of the present study has led to identify an alternative and rational mechanism, and to formulate the hypothesis about CEP involvement in the disturbance of disc nutrition. The study of Benneker et al. (2005) showed that alterations in the CEP are one of the first MRI signs to appear. Moreover, according to our results CEP permeability would increase with ageing. In consequence, the exchange of fluid increases generating a high tissue consolidation, i.e. porosity reduction. This reduction leads to the dehydration of the NP, that combined to the

NP proteoglycan depletion decrease the levels of glucose and pH. Such fall in the level of solutes might downregulate the expression of matrix proteins and/or activate catabolic cell activities, e.g. expression of matrix metalloproteinase (MMP), especially MMP-3, which might contribute to accelerated disc degeneration.

As any numerical study, the present study has limitations. Firstly, it only considered compression loads in the 3D simulations. Within a regular day the disc is subjected to different static and dynamic load variations. However, in Chapter 5 it was shown that the consideration of peaks of pressure did not affect the transport of solute. Also, Malandrino et al. (2011) showed that sustained compression effects the most disc nutrition. As such, only this type of load was considered. Secondly, an average content for all disc biochemical components was considered. Thirdly, the geometry of the 3D disc model remained generic. Patient specific geometries might give different shapes of CEPs and in addition with new techniques for measuring disc composition could provide further information about the influence of the CEP on disc degeneration. Fourthly, the initial cell density was not changed when all disc tissue were considered degenerated. However the cell density in the transport model is updated with the tissue deformations which change with degeneration. Finally, mean homogenized permeability was considered for all disc tissue in the 3D simulations. However, the results obtained in the 2D model related to the increment in permeability with degenerative changes in CEP composition gave a good start point for the 3D simulations in order to evaluate the role of the whole CEP tissue in the nutrition phenomena. Interestingly, changes in CEP composition with ageing might make the tissue structure weaker and probably could explain the microfractures observed in cadaveric specimens (Adams 2004). Extending the 2D model permeability gradient approach developed in this study to a 3D model may provide a better idea of influence of such gradient of composition on the releases of inflammatory factors that, combined with Modic changes, might be a cause for low back pain (Zhang et al. 2008).

6.5 Conclusions

This Chapter presented a novel approach for simulating the permeability gradient of the cartilage endplate to evaluate the role of this tissue in disc nutrition and cell viability. The results of the 2D model showed that alterations in the proteoglycan content would largely affect the CEP permeability. In addition, the degeneration of the CEP led to the increment of the permeability of the tissue.

The consideration of CEP matrix composition and CEP composition-based permeability mean values allowed to evaluate the importance of the CEP in disc degeneration. Moreover, the results presented in this Chapter allowed the proposal of an alternative path to disc generation: when the CEP degenerates, the NP dehydrates leading to a reduction in the levels of solutes. The fall in solute concentrations produces cell death and also might activate the release of enzymes that disintegrate the disc extracellular matrix possibly leading to disc degeneration. This statement identifies the CEP as a key factor in disc degeneration. The present study opens a new insight for regenerative strategies in order to generate alternative therapies to deal with disc degeneration.

7 GENERAL DISCUSSION AND CONCLUSIONS

As mentioned in Chapter 2, disc degeneration involves several changes in the disc, e.g. morphological and biochemical. Among the biochemical changes, proteoglycan loss is the major one, which produces alterations at disc mechanical behaviour, but its influence on disc cell nutrition that in turn largely controls disc cell viability, remained poorly addressed. In general, the literature review revealed that the influence of degenerative changes of disc tissues on cell activity lacked comprehensive explorations. Also, CEP calcification was suggested to have a major impact on the nutrition-dependent viability of disc cells. However, while this hypothesis remains controversial, the specific role of CEP composition in terms of collagen, water and proteoglycans, remained unknown in disc cell nutrition. The study of all the unknown points mentioned earlier represent a major challenge for experimental studies, in order to find a link between disc degeneration and cell nutrition, since:

- Many processes occur simultaneously and an experimental model that captures these processes and the interactions thereof is difficult to achieve.
- The history of coupled processes in different regions of the disc e.g. NP centre, boundary NP-AF and boundary NP-CEP is difficult to assess experimentally.

- Controlling the influence of each parameter of disc composition, e.g. collagen and proteoglycans simultaneously, on measured biological processes is not an easy task.
- The experimental or clinical exploration of degenerative changes in the CEP is hard, since the latter is a very thin layer of hyaline cartilage with a thickness no larger than 1 mm.

Finite element modelling, in particular poromechanical analyses, appeared as an appropriate alternative/complement to experimental studies, in order to tackle the difficulties mentioned above. In Chapter 2, it was also mentioned that the mesh of the finite element models might have to be finely tuned to ensure accurate results, and mesh convergence studies are mandatory. In this sense, the challenge is to find the best relation element size-computational cost that allows the simulation of disc tissue poromechanics and all other coupled processes with accuracy. Overall, the numerical approaches developed in this thesis were used to reveal different spatiotemporal sequences of indirect mechanotransduction that can occur during disc degeneration.

7.1 Technological development in IVD modelling

In Chapter 3, different mesh refinements were tested to evaluate the accuracy of poromechanical predictions under loads rates involved in physiological cyclic loads. The convergence study led to the addition of a material transition zone that combined with local mesh refinement generated a model that largely reduced FV oscillations under extension and ensured the convergence of SED predictions under axial rotation. In Chapter 4 the disc model was updated through the incorporation of a constitutive formulation that considered the biochemical composition of disc tissues. The model was coupled to a transport-cell viability model. Such coupling allowed the study of the influence of degenerative changes of disc tissues on nutrition. In Chapter 5, a novel approach for the NP proteoglycan turnover was incorporated to the model. Accordingly, the simulation workflow was changed so as to evaluate how solute transport and cell nutrition can influence the disc poromechanical behaviour. Finally in Chapter 6, the biochemical composition formulation was extended to the CEP matrix and the initial CEP permeability value was obtained from a novel composition-dependent

formulation for the CEP gradient composition permeability. This last update allowed the exploration of the role of the CEP in disc degeneration.

7.2 Major findings

Pore pressure oscillations in poromechanical models had been identified for fast load rates (Stokes et al. 2010). Chapter 3 revealed that FV (first spatial derivative of the pore pressure) oscillations were also caused by material discontinuities, e.g. boundary NP-AF. The application of the Vermeer-Veruijt criterion, suggested to stabilize pore pressure predictions at order zero through guided mesh refinement, was insufficient to solve these weak discontinuity effects. However, the creation of a transition zone with material-depend mesh refinement led to a stable IVD mesh template for the other explorations of this thesis, at the tissue level.

In Chapter 4, water content was identified as the disc composition parameter that affected the most the calculated cell nutrition, through load-induced tissue consolidation. None of the simulated degenerative changes affected cell viability, however. Changes in the proteoglycan content in the NP affected disc height, and remarkably, degeneration of the NP affected AF nutrition, especially the posterior AF. Such a process might be proposed as a specific mechanism able to debilitate the AF structure through local cell responses to nutritional stress, favouring the eventual occurrence of radial tears in the posterior AF.

Chapter 5 showed that disc nutrition might controls the proteoglycan content inside the NP along ageing. Calculations pointed out the relevance of oxygen level in the control of proteoglycan production rates per disc cell. The loss of proteoglycan due to limited oxygen transport affected the mechanical behaviour of the disc by reducing the osmotic pressure and disc height, but it did not significantly alter disc cell nutrition. Nevertheless, additional dehydration of the NP, as measured in mildly degenerated discs, led to reduced solute concentrations under mechanical loads. These results suggested that proteoglycan-independent water loss is a major risk factor for disc degeneration. Should such a disc desiccation happen, experimental research should inform about whether the reduction of glucose concentration (around 1 mM) and pH might trigger cell catabolic activity.

Finally, Chapter 6 revealed that CEP permeability is likely to increase with disc degeneration. Simulating the degeneration of the CEP alone generated dehydration of the NP under mechanical loads, and already reduced the solute concentrations. In addition, CEP degeneration combined with the AF and NP degeneration led to nutrition-induced cell death. Overall, Chapter 6 results led to speculate about an alternative path for disc degeneration: early CEP degeneration produces a load-induced dehydration of the NP that chronically reduces the solute concentration, which might trigger catabolic cell activity and degrade disc matrix possibly accelerating the degeneration process.

7.3 Integrated view of the major findings

The major findings mentioned in the previous section allowed mapping different sequences of nutrition-related events associated to ageing and disc degeneration (Figure 7.1). In general, results suggested that the NP degeneration could produce a biochemical weakening of the AF structure, depending on the sensitivity of disc cell responses to reduced nutrition, which remains poorly explored experimentally. Such weakening might contribute to the occurrence of tears at the posterior AF in a grade III disc. In addition, the loss of proteoglycan possibly due to limited oxygen concentrations along simulated ageing reduced the osmotic pressure, which might favour the propagation of the tears, according to earlier simulation findings from Wognum et al. (2006).

Simulations from Chapter 5 revealed that the loss of proteoglycan in the NP due to ageing might not affect significantly disc cell nutrition. Although such loss reduced the disc height possibly enhancing nutrition, it was showed in Chapter 4 that the reduction of porosity, i.e. water content has a stronger affect on nutrition for the specific modelled disc geometry. In this sense, the combination of NP proteoglycan loss and NP dehydration reduced solute concentration in the disc, confirming the results of Chapter 4 where it was showed that the water content was the parameter that affected the most disc nutrition. Overall, disc dehydration achieved through other mechanisms than osmotic pressure loss seemed to be particularly critical.

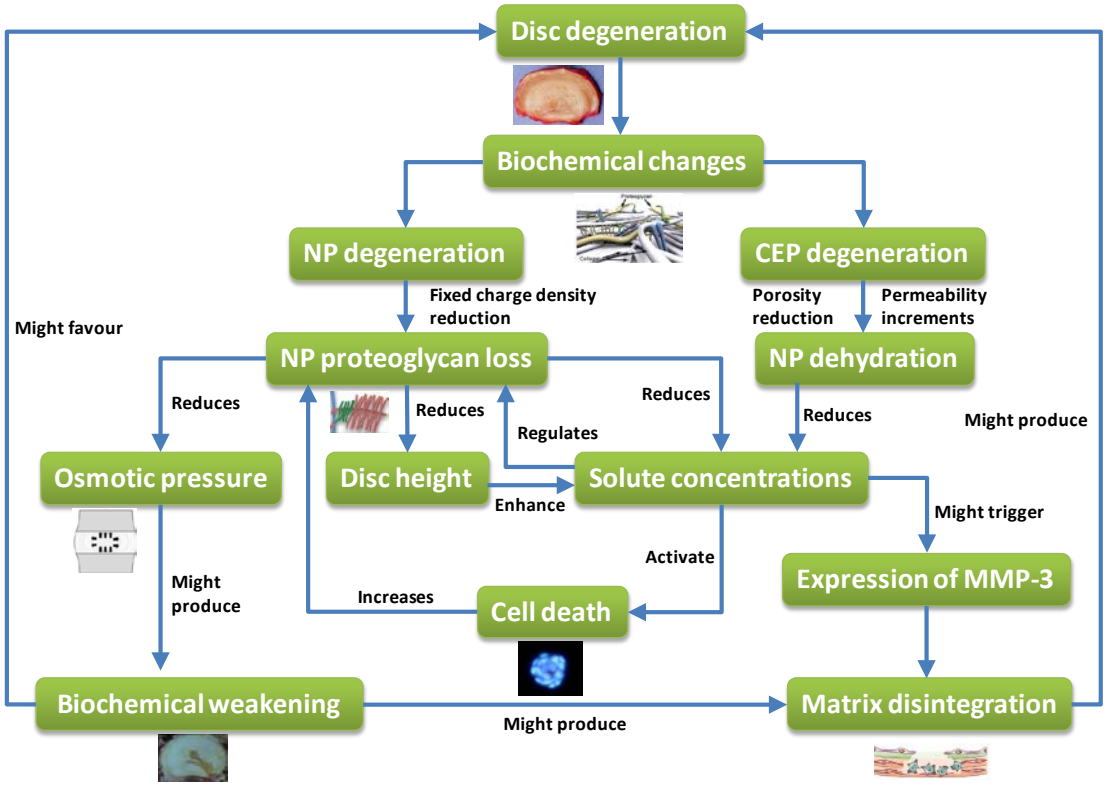

Figure 7.1: Integrated general scheme of the main results obtained in this thesis

Both Chapter 4 and 5 results showed that the reduction of solute concentrations due to combined or separated AF and NP degeneration did not lead to nutrition-induced cell death. The inclusion of the CEP degeneration was necessary to observe cell death (Chapter 6). Interestingly, simulating CEP degeneration through composition changes led to a more permeable CEP according to experimental findings reported in the literature (Rodriguez et al. 2011). Hence CEP degeneration could contribute to increased disc dehydration under mechanical loads, independently on the condition of the NP.

Furthermore, Chapter 6 showed that CEP degeneration alone had a stronger effect on disc nutrition that the combined degeneration of AF and NP. This result confirmed the importance that the CEP has on disc nutrition. Both, lower oxygen transport due to reduced water content, and lower cell density due to cell death might accelerate the proteoglycan loss according to Chapter 5 simulations. Moreover, the reduction of solute concentrations either by combined NP proteoglycan loss and NP dehydration (Chapter 5) or by CEP degeneration only (Chapter 6) might (i) generate the release of enzymes like the MMP-3, and (ii) further reduce the expression of ECM components (Rinkler et al. 2010; Neidlinger-Wilke et al. 2012).

7.4 Future works

The findings of this thesis may lead to new studies. Firstly, the model could be updated with a patient-specific geometry, since it was shown that diffusion distances might change with the person and with the level in the spine (Malandrino et al. 2015a). In consequence, the effect that such variety of geometries can have on disc nutrition and cell viability need to be further explored. Secondly, the concentration of glucose and pH found in Chapter 5 might activate catabolic processes. New experimental studies that would take into account the range of calculated solute concentrations would confirm such activation, and would determine if the amount of enzymes released can affect the ECM and accelerate disc degeneration. Finally, the composition-dependent heterogeneous CEP model developed in Chapter 6 should be extended to a 3D model. This extension would allow the evaluation of the effect of the CEP gradient of composition on disc nutrition and the verification of the role of the CEP on disc degeneration.

7.5 Novelty in relation to the current literature and conclusion

This thesis identified links between processes that occur during the intervertebral disc degeneration, providing important knowledge in order to have a better understanding of this pathology. In this sense, Chapter 3 provided an IVD poromechanics FE model that guarantees the stability of local predictions, allowing the study of long lasting phenomena such as diffusion or disc degeneration.

Matrix composition is suggested to be a factor that controls the movement of solutes along the disc. Although proteoglycans might regulate the tissue pore size (Grunhagen et al. 2011), in Chapter 4 the water content was identified as the biochemical component of disc matrix that affects the most the nutrition. Moreover, in the same Chapter it is suggested that NP degeneration might weaken the structure of the AF, giving a possible explanation to the appearance of tears at the posterior AF in grade III discs.

It is known that the main biochemical change in disc degeneration is the proteoglycan loss, that produce the fall of the osmotic pressure (Urban & Roberts

2003). Chapter 5 suggested that disc cell nutrition might explain this change along ageing. However, alone, this proteoglycan loss might not have dramatic effects in terms of indirect mechanotransduction, in healthy to mildly degenerated discs. It was further pointed out that NP dehydration through other mechanisms might be needed to alter disc nutrition. Also Chapter 5 revealed that the effect of low levels of glucose, e.g. 1.06 mM and pH, e.g. 6.98 might be explored against their capacity to trigger the expression of MMP-3 or other proteases that might weaken the ECM especially nearby the inner AF. Current experimental data are only available for MMP-3 and ECM components expression with levels of glucose of 0, 0.5, and 5 mM (Neidlinger-Wilke et al. 2012). Simulation findings strongly suggest the necessity to screen the effect of reduced glucose concentrations at intermediate concentration values, between 0.5 and 5 mM.

It has been reported in the literature that CEP permeability decreases with disc degeneration. This decrease is attributed to the sclerosis and CEP calcification (Roberts et al. 1996; Riches & McNally 2005). However, an opposite outcome was obtained in Chapter 6, where the value of CEP permeability increases with degeneration. Interestingly, this result is in agreement with the study of Rodriguez et al. (2011). Chapter 6 also showed that CEP degeneration combined with the AF and NP degeneration due to natural ageing provoked nutrition-induced cell death under mechanical loads. This result contradicts the general idea that CEP calcification is needed to observe cell death. Moreover, this Chapter showed an alternative path for disc degeneration where CEP degeneration plays a key role.

Although this thesis established links between diverse processes that occur during the intervertebral disc degeneration, still many issues remain. The combined use of advanced disc models such as the one presented in this thesis with experimental tests could provide a more complete vision of the degenerative processes that occur inside the disc including precise spatiotemporal sequences. This knowledge can be used in the creation of new regenerative strategies in order to achieve improved treatments that cure patients with low back pain.

REFERENCES

Abbott, R.D. et al., 2012. Live free or die: Stretch-induced apoptosis occurs when adaptive reorientation of annulus fibrosus cells is restricted. *Biochemical and Biophysical Research Communications*, 421(2), pp.361–366. Available at: http://www.ncbi.nlm.nih.gov/pubmed/22516752.

Accadbled, F. et al., 2008. Influence of location, fluid flow direction, and tissue maturity on the macroscopic permeability of vertebral end plates. *Spine*, 33(6), pp.612–9. Available at: http://www.ncbi.nlm.nih.gov/pubmed/18344854.

Adams, M. a et al., 2014. Why do some intervertebral discs degenerate, when others (in the same spine) do not? *Clinical anatomy (New York, N.Y.)*, 00(April). Available at: http://www.ncbi.nlm.nih.gov/pubmed/24753325 [Accessed August 18, 2014].

Adams, M.A., 2004. Biomechanics of back pain. *Acupuncture in Medicine*, 22(4), pp.178–188. Available at: http://www.ncbi.nlm.nih.gov/pubmed/15628775.

Adams, M.A. et al., 1990. Diurnal changes in spinal mechanics and their clinical significance. *The Journal of bone and joint surgery. British volume*, 72(2), pp.266–270. Available at: http://www.ncbi.nlm.nih.gov/pubmed/2138156.

Adams, M.A. & Hutton, W.C., 1983. The effect of posture on the fluid content of lumbar intervertebral discs. *Spine*, 8(6), pp.665–671. Available at: http://www.ncbi.nlm.nih.gov/pubmed/6685921.

Adams, M.A., McNally, D.S. & Dolan, P., 1996. "Stress" distributions inside intervertebral discs. The effects of age and degeneration. *The Journal of bone and joint surgery. British volume*, 78(6), pp.965–972. Available at: http://www.ncbi.nlm.nih.gov/pubmed/8951017.

Alenghat, F.J. & Ingber, D.E., 2002. Mechanotransduction: all signals point to cytoskeleton, matrix, and integrins. *Science's STKE : signal transduction knowledge environment*, 2002(119), p.pe6. Available at: http://www.ncbi.nlm.nih.gov/pubmed/11842240.

Ali, A. a. et al., 2014. Specimen-specific modeling of hip fracture pattern and repair. *Journal of Biomechanics*, 47(2), pp.536–543. Available at: http://www.ncbi.nlm.nih.gov/pubmed/24275435.

Alini, M. et al., 2008. Are animal models useful for studying human disc disorders/degeneration? *European Spine Journal*, 17(1), pp.2–19. Available at: http://www.ncbi.nlm.nih.gov/pubmed/17632738.

Anderson, A.E., Ellis, B.J. & Weiss, J. a, 2007. Verification, validation and sensitivity studies in computational biomechanics. *Computer methods in biomechanics and biomedical engineering*, 10(3), pp.171–184. Available at: http://www.ncbi.nlm.nih.gov/pubmed/17558646.

Andersson, G.B., 1999. Epidemiological features of chronic low-back pain. *Lancet*, 354(9178), pp.581–585. Available at: http://www.ncbi.nlm.nih.gov/pubmed/10470716.

Antoniou, J. et al., 1996. The human lumbar intervertebral disc: Evidence for changes in the biosynthesis and denaturation of the extracellular matrix with growth, maturation, ageing, and degeneration. *Journal of Clinical Investigation*, 98(4), pp.996–1003. Available at: http://www.ncbi.nlm.nih.gov/pubmed/8770872.

Argoubi, M. & Shirazi-Adl, A., 1996. Poroelastic creep response analysis of a lumbar motion segment in compression. *Journal of Biomechanics*, 29(10), pp.1331–1339. Available at: http://www.ncbi.nlm.nih.gov/pubmed/8884478.

Arun, R. et al., 2009. 2009 ISSLS Prize Winner: What influence does sustained mechanical load have on diffusion in the human intervertebral disc?: an in vivo study using serial postcontrast magnetic resonance imaging. *Spine*, 34(21), pp.2324–2337. Available at: http://www.ncbi.nlm.nih.gov/pubmed/19755934.

Asfour, S. et al., 2015. A computational analysis on the implications of age-related changes in the expression of cellular signals on the role of IGF-1 in intervertebral disc homeostasis. *Journal of Biomechanics*, 48(2), pp.332–339. Available at: http://www.ncbi.nlm.nih.gov/pubmed/25488135.

Ayotte, D.C. et al., 2000. Direction-dependent constriction flow in a poroelastic solid: the intervertebral disc valve. *Journal of biomechanical engineering*, 122(6), pp.587–593. Available at: http://www.ncbi.nlm.nih.gov/pubmed/11192378.

Ayotte, D.C., Ito, K. & Tepic, S., 2001. Direction-dependent resistance to flow in the endplate of the intervertebral disc: an ex vivo study. *Journal of orthopaedic research : official publication of the Orthopaedic Research Society*, 19(6), pp.1073–7. Available at: http://www.ncbi.nlm.nih.gov/pubmed/11781007.

Bartels, E.M. et al., 1998. Oxygen and lactate concentrations measured in vivo in the intervertebral discs of patients with scoliosis and back pain. *Spine*, 23(1), pp.1–7; discussion 8. Available at: http://www.ncbi.nlm.nih.gov/pubmed/9460145.

Belytschko, T. & Black, T., 1999. Elastic Crack Growth in Finite Elements. *International Journal for Numerical Methods in Engineering*, 620(July 1998), pp.601–620. Available at: http://doi.wiley.com/10.1002/(SICI)1097-0207(19990620)45:5<601::AID-NME598>3.0.CO;2-S.

Benallaoua, M. et al., 2006. Modulation of proteoglycan production by cyclic tensile stretch in intervertebral disc cells through a post-translational mechanism. *Biorheology*, 43(3-4), pp.303–10. Available at: http://www.ncbi.nlm.nih.gov/pubmed/16912403.

Benneker, L.M. et al., 2005. Correlation of radiographic and MRI parameters to morphological and biochemical assessment of intervertebral disc degeneration. *European Spine Journal*, 14(1), pp.27–35.

Bernick, S. & Cailliet, R., 1982. Vertebral end-plate changes with aging of human vertebrae. *Spine*, 7(2), pp.97–102. Available at: http://www.ncbi.nlm.nih.gov/pubmed/7089697.

Bibby, S.R.S. et al., 2005. Metabolism of the intervertebral disc: effects of low levels of oxygen, glucose, and pH on rates of energy metabolism of bovine nucleus pulposus cells. *Spine*, 30(5), pp.487–96. Available at: http://www.ncbi.nlm.nih.gov/pubmed/15738779.

Bibby, S.R.S. et al., 2001. Pathophysiology of the human intervertebral disc. *Joint Bone Spine*, 68, pp.537–42. Available at: http://www.sciencedirect.com/science/article/pii/S1297319X01003323.

Bibby, S.R.S. & Urban, J.P.G., 2004. Effect of nutrient deprivation on the viability of intervertebral disc cells. *European spine journal : official publication of the European Spine Society, the European Spinal Deformity Society, and the European Section of the Cervical Spine Research Society*, 13(8), pp.695–701. Available at: http://www.ncbi.nlm.nih.gov/pubmed/15048560 [Accessed August 18, 2014].

Biot, M. a., 1941. General theory of three-dimensional consolidation. *Journal of Applied Physics*, 12(2), pp.155–164.

Bischoff, M. & Ramm, E., 2000. On the physical significance of higher order kinematic and static variables in a three-dimensional shell formulation. *International Journal of Solids and Structures*, 37(46-47), pp.6933–6960. Available at: http://www.sciencedirect.com/science/article/pii/S0020768399003212.

Bogduk, N., 2005. *Clinical Anatomy of the Lumbar Spine and Sacrum* 4th editio., Oxford: Churchill Livingstone.

Boos, N. et al., 2002. Classification of age-related changes in lumbar intervertebral discs: 2002 Volvo Award in basic science. *Spine*, 27(23), pp.2631–2644. Available at: http://www.ncbi.nlm.nih.gov/pubmed/12461389.

Boubriak, O.A. et al., 2013. Factors regulating viable cell density in the intervertebral disc: blood supply in relation to disc height. *Journal of anatomy*, 222(3), pp.341–348. Available at: http://www.ncbi.nlm.nih.gov/pubmed/23311982 [Accessed February 12, 2013].

Brown, T., Hansen, R.J. & Yorra, A.J., 1957. Some mechanical tests on the lumbosacral spine with particular reference to the intervertebral discs; a preliminary report. *The Journal of bone and joint surgery. American volume*, 39-A(5), pp.1135–1164.

Bruehlmann, S.B. et al., 2002. Regional variations in the cellular matrix of the annulus fibrosus of the intervertebral disc. *Journal of Anatomy*, 201(2), pp.159–171. Available at: http://www.ncbi.nlm.nih.gov/pubmed/12220124.

Büchter, N., Ramm, E. & Roehl, D., 1994. Three-dimensional extension of non-linear shell formulation based on the enhanced assumed strain concept. *International Journal for Numerical Methods in Engineering*, 37(15), pp.2551–2568. Available at: http://dx.doi.org/10.1002/nme.1620371504.

Buckwalter, J.A., 1995. Aging and degeneration of the human intervertebral disc. *Spine*, 20(11), pp.1307–1314. Available at: http://www.ncbi.nlm.nih.gov/pubmed/7660243.

Caner, F.C. et al., 2007. Hyperelastic anisotropic microplane constitutive model for annulus fibrosus. *Journal of biomechanical engineering*, 129(5), pp.632–641. Available at: http://www.ncbi.nlm.nih.gov/pubmed/17887888.

Cassinelli, E.H., Hall, R. a & Kang, J.D., 2001. Biochemistry of intervertebral disc degeneration and the potential for gene therapy applications. *The spine journal : official journal of the North American Spine Society*, 1(3), pp.205–14. Available at: http://www.ncbi.nlm.nih.gov/pubmed/14588349.

Chen, J. et al., 2002. Matrix protein gene expression in intervertebral disc cells subjected to altered osmolarity. *Biochemical and biophysical research communications*, 293(3), pp.932–8. Available at: http://www.ncbi.nlm.nih.gov/pubmed/12051748.

Chou, R. et al., 2009. Nonsurgical interventional therapies for low back pain: a review of the evidence for an American Pain Society clinical practice guideline. *Spine*, 34(10), pp.1078–93. Available at: http://www.ncbi.nlm.nih.gov/pubmed/19363456.

Comí, M. et al., 1995. *Biomecánica del raquis y sistemas de reparación* 2nd Editio., Valencia: Insituto de Biomecánica de Valencia.

Comper, W.D. & Lyons, K.C., 1993. Non-electrostatic factors govern the hydrodynamic properties of articular cartilage proteoglycan. *The Biochemical journal*, 289 (Pt 2(109), pp.543–547. Available at: http://www.ncbi.nlm.nih.gov/pubmed/8424796/.

Courtecuisse, H., Kerfriden, P. & Bordas, S., 2013. Cutting in Real Time in Corotational Elasticity and Perspectives on Simulating Cuts. In *Computational Biomechanics for Medicine*. pp. 3–5.

Crean, J.K. et al., 1997. Matrix metalloproteinases in the human intervertebral disc: role in disc degeneration and scoliosis. *Spine*, 22(24), pp.2877–2884. Available at: http://www.ncbi.nlm.nih.gov/pubmed/9431623.

Crock, H. V & Goldwasser, M., 1984. Anatomic studies of the circulation in the region of the vertebral end-plate in adult Greyhound dogs. *Spine*, 9(7), pp.702–706.

Dao, T.T. et al., 2014. In vitro Assessment of Micro-structural Properties of Intervertebral Disc using 1.5T Magnetic Resonance T2 and ADC Mappings. In *7th World Congress of Biomechanics*. Boston.

Doyle, A.D. & Yamada, K.M., 2010. Cell biology: Sensing tension. *Nature*, 466(7303), pp.192–193. Available at: http://www.ncbi.nlm.nih.gov/pubmed/20613830.

Drescher, W. et al., 2000. Vertebral blood flow and bone mineral density during long-term corticosteroid treatment: An experimental study in immature pigs. *Spine*, 25(23), pp.3021–3025. Available at: http://www.ncbi.nlm.nih.gov/pubmed/11145813.

Drew, S.C. et al., 2004. A diffusion and T2 relaxation MRI study of the ovine lumbar intervertebral disc under compression in vitro. *Physics in medicine and biology*, 49(16), pp.3585–3592. Available at: http://www.ncbi.nlm.nih.gov/pubmed/15446789.

Duarte, C.A. & Oden, J.T., 1996. H-p clouds-an h-p meshless method. *Numerical Methods for Partial Differential Equations*, 12(6), pp.673–705. Available at: http://dx.doi.org/10.1002/(SICI)1098-2426(199611)12:6<673::AID-NUM3>3.0.CO;2-P.

Dynamic Disc Designs, 2015. Professional LxH Disc Model. *Spine Education Models*. Available at: http://www.dynamicdiscdesigns.com/shop/professional-lxh-disc-model/.

Eyre, D.R., Dickson, I.R. & Van Ness, K., 1988. Collagen cross-linking in human bone and articular cartilage. Age-related changes in the content of mature hydroxypyridinium residues. *The Biochemical journal*, 252(2), pp.495–500. Available at: http://www.ncbi.nlm.nih.gov/pubmed/3415669/.

Fagan, M.J., Julian, S. & Mohsen, a M., 2002. Finite element analysis in spine research. *Proceedings of the Institution of Mechanical Engineers. Part H, Journal of engineering in medicine*, 216(5), pp.281–298. Available at: http://www.ncbi.nlm.nih.gov/pubmed/12365787.

Ferguson, S.J., Ito, K. & Nolte, L.P., 2004. Fluid flow and convective transport of solutes within the intervertebral disc. *Journal of Biomechanics*, 37(2), pp.213–221. Available at: http://www.ncbi.nlm.nih.gov/pubmed/14706324 [Accessed July 23, 2014].

Fernando, H.N. et al., 2011. Mechanical loading affects the energy metabolism of intervertebral disc cells. *Journal of orthopaedic research : official publication of the Orthopaedic Research Society*, 29(11), pp.1634–41. Available at: http://www.ncbi.nlm.nih.gov/pubmed/21484859 [Accessed November 14, 2014].

Fields, A.J. et al., 2015. Cartilaginous End Plates: Quantitative MR Imaging with Very Short Echo Times—Orientation Dependence and Correlation with Biochemical Composition. *Radiology*.

Freemont, a J., 2009. The cellular pathobiology of the degenerate intervertebral disc and discogenic back pain. *Rheumatology (Oxford, England)*, 48(1), pp.5–10. Available at: http://www.ncbi.nlm.nih.gov/pubmed/18854342 [Accessed November 13, 2014].

Galbusera, F., Schmidt, H., et al., 2011a. Comparison of four methods to simulate swelling in poroelastic finite element models of intervertebral discs. *Journal of the Mechanical Behavior of Biomedical Materials*, 4(7), pp.1234–1241. Available at: http://www.ncbi.nlm.nih.gov/pubmed/21783132 [Accessed November 20, 2014].

Galbusera, F., Mietsch, A., et al., 2011b. Effect of intervertebral disc degeneration on disc cell viability: a numerical investigation. *Computer Methods in Biomechanics and Biomedical Engineering*, 16(3), pp.1–10. Available at: http://www.ncbi.nlm.nih.gov/pubmed/21970697 [Accessed September 3, 2014].

Gasser, T.C., Ogden, R.W. & Holzapfel, G. a, 2006. Hyperelastic modelling of arterial layers with distributed collagen fibre orientations. *Journal of the Royal Society, Interface / the Royal Society*, 3(6), pp.15–35. Available at: http://www.ncbi.nlm.nih.gov/pubmed/16849214.

Gatenby, R. a & Gillies, R.J., 2004. Why do cancers have high aerobic glycolysis? *Nature reviews. Cancer*, 4(11), pp.891–899.

Grant, J.P. et al., 2002. The effects of bone density and disc degeneration on the structural property distributions in the lower lumbar vertebral endplates. *Journal of orthopaedic research : official publication of the Orthopaedic Research Society*, 20(5), pp.1115–20. Available at: http://www.ncbi.nlm.nih.gov/pubmed/12382980.

Grunhagen, T. et al., 2011. Intervertebral Disk Nutrition: A Review of Factors Influencing Concentrations of Nutrients and Metabolites. *Orthopedic Clinics of North America*, 42(4), pp.465–477. Available at: http://www.ncbi.nlm.nih.gov/pubmed/21944584.

Gu, W. et al., 2014. Simulation of the Progression of Intervertebral Disc Degeneration Due to Decreased Nutritional Supply. *Spine*, 39(24), pp.E1411–E1417. Available at: http://www.ncbi.nlm.nih.gov/pubmed/25188596.

Guehring, T. et al., 2009. Notochordal intervertebral disc cells: sensitivity to nutrient deprivation. *Arthritis and rheumatism*, 60(4), pp.1026–34. Available at: http://www.ncbi.nlm.nih.gov/pubmed/19333932 [Accessed August 18, 2014].

Guilak, F. et al., 1999. Viscoelastic properties of intervertebral disc cells. Identification of two biomechanically distinct cell populations. *Spine*, 24(23), pp.2475–83. Available at: http://www.ncbi.nlm.nih.gov/pubmed/10626310.

Hangai, M. et al., 2009. Lumbar intervertebral disk degeneration in athletes. *The American journal of sports medicine*, 37, pp.149–155. Available at: http://www.ncbi.nlm.nih.gov/pubmed/18799691.

Harrop, J.S. et al., 2008. Lumbar adjacent segment degeneration and disease after arthrodesis and total disc arthroplasty. *Spine*, 33(15), pp.1701–7. Available at: http://www.ncbi.nlm.nih.gov/pubmed/18594464.

Heuer, F. et al., 2007. Creep associated changes in intervertebral disc bulging obtained with a laser scanning device. *Clinical biomechanics (Bristol, Avon)*, 22(7), pp.737–44. Available at: http://www.ncbi.nlm.nih.gov/pubmed/17561321 [Accessed August 18, 2014].

Holm, S. et al., 1981. Nutrition of the intervertebral disc: solute transport and metabolism. *Connective tissue research*, 8(2), pp.101–119. Available at: http://www.ncbi.nlm.nih.gov/pubmed/6453689.

Holzer, L. et al., 2012. The influence of constrictivity on the effective transport properties of porous layers in electrolysis and fuel cells. *Journal of Materials Science*, 48(7), pp.2934–2952. Available at: http://link.springer.com/10.1007/s10853-012-6968-z [Accessed September 3, 2014].

Horner, H. a & Urban, J.P., 2001. 2001 Volvo Award Winner in Basic Science Studies: Effect of nutrient supply on the viability of cells from the nucleus pulposus of the intervertebral disc. *Spine*, 26(23), pp.2543–9. Available at: http://www.ncbi.nlm.nih.gov/pubmed/11725234.

Horner, H.A. et al., 2002. Cells From Different Regions of the Intervertebral Disc Effect of Culture System on Matrix Expression and Cell Phenotype. , 27(10), pp.1018–1028.

Hsieh, A.H. & Twomey, J.D., 2010. Cellular mechanobiology of the intervertebral disc: New directions and approaches. *Journal of Biomechanics*, 43(1), pp.137–145. Available at: http://www.ncbi.nlm.nih.gov/pubmed/ [Accessed November 12, 2014].

Huang, C.Y. & Gu, W.Y., 2008. Effects of mechanical compression on metabolism and distribution of oxygen and lactate in intervertebral disc. *Journal of Biomechanics*, 41(6), pp.1184–1196. Available at: http://www.ncbi.nlm.nih.gov/pubmed/18374341 [Accessed August 20, 2014].

Huang, K.-Y. et al., 2008. IL-20 may contribute to the pathogenesis of human intervertebral disc herniation. *Spine*, 33(19), pp.2034–40. Available at: http://www.ncbi.nlm.nih.gov/pubmed/18758357.

Huang, Y.-C., Urban, J.P.G. & Luk, K.D.K., 2014. Intervertebral disc regeneration: do nutrients lead the way? *Nature reviews. Rheumatology*, 10(9), pp.561–6. Available at: http://www.ncbi.nlm.nih.gov/pubmed/24914695 [Accessed October 28, 2014].

Huyghe, J.M. et al., 2003. An ionised/non-ionised dual porosity model of intervertebral disc tissue. *Biomechanics and modeling in mechanobiology*, 2(1), pp.3–19. Available at: http://www.ncbi.nlm.nih.gov/pubmed/14586814 [Accessed September 3, 2014].

Huyghe, J.M. & Janssen, J.D., 1997. Quadriphasic mechanics of swelling incompressible porous media. *International Journal of Engineering Science*, 35(8), pp.793–802. Available at: www.sciencedirect.com/science/article/pii/S002072259600119X.

Huyghe, J.M., Wilson, W. & Malakpoor, K., 2009. On the thermodynamical admissibility of the triphasic theory of charged hydrated tissues. *Journal of biomechanical engineering*, 131(4), p.044504. Available at: http://www.ncbi.nlm.nih.gov/pubmed/19275446.

Iatridis, J.C. et al., 2006. Effects of mechanical loading on intervertebral disc metabolism in vivo. *The Journal of bone and joint surgery. American volume*, 88 Suppl 2(6), pp.41–46. Available at: http://www.ncbi.nlm.nih.gov/pubmed/16595442.

Iatridis, J.C. et al., 2007. Measurements of proteoglycan and water content distribution in human lumbar intervertebral discs. *Spine*, 32(14), pp.1493–1497. Available at: http://www.ncbi.nlm.nih.gov/pubmed/17572617.

Iatridis, J.C. & Ap Gwynn, I., 2004. Mechanisms for mechanical damage in the intervertebral disc annulus fibrosus. *Journal of Biomechanics*, 37(8), pp.1165–1175. Available at: http://www.ncbi.nlm.nih.gov/pubmed/15212921.

Ishihara, H. & Urban, J.P., 1999. Effects of low oxygen concentrations and metabolic inhibitors on proteoglycan and protein synthesis rates in the intervertebral disc. *Journal of orthopaedic research : official publication of the Orthopaedic Research Society*, 17(6), pp.829–35. Available at: http://www.ncbi.nlm.nih.gov/pubmed/10632449.

Jackson, A. et al., 2006. Anisotropic ion diffusivity in intervertebral disc: an electrical conductivity approach. *Spine*, 31(24), pp.2783–2789. Available at: http://www.ncbi.nlm.nih.gov/pubmed/17108829.

Jackson, A.R., Huang, C.-Y.C., et al., 2011a. 3D Finite Element Analysis of Nutrient Distributions and Cell Viability in the Intervertebral Disc: Effects of Deformation and Degeneration. *Journal of Biomechanical Engineering*, 133(9), pp.091006–1–7. Available at: http://www.ncbi.nlm.nih.gov/pubmed/22010741 [Accessed August 25, 2014].

Jackson, A.R. et al., 2008. Effect of compression and anisotropy on the diffusion of glucose in annulus fibrosus. *Spine*, 33(1), pp.1–7. Available at: http://www.ncbi.nlm.nih.gov/pubmed/18165741.

Jackson, A.R., Huang, C.-Y. & Gu, W.Y., 2011b. Effect of endplate calcification and mechanical deformation on the distribution of glucose in intervertebral disc: a 3D finite element study. *Computer methods in biomechanics and biomedical engineering*, 14(2), pp.195–204. Available at: http://www.ncbi.nlm.nih.gov/pubmed/21337225.

Jaumard, N. V. et al., 2007. Synthetic Lumbar Intervertebral Disk for Medical Education. *Journal of Medical Devices*, 1(September 2007), p.212.

Johannessen, W. et al., 2006. Assessment of human disc degeneration and proteoglycan content using T1rho-weighted magnetic resonance imaging. *Spine*, 31(11), pp.1253–1257. Available at: http://www.ncbi.nlm.nih.gov/pubmed/16688040.

Jones, A.C. & Wilcox, R.K., 2008. Finite element analysis of the spine: Towards a framework of verification, validation and sensitivity analysis. *Medical Engineering and Physics*, 30(10), pp.1287–1304. Available at: http://www.ncbi.nlm.nih.gov/pubmed/18986824.

Jünger, S. et al., 2009. Effect of limited nutrition on in situ intervertebral disc cells under simulated-physiological loading. *Spine*, 34(12), pp.1264–1271. Available at: http://www.ncbi.nlm.nih.gov/pubmed/19455001.

Juniper, M., Le, T.K. & Mladsi, D., 2009. The epidemiology, economic burden, and pharmacological treatment of chronic low back pain in France, Germany, Italy, Spain and the UK: a literature-based review. *Expert opinion on pharmacotherapy*, 10(16), pp.2581–2592. Available at: http://www.ncbi.nlm.nih.gov/pubmed/19874246.

Karoui, A. et al., 2014. The eXtended finite element method for cracked hyperelastic materials: A convergence study. *International Journal for Numerical Methods in Engineering*, 100(3), pp.222–242. Available at: http://doi.wiley.com/10.1002/nme.4736.

Katz, J.N., 2006. Lumbar disc disorders and low-back pain: socioeconomic factors and consequences. *The Journal of bone and joint surgery. American volume*, 88 Suppl 2, pp.21–4. Available at: http://www.ncbi.nlm.nih.gov/pubmed/16595438.

Kim, K.-W. et al., 2003. The origin of chondrocytes in the nucleus pulposus and histologic findings associated with the transition of a notochordal nucleus pulposus to a fibrocartilaginous

nucleus pulposus in intact rabbit intervertebral discs. *Spine*, 28(10), pp.982–990. Available at: http://www.ncbi.nlm.nih.gov/pubmed/12768135.

Klionsky, D.J., 2005. The molecular machinery of autophagy: unanswered questions. *Journal of cell science*, 118(Pt 1), pp.7–18. Available at: http://www.ncbi.nlm.nih.gov/pubmed/15615779.

Lai, W.M., Hou, J.S. & Mow, V.C., 1991. A triphasic theory for the swelling and deformation behaviors of articular cartilage. *Journal of biomechanical engineering*, 113(3), pp.245–258.

Laible, J.P. et al., 1993. A poroelastic-swelling finite element model with application to the intervertebral disc. *Spine*, 18(5), pp.659–670. Available at: http://www.ncbi.nlm.nih.gov/pubmed/8484158.

Liebscher, T. et al., 2011. Age-related variation in cell density of human lumbar intervertebral disc. *Spine*, 36(2), pp.153–9. Available at: http://www.ncbi.nlm.nih.gov/pubmed/20671592 [Accessed September 3, 2014].

Lockshin, R. a. & Zakeri, Z., 2004. Apoptosis, autophagy, and more. *International Journal of Biochemistry and Cell Biology*, 36(12), pp.2405–2419. Available at: http://www.ncbi.nlm.nih.gov/pubmed/15325581.

Lotz, J.C. & Hsieh, A.H., 2014. The effect of mechanical forces on nucleus pulposus and annulus fibrosus cells. In I. M. Shapiro & M. V Risbud, eds. *The intervertebral disc*. Wien: Springer, pp. 109–23.

Lotz, J.C. & Ulrich, J.A., 2006. Innervation, inflammation, and hypermobility may characterize pathologic disc degeneration: review of animal model data. *The Journal of bone and joint surgery. American volume*, 88 Suppl 2(2), pp.76–82. Available at: http://www.ncbi.nlm.nih.gov/pubmed/16595449.

Lyons, G., Eisenstein, S.M. & Sweet, M.B., 1981. Biochemical changes in intervertebral disc degeneration. *Biochimica et biophysica acta*, 673(4), pp.443–453. Available at: http://www.ncbi.nlm.nih.gov/pubmed/7225426.

Mackie, J.S. & Meares, P., 1955. The Diffusion of Electrolytes in a Cation-Exchange Resin Membrane. II. Experimental. *Proceedings of the Royal Society A: Mathematical, Physical and Engineering Sciences*, 232(1191), pp.510–518. Available at: http://www.jstor.org/stable/99827.

Mahmoodian, R. et al., 2011. Changes in mechanics and composition of human talar cartilage anlagen during fetal development. *Osteoarthritis and Cartilage*, 19(10), pp.1199–1209. Available at: http://www.ncbi.nlm.nih.gov/pubmed/21843650.

Malandrino, A., Pozo, J.M., et al., 2015a. On the Relative Relevance of Subject-Specific Geometries and Degeneration-Specific Mechanical Properties for the Study of Cell Death in Human Intervertebral Disk Models. *Frontiers in Bioengineering and Biotechnology*.

Malandrino, A., Jackson, A.R., et al., 2015b. Poroelastic modeling of the intervertebral disc: A path toward integrated studies of tissue biophysics and organ degeneration. *MRS Bulletin*, 40(04), pp.324–332. Available at: http://www.journals.cambridge.org/abstract_S0883769415000688.

Malandrino, A. et al., 2014b. The role of endplate poromechanical properties on the nutrient availability in the intervertebral disc. *Osteoarthritis and Cartilage*, 22(7), pp.1053–1060. Available at: http://www.ncbi.nlm.nih.gov/pubmed/24857972 [Accessed September 3, 2014].

Malandrino, A., Noailly, J. & Lacroix, D., 2014a. Numerical exploration of the combined effect of nutrient supply, tissue condition and deformation in the intervertebral disc. *Journal of*

Biomechanics, 47(6), pp.1520–1525. Available at: http://www.ncbi.nlm.nih.gov/pubmed/24612720 [Accessed September 3, 2014].

Malandrino, A., Noailly, J. & Lacroix, D., 2011. The effect of sustained compression on oxygen metabolic transport in the intervertebral disc decreases with degenerative changes. *PLoS computational biology*, 7(8), p.e1002112. Available at: http://www.ncbi.nlm.nih.gov/pubmed/21829341 [Accessed November 24, 2014].

Malandrino, A., Planell, J. a. & Lacroix, D., 2009. Statistical factorial analysis on the poroelastic material properties sensitivity of the lumbar intervertebral disc under compression, flexion and axial rotation. *Journal of Biomechanics*, 42(16), pp.2780–2788. Available at: http://www.ncbi.nlm.nih.gov/pubmed/19796766 [Accessed May 4, 2011].

Malko, J. a., Hutton, W.C. & Fajman, W. a., 2002. An in vivo MRI study of the changes in volume (and fluid content) of the lumbar intervertebral disc after overnight bed rest and during an 8-hour walking protocol. *Journal of spinal disorders & techniques*, 15(2), pp.157–163. Available at: http://www.ncbi.nlm.nih.gov/pubmed/11927827.

Marchand, F. & Ahmed, A.M., 1990. Investigation of the laminate structure of lumbar disc anulus fibrosus. *Spine*, 15(5), pp.402–410. Available at: http://www.ncbi.nlm.nih.gov/pubmed/2363068.

Mariconda, M. et al., 2010. Frequency and clinical meaning of long-term degenerative changes after lumbar discectomy visualized on imaging tests. *European Spine Journal*, 19(1), pp.136–143. Available at: http://www.ncbi.nlm.nih.gov/pubmed/19894068 [Accessed October 25, 2014].

Markolf, K.L. & Morris, J.M., 1974. The structural components of the intervertebral disc. A study of their contributions to the ability of the disc to withstand compressive forces. *The Journal of bone and joint surgery. American volume*, 56(4), pp.675–687. Available at: http://www.ncbi.nlm.nih.gov/pubmed/4835815.

Maroudas, a et al., 1975. Factors involved in the nutrition of the human lumbar intervertebral disc: cellularity and diffusion of glucose in vitro. *Journal of anatomy*, 120(Pt 1), pp.113–130. Available at: http://www.ncbi.nlm.nih.gov/pubmed/1184452.

Maroudas, A., 1968. Physicochemical properties of cartilage in the light of ion exchange theory. *Biophysical journal*, 8(5), pp.575–595. Available at: http://www.ncbi.nlm.nih.gov/pubmed/5699797.

Mawatari, T. et al., 2010. Effects of tensile strain and fluid flow on osteoarthritic human chondrocyte metabolism in vitro. *Journal of Orthopaedic Research*, 28(7), pp.907–913. Available at: http://www.ncbi.nlm.nih.gov/pubmed/20063382.

McMillan, D.W., Garbutt, G. & Adams, M. a, 1996. Effect of sustained loading on the water content of intervertebral discs: implications for disc metabolism. *Annals of the rheumatic diseases*, 55(12), pp.880–887. Available at: http://www.ncbi.nlm.nih.gov/pubmed/9014581.

McNally, D.S. et al., 1996. In vivo stress measurement can predict pain on discography. *Spine*, 21(22), pp.2580–2587. Available at: http://www.ncbi.nlm.nih.gov/pubmed/8961445.

Melenk, J.M. & Babuška, I., 1996. The partition of unity finite element method: Basic theory and applications. *Computer Methods in Applied Mechanics and Engineering*, 139(1-4), pp.289–314. Available at: http://citeseerx.ist.psu.edu/viewdoc/summary?doi=10.1.1.55.5239.

Mokhbi Soukane, D., Shirazi-Adl, A. & Urban, J.P.G., 2009. Investigation of solute concentrations in a 3D model of intervertebral disc. *European Spine Journal*, 18(2), pp.254–262. Available at: http://www.ncbi.nlm.nih.gov/pubmed/19015897 [Accessed September 3, 2014].

Mow, V.C. et al., 1980. Biphasic creep and stress relaxation of articular cartilage in compression? Theory and experiments. *Journal of biomechanical engineering*, 102(1), pp.73–84. Available at: http://www.ncbi.nlm.nih.gov/pubmed/7382457.

Nachemson, A. et al., 1970. In vitro diffusion of dye through the end-plates and the annulus fibrosus of human lumbar inter-vertebral discs. *Acta orthopaedica Scandinavica*, 41(6), pp.589–607. Available at: http://www.ncbi.nlm.nih.gov/pubmed/5516549.

Negrini, S. et al., 2006. Diagnostic therapeutic flow-charts for low back pain patients: the Italian clinical guidelines. *Europa medicophysica*, 42(2), pp.151–170. Available at: http://www.ncbi.nlm.nih.gov/pubmed/16767064.

Neidlinger-Wilke, C. et al., 2012. Interactions of environmental conditions and mechanical loads have influence on matrix turnover by nucleus pulposus cells. *Journal of orthopaedic research : official publication of the Orthopaedic Research Society*, 30(1), pp.112–21. Available at: http://www.ncbi.nlm.nih.gov/pubmed/21674606 [Accessed August 25, 2014].

Neumann, D.A., 2009. *Kinesiology of the musculoskeletal system: Foundations for rehabilitation* 2 edition., London: Mosby.

Noailly, J. et al., 2007. How does the geometry affect the internal biomechanics of a lumbar spine bi-segment finite element model? Consequences on the validation process. *Journal of Biomechanics*, 40(11), pp.2414–25. Available at: http://www.ncbi.nlm.nih.gov/pubmed/17257603.

Noailly, J. & Lacroix, D., 2012b. Cartilage Endplate Composition Controls the Functional Fluid Transport in and Out of the Disc. *Journal of Biomechanics*, 45, p.S610. Available at: http://linkinghub.elsevier.com/retrieve/pii/S0021929012706115 [Accessed December 2, 2014].

Noailly, J. & Lacroix, D., 2012a. Finite element modelling of the spine. In L. Ambrosio & E. Tanner, eds. *Biomaterials for spinal surgery*. Cambridge: Woodhead Publishing Ltd, pp. 144–232.

Noailly, J., Malandrino, A. & Galbusera, F., 2014. Computational modelling of spinal implants. In Z. Jin, ed. *Computational Modelling of Biomechanics and Biotribology in the Musculoskeletal System*.

Noailly, J., Planell, J.A. & Lacroix, D., 2011. On the collagen criss-cross angles in the annuli fibrosi of lumbar spine finite element models. *Biomechanics and Modeling in Mechanobiology*, 10, pp.203–219. Available at: http://www.ncbi.nlm.nih.gov/pubmed/20532944 [Accessed August 6, 2010].

Oegema, T.R. et al., 2000. Fibronectin and its fragments increase with degeneration in the human intervertebral disc. *Spine*, 25(21), pp.2742–2747. Available at: http://www.ncbi.nlm.nih.gov/pubmed/11064518.

Osti, O.L. et al., 1992. Annular tears and disc degeneration in the lumbar spine. A post-mortem study of 135 discs. *The Journal of bone and joint surgery. British volume*, 74(5), pp.678–682.

Pazzaglia, U.E., Salisbury, J.R. & Byers, P.D., 1989. Development and involution of the notochord in the human spine. *Journal of the Royal Society of Medicine*, 82(7), pp.413–415. Available at: http://www.ncbi.nlm.nih.gov/pubmed/2585428.

Pfirrmann, C.W. et al., 2001. Magnetic resonance classification of lumbar intervertebral disc degeneration. *Spine*, 26(17), pp.1873–8. Available at: http://www.ncbi.nlm.nih.gov/pubmed/11568697.

Podniece, Z., 2008. *Work-related musculoskeletal disorders: Prevention report*, European Agency for Safety and Health at Work. Available at: http://europa.eu.

Postacchini, F. et al., 1994. Ligamenta flava in lumbar disc herniation and spinal stenosis. Light and electron microscopic morphology. *Spine*, 19(8), pp.917–922. Available at: http://www.ncbi.nlm.nih.gov/pubmed/8009349.

Raj, P.P., 2008. Intervertebral disc: Anatomy-physiology-pathophysiology-treatment. *Pain Practice*, 8(1), pp.18–44. Available at: http://www.ncbi.nlm.nih.gov/pubmed/18211591 [Accessed April 11, 2013].

Rajasekaran, S. et al., 2004. ISSLS prize winner: A study of diffusion in human lumbar discs: a serial magnetic resonance imaging study documenting the influence of the endplate on diffusion in normal and degenerate discs. *Spine*, 29(23), pp.2654–2667. Available at: http://www.ncbi.nlm.nih.gov/pubmed/15564914.

Razaq, S., Wilkins, R.J. & Urban, J.P.G., 2003. The effect of extracellular pH on matrix turnover by cells of the bovine nucleus pulposus. *European Spine Journal*, 12(4), pp.341–349. Available at: http://www.ncbi.nlm.nih.gov/pubmed/12883962 [Accessed November 13, 2014].

Reutlinger, C. et al., 2014. Specimen specific parameter identification of ovine lumbar intervertebral discs: On the influence of fibre-matrix and fibre-fibre shear interactions. *Journal of the Mechanical Behavior of Biomedical Materials*, 30, pp.279–289. Available at: http://www.ncbi.nlm.nih.gov/pubmed/24361932.

Riches, P.E. & McNally, D.S., 2005. A one-dimensional theoretical prediction of the effect of reduced end-plate permeability on the mechanics of the intervertebral disc. *Proceedings of the Institution of Mechanical Engineers. Part H, Journal of engineering in medicine*, 219(5), pp.329–335. Available at: http://www.ncbi.nlm.nih.gov/pubmed/16225149 [Accessed September 3, 2014].

Rinkler, C. et al., 2010. Influence of low glucose supply on the regulation of gene expression by nucleus pulposus cells and their responsiveness to mechanical loading. *Journal of neurosurgery: Spine*, 13(4), pp.535–42. Available at: http://www.ncbi.nlm.nih.gov/pubmed/20887152 [Accessed May 30, 2011].

Del Rio, A. et al., 2009. Stretching single talin rod molecules activates vinculin binding. *Science (New York, N.Y.)*, 323(5914), pp.638–641. Available at: http://www.ncbi.nlm.nih.gov/pubmed/19179532.

Roberts, S. et al., 1996. Transport properties of the human cartilage endplate in relation to its composition and calcification. *Spine*, 21(4), pp.415–420. Available at: http://www.ncbi.nlm.nih.gov/pubmed/8658243.

Roberts, S., Menage, J. & Urban, J.P., 1989. Biochemical and structural properties of the cartilage end-plate and its relation to the intervertebral disc. *Spine*, 14(2), pp.166–174. Available at: http://www.ncbi.nlm.nih.gov/pubmed/2922637.

Roberts, S. & Urban, J.P.G., 2011. Intervertebral discs. In *Encyclopaedia of Occupational health and Safety*. Geneva. Available at: http://www.ilocis.org/en/contilo1.html.

Rodriguez, A.G. et al., 2011. Human disc nucleus properties and vertebral endplate permeability. *Spine*, 36(7), pp.512–520. Available at: http://www.ncbi.nlm.nih.gov/pubmed/21240044.

Rodriguez, A.G. et al., 2012. Morphology of the human vertebral endplate. *Journal of Orthopaedic Research*, 30(2), pp.280–287. Available at: http://www.ncbi.nlm.nih.gov/pubmed/21812023 [Accessed November 24, 2014].

Rohlmann, A. et al., 2008. Loads on a telemeterized vertebral body replacement measured in three patients within the first postoperative month. *Clinical Biomechanics*, 23(2), pp.147–158. Available at: http://www.ncbi.nlm.nih.gov/pubmed/18469689.

Salvatierra, J.C. et al., 2011. Difference in energy metabolism of annulus fibrosus and nucleus pulposus cells of the intervertebral disc. *Cellular and Molecular Bioengineering*, 4(2), pp.302–310. Available at: http://www.ncbi.nlm.nih.gov/pubmed/21625336.

Schmidt, H. et al., 2010. Response analysis of the lumbar spine during regular daily activities--a finite element analysis. *Journal of biomechanics*, 43(10), pp.1849–56. Available at: http://www.ncbi.nlm.nih.gov/pubmed/20394933 [Accessed November 18, 2014].

Schroeder, Y. et al., 2010. A biochemical/biophysical 3D FE intervertebral disc model. *Biomechanics and modeling in mechanobiology*, 9(5), pp.641–50. Available at: http://www.ncbi.nlm.nih.gov/pubmed/20229171 [Accessed September 3, 2014].

Schroeder, Y. et al., 2007. Are disc pressure, stress, and osmolarity affected by intra- and extrafibrillar fluid exchange? *Journal of orthopaedic research : official publication of the Orthopaedic Research Society*, 25(10), pp.1317–24. Available at: http://www.ncbi.nlm.nih.gov/pubmed/17557324.

Schroeder, Y. et al., 2006. Osmoviscoelastic finite element model of the intervertebral disc. In *European Spine Journal*. pp. S361–71. Available at: http://www.ncbi.nlm.nih.gov/pubmed/16724211 [Accessed September 3, 2014].

Setton, L. a, 2005. Cell mechanics and mechanobiology in the intervertebral disc. In *European Cells and Materials*. Davos, p. 22.

Setton, L. a & Chen, J., 2004. Cell mechanics and mechanobiology in the intervertebral disc. *Spine*, 29(23), pp.2710–23. Available at: http://www.ncbi.nlm.nih.gov/pubmed/15564920.

Shah, J.S., Hampson, W.G. & Jayson, M.I., 1978. The distribution of surface strain in the cadaveric lumbar spine. *The Journal of bone and joint surgery. British volume*, 60-B(2), pp.246–251. Available at: http://www.ncbi.nlm.nih.gov/pubmed/659474.

Shankar, H., Scarlett, J. a. & Abram, S.E., 2009. Anatomy and pathophysiology of intervertebral disc disease. *Techniques in Regional Anesthesia and Pain Management*, 13(2), pp.67–75. Available at: http://linkinghub.elsevier.com/retrieve/pii/S1084208X09000135 [Accessed March 7, 2013].

Shinmei, M. et al., 1988. The role of interleukin-1 on proteoglycan metabolism of rabbit annulus fibrosus cells cultured in vitro. *Spine*, 13(11), pp.1284–1290. Available at: http://www.ncbi.nlm.nih.gov/pubmed/3264623.

Shirazi-Adl, a, Taheri, M. & Urban, J.P.G., 2010. Analysis of cell viability in intervertebral disc: Effect of endplate permeability on cell population. *Journal of biomechanics*, 43(7), pp.1330–6. Available at: http://www.ncbi.nlm.nih.gov/pubmed/20167323 [Accessed August 29, 2014].

Simon, B.R. et al., 1998. Identification and determination of material properties for porohyperelastic analysis of large arteries. *Journal of biomechanical engineering*, 120(2), pp.188–194. Available at: http://www.ncbi.nlm.nih.gov/pubmed/10412379.

Simon, B.R. et al., 1985. Structural models for human spinal motion segments based on a poroelastic view of the intervertebral disk. *Journal of Biomechanical Engineering*, 107(4), pp.327–35.

Sivan, S. et al., 2006a. Correlation of swelling pressure and intrafibrillar water in young and aged human intervertebral discs. *Journal of orthopaedic research : official publication of the*

Orthopaedic Research Society, 24(6), pp.1292–8. Available at: http://www.ncbi.nlm.nih.gov/pubmed/16649177.

Sivan, S.S. et al., 2006b. Aggrecan turnover in human intervertebral disc as determined by the racemization of aspartic acid. *The Journal of biological chemistry*, 281(19), pp.13009–14. Available at: http://www.ncbi.nlm.nih.gov/pubmed/16537531 [Accessed August 28, 2014].

Sivan, S.S. et al., 2008. Collagen turnover in normal and degenerate human intervertebral discs as determined by the racemization of aspartic acid. *Journal of Biological Chemistry*, 283(14), pp.8796–8801. Available at: http://www.ncbi.nlm.nih.gov/pubmed/18250164.

Smith, L.J. et al., 2011. Degeneration and regeneration of the intervertebral disc: lessons from development. *Disease models & mechanisms*, 4(1), pp.31–41. Available at: http://www.ncbi.nlm.nih.gov/pubmed/21123625 [Accessed August 29, 2014].

Soukane, D.M., Shirazi-Adl, A. & Urban, J.P.G., 2005. Analysis of nonlinear coupled diffusion of oxygen and lactic acid in intervertebral discs. *Journal of biomechanical engineering*, 127(7), pp.1121–1126. Available at: http://www.ncbi.nlm.nih.gov/pubmed/16502654 [Accessed September 3, 2014].

Specchia, N. et al., 2002. Cytokines and growth factors in the protruded intervertebral disc of the lumbar spine. *European Spine Journal*, 11(2), pp.145–151. Available at: http://www.ncbi.nlm.nih.gov/pubmed/11956921 [Accessed October 28, 2014].

Stokes, I. a et al., 2010. Limitation of finite element analysis of poroelastic behavior of biological tissues undergoing rapid loading. *Annals of Biomedical Engineering*, 38(5), pp.1780–1788. Available at: http://www.ncbi.nlm.nih.gov/pubmed/20306136 [Accessed November 18, 2014].

Stokes, I. a. F. & Iatridis, J.C., 2004. Mechanical conditions that accelerate intervertebral disc degeneration: overload versus immobilization. *Spine*, 29(23), pp.2724–2732. Available at: http://www.ncbi.nlm.nih.gov/pubmed/15564921.

Sun, F., Qu, J.-N. & Zhang, Y.-G., 2013. Animal models of disc degeneration and major genetic strategies. *Pain physician*, 16(3), pp.E267–75. Available at: http://www.ncbi.nlm.nih.gov/pubmed/23703425.

Sztrolovics, R. et al., 1997. Aggrecan degradation in human intervertebral disc and articular cartilage. *The Biochemical journal*, 326 (Pt 1, pp.235–241. Available at: http://www.ncbi.nlm.nih.gov/pubmed/9337874.

Thompson, J.P., Oegema, T.R. & Bradford, D.S., 1991. Stimulation of mature canine intervertebral disc by growth factors. *Spine*, 16(3), pp.253–260. Available at: http://www.ncbi.nlm.nih.gov/pubmed/2028297.

Travascio, F. & Gu, W.Y., 2007. Anisotropic diffusive transport in annulus fibrosus: Experimental determination of the diffusion tensor by FRAP technique. *Annals of Biomedical Engineering*, 35(10), pp.1739–1748. Available at: http://www.ncbi.nlm.nih.gov/pubmed/17605108.

Tsai, T.-T. et al., 2014. Mechanotransduction in intervertebral discs. *Journal of cellular and molecular medicine*, 18(12), pp.2351–2360. Available at: http://www.ncbi.nlm.nih.gov/pubmed/25267492.

Urban, J.P. et al., 1982. Nutrition of the intervertebral disc: effect of fluid flow on solute transport. *Clinical orthopaedics and related research*, 170(170), pp.296–302. Available at: http://www.ncbi.nlm.nih.gov/pubmed/7127960.

Urban, J.P. et al., 1979. Swelling pressures of proteoglycans at the concentrations found in cartilaginous tissues. *Biorheology*, 16(6), pp.447–464. Available at: http://www.ncbi.nlm.nih.gov/pubmed/534768.

Urban, J.P.G. & Maroudas, A., 1979. The measurement of fixed charged density in the intervertebral disc. *Biochimica et Biophysica Acta (BBA) - General Subjects*, 586(1), pp.166–78. Available at: http://www.sciencedirect.com/science/article/pii/030441657990415X.

Urban, J.P.G. & Roberts, S., 2003. Degeneration of the intervertebral disc. *Arthritis research & therapy*, 5(3), pp.120–130. Available at: http://www.ncbi.nlm.nih.gov/pubmed/12723977.

Urban, J.P.G., Roberts, S. & Ralphs, J.R., 2000. The Nucleus of the Intervertebral Disc from Development to Degeneration1. *American Zoologist*, 40(1), pp.53–61.

Urban, J.P.G., Smith, S. & Fairbank, J.C.T., 2004. Nutrition of the intervertebral disc. *Spine*, 29(23), pp.2700–2709. Available at: http://www.ncbi.nlm.nih.gov/pubmed/15564919 [Accessed April 11, 2013].

Vigneron, L.M. et al., 2012. Serial FEM/XFEM-based update of preoperative brain images using intraoperative MRI. *International Journal of Biomedical Imaging*, 2012, pp.1–17. Available at: http://www.ncbi.nlm.nih.gov/pubmed/22287953.

Wallace, A.L. et al., 1994. Humoral regulation of blood flow in the vertebral endplate. *Spine*, 19(12), pp.1321–8. Available at: http://www.ncbi.nlm.nih.gov/pubmed/8066511.

Wang, P., Yang, L. & Hsieh, A.H., 2011. Nucleus pulposus cell response to confined and unconfined compression implicates mechanoregulation by fluid shear stress. *Annals of biomedical engineering*, 39(3), pp.1101–11. Available at: http://www.ncbi.nlm.nih.gov/pubmed/21132369 [Accessed November 21, 2014].

Weiler, C. et al., 2002. 2002 SSE award competition in basic science: Expression of major matrix metalloproteinases is associated with intervertebral disc degradation and resorption. *European Spine Journal*, 11(4), pp.308–320. Available at: http://www.ncbi.nlm.nih.gov/pubmed/12193691 [Accessed October 25, 2014].

Van Der Werf, M. et al., 2007. Inhibition of vertebral endplate perfusion results in decreased intervertebral disc intranuclear diffusive transport. *Journal of Anatomy*, 211(6), pp.769–774. Available at: http://www.ncbi.nlm.nih.gov/pubmed/17953653 [Accessed September 3, 2014].

White, A. & Panjabi, M.M., 1978. *Clinical Biomechanics of the Spine* 1st editio., J. B. Lippincott Company.

Wilke, H.J. et al., 1999. New in vivo measurements of pressures in the intervertebral disc in daily life. *Spine*, 24(8), pp.755–62. Available at: http://www.ncbi.nlm.nih.gov/pubmed/10222525.

Williamson, A.K., Chen, A.C. & Sah, R.L., 2001. Compressive properties and function-composition relationships of developing bovine articular cartilage. *Journal of Orthopaedic Research*, 19(6), pp.1113–1121. Available at: http://www.ncbi.nlm.nih.gov/pubmed/11781013.

Wilson, W., van Donkelaar, C.C. & Huyghe, J.M., 2005. A Comparison Between Mechano-Electrochemical and Biphasic Swelling Theories for Soft Hydrated Tissues. *Journal of Biomechanical Engineering*, 127(1), p.158. Available at: http://biomechanical.asmedigitalcollection.asme.org/article.aspx?doi=10.1115/1.1835361 [Accessed November 12, 2014].

Wognum, S., Huyghe, J.M. & Baaijens, F.P.T., 2006. Influence of osmotic pressure changes on the opening of existing cracks in 2 intervertebral disc models. *Spine*, 31(16), pp.1783–1788. Available at: http://www.ncbi.nlm.nih.gov/pubmed/16845351.

Wolfe, H.J., Putschar, W.G. & Vickery, A.L., 1965. Role of the notochord in human intervertebral disk. I. Fetus and infant. *Clinical orthopaedics and related research*, 39, pp.205–212. Available at: http://www.ncbi.nlm.nih.gov/pubmed/14288176.

Zaafouri, M. et al., 2015. *Multiphysics Modelling and Simulation for Systems Design and Monitoring*, Available at: http://link.springer.com/10.1007/978-3-319-14532-7.

Zhang, Y.-H. et al., 2008. Modic changes: a systematic review of the literature. *European spine journal : official publication of the European Spine Society, the European Spinal Deformity Society, and the European Section of the Cervical Spine Research Society*, 17(10), pp.1289–99. Available at: http://www.pubmedcentral.nih.gov/articlerender.fcgi?artid=2556462&tool=pmcentrez&rendertype=abstract [Accessed September 3, 2014].

Zhu, Q., Gao, X. & Gu, W., 2014. Temporal changes of mechanical signals and extracellular composition in human intervertebral disc during degenerative progression. *Journal of Biomechanics*, 47(15), pp.3734–3743. Available at: http://www.ncbi.nlm.nih.gov/pubmed/25305690.

Zhu, Q., Jackson, A.R. & Gu, W.Y., 2012. Cell viability in intervertebral disc under various nutritional and dynamic loading conditions: 3d Finite element analysis. *Journal of Biomechanics*, 45(16), pp.2769–2777. Available at: http://www.ncbi.nlm.nih.gov/pubmed/23040882 [Accessed August 20, 2014].